TH 1137

THE GEOLOGY AND GEOCHEMISTRY OF ARCHEAN VOLCANIC ROCKS IN DANIEL TOWNSHIP, MATAGAMI, QUEBEC

Documents complémentaires

Additional Files





Licence



License

Cette première page a été ajoutée
au document et ne fait pas partie du
rapport tel que soumis par les auteurs.

Énergie et Ressources naturelles
Québec

THE GEOLOGY AND GEOCHEMISTRY OF ARCHEAN VOLCANIC ROCKS IN DANIEL TOWNSHIP, MATAGAMI, QUEBEC

PAR

Charles Beaudry

1984

1H 1137

THE GEOLOGY AND GEOCHEMISTRY OF ARCHEAN VOLCANIC ROCKS IN DANIEL TOWNSHIP, MATAGAMI, QUEBEC

by

CHARLES BEAUDRY

A thesis submitted to the Faculty of Graduate Studies and Research of McGill University, in partial fulfillment of the requirements for the degree of Master of Science.

Department of Geological Sciences
McGill University, Montreal, Quebec, Canada

Copyright © Charles Beaudry, 1984

THE GEOLOGY AND GEOCHEMISTRY OF ARCHEAN VOLCANIC ROCKS IN DANIEL TOWNSHIP, MATAGAMI, QUEBEC

by

CHARLES BEAUDRY

A thesis submitted to the Faculty of Graduate Studies and Research of McGill University, in partial fulfillment of the requirements for the degree of Master of Science.

Department of Geological Sciences
McGill University, Montreal, Quebec, Canada

Copyright © Charles Beaudry, 1984

C. Beaudry - The Geology and Geochemistry of Archean Volcanic rocks in Daniel Township, Matagami, Quebec

Department of Geological Sciences, Master of Science

Volcanic rocks of the Wabassee Group in Daniel township, near Matagami, Quebec are composed of tholeiitic basalt and calc-alkaline basaltic-andesite to rhyolite. Pillowed and massive submarine flows and rare pyroclastic horizons are intruded by synvolcanic gabbro-norite stocks and sills. The area has been folded into an open, gently westerly plunging anticline with a subvertically dipping east-west striking axial plane. In the east and central part of the map area the rocks are in the prehnite-pumpellyite and lower greenschist facies. In the west, near gabbro-norite stocks, the metamorphic grade reaches amphibolite facies.

Petrographic relations and AFM, Jensen, Harker, Zr vs Ti-Y-Nb and other variation diagrams suggest the tholeiitic and calc-alkaline volcanics are related by fractionation of clinopyroxene, orthopyroxene, plagioclase, and magnetite. Increasing Zr/Nb and La/Yb ratios with differentiation indicate the magma was assimilating crustal material during crystallization.

C. Beaudry - Géologie et Lithogéochimie des Volcanites Archéennes du Canton de Daniel, Matagami, Québec

Département des Sciences Géologiques, Maitrise en Sciences

Les volcanites du groupe de Wabassee dans le canton de Daniel, près de Matagami au Québec se composent de basalte tholéiitique et de roches calco-alcalines variant d'andésite-basaltique à ryolite. Des coulées de laves sous-marines massives et coussinées et de rares horizons pyroclastiques sont recoupés par des intrusions syn-volcaniques gabbro-noritiques. Les roches sont plissées en un anticlinale plongeant légèrement vers l'ouest avec une surface axiale verticale orienté est-ouest. Le métamorphisme dans le faciès préhnite-pumpellyite et chlorite vert inférieur prédomine à l'est et au centre de la région d'étude. A l'ouest, les roches atteignent le faciès amphibolite près des intrusions gabbro-noritiques.

Les relations pétrographiques et les diagrammes de variations chimiques usuels suggèrent que les roches tholéiitiques et calco-alcalines sont co-magmatiques. Ces variations sont le résultat de la cristallisation de clinopyroxène, orthopyroxène, plagioclase et magnétite. L'augmentation des rapports Zr/Nb et La/Yb durant le processus de cristallisation nous indique l'assimilation de matériel crustal par le magma.

TABLE OF CONTENTS

1. Introduction
1.1 General statement----------1
1.2 Location and access----------1
1.3 Summary of geology and previous work----------5
1.4 Nature and purpose of study----------7

2. Geology
2.1 General statement----------10
2.2 Petrography of rock units----------11
2.3 Structural geology----------31

3. Geochemistry
3.1 General statement----------41
3.2 Effects of alteration----------42
3.3 General geochemistry----------51
3.4 Comparison of chemistry of Allard River volcanics with other Archean volcanics in Abitibi greenstone belt----------66
3.5 Petrogenetic modelling----------71
3.6 Discriminant analysis----------78

4. Discussion----------81

5. Conclusions----------91

Contributions to knowledge and suggested work----------93
References----------94

Appendix 1 Sample preperation procedures and analytical techniques----------100

Appendix 2 Results of XRF analyses----------103

Appendix 3 Calculation of precision and accuracy-----109

Appendix 4 Results of rare earth element analyses----114

Appendix 5 Discriminant analysis----------115

LIST OF TABLES

Table 1: Table of formations----------11

2: Metamorphic-alteration mineral assemblages in Wabassee Group----------12

3: Mean modal composition of diabase----------30

4: Summary of alteration studies on spilites----43

5: Mobility of elements during alteration of pillows----------44

6: Chemical analyses of Watson Lake Group rhyolites----------51

7: Comparison between average chemistry of gabbro-norites and Allard River volcanics--56

8: Chemistry of rhyolitic rocks in Wabassee Group----------63

9: Chemistry of basic dikes----------64

10: Analysis of tonalite----------65

11: Analyses of diabase dikes----------66

12: Comparison of Allard River volcanics, Bell River lavas and Watson Lake Group basalts-67

13: Comparison of Allard River volcanics with compiled averages for Timmins-Kirkland Lake-Noranda regions----------69

14: Comparison of Allard River volcanics with Pelletier-Rouyn-Noranda series----------71

15: Discriminant functions for Matagami area volcanic suites----------79

16: Comparison of stratigraphy around Mattagami Lake and New Hosco Mines----------82

LIST OF FIGURES

Figure 1: Regional geology, Matagami district, Quebec----------3

2: Vertical sections through Daniel township---22

3: Sketch of pillows from outcrop north of North McIvor Hill (near station 82c-18)---33

4: Harker diagrams of Allard River of Allard River volcanics----------45,46

5: Hughes diagram----------48

6: FeO and CaO vs Zr diagram----------48

7: Na2O, K2O, and CaO vs LOI----------50

8: Histograms of Allard River volcanics--------53,54

9: AFM diagram----------55

10: MgO vs FeO(Total) diagram----------58

11: Jensen diagram----------58

12: Pearce and Cann diagrams----------59

13: Chondrite normalized rare earth element profiles----------61

14: TiO2, Nb, and Y vs Zr diagrams----------74

15: Zr/Nb, Zr/Y, Zr/TiO2*0.01 vs Zr diagrams----------77

16: Discriminant diagram----------80

17: Cartoon of geology of map area----------84

LIST OF PLATES

Plate 1: Photograph showing typical physiography of thesis area----------36

2: Photograph similar to plate 1----------36

3: Photomicrograph of spherulitic rhyolite from Watson Lake Group----------36

4: Photomicrograph of rhyolite from Watson Lake Group----------36

5: Photomicrograph of rhyolite from Watson Lake Group----------36

6: Photograph of pillow near station 81c-004----36

7: Photograph of hyaloclastic tuff near station 81c-135----------36

8: Photograph of pillow breccia----------36

9: Photomicrograph of prehnite-clinozoisite bearing amygdule in andesite----------38

10: Photomicrograph of plagioclase phenocryst in andesite----------38

11: Photomicrograph of clinopyroxene phenocryst in basalt----------38

12: Photomicrograph of altered prehnite-bearing amygdule----------38

13: Photomicrograph of accretionnary lapilli tuff----------38

14: Photograph of rhyolite breccia in Wabassee Group near station 82c-06--------38

15: Close-up of outcrop in plate 14----------38

16: Photomicrograph of rhyolite fragment from outcrop in plate 14----------38

17: Photomicrograph of gabbro-norite----------40

18: Photomicrograph of gabbro-norite----------40

19: Photomicrograph of porphyritic dike---------40

20: Photomicrograph of hornblende-rich dike-----40

21: Photomicrograph of tonalite-----------------40

22: Photomicrograph of tonalite-----------------40

23: Photograph of tonalite outcrop near station 81c-181 showing mafic xenolith----40

24: Photomicrograph of diabase------------------40

AKNOWLEDGEMENTS

This report has used up a large fraction of my time for the past three years. This could not have been possible save for the love and patience of my wife and best friend Joanne Dubois.

A special thanks to Explorations Noranda Ltee. for field support and particularly to Denis Francoeur and Claude Durocher for showing interest in this project.

The thesis was supported by the governments of Canada (NSERC) and Quebec (FCAC) through operating grants to Prof. Wallace H. MacLean and by two Carl Reinhart Scholarships from McGill University. Special thanks to Prof. Wallace H. MacLean for help and encouragement during all phases of this research.

Other technical assistance from Richard Yates, Shirley Jackson, and Mr. Weiss are aknowledged.

Numerous highly fruitful discussions with F. Bonavia, P. Kranidiotis, J. Gartner, and Laurent Halle are also warmly aknowledged. I assume responsiblity however, for all the conclusions in this report.

CHAPTER 1

I N T R O D U C T I O N

1.1 GENERAL STATEMENT

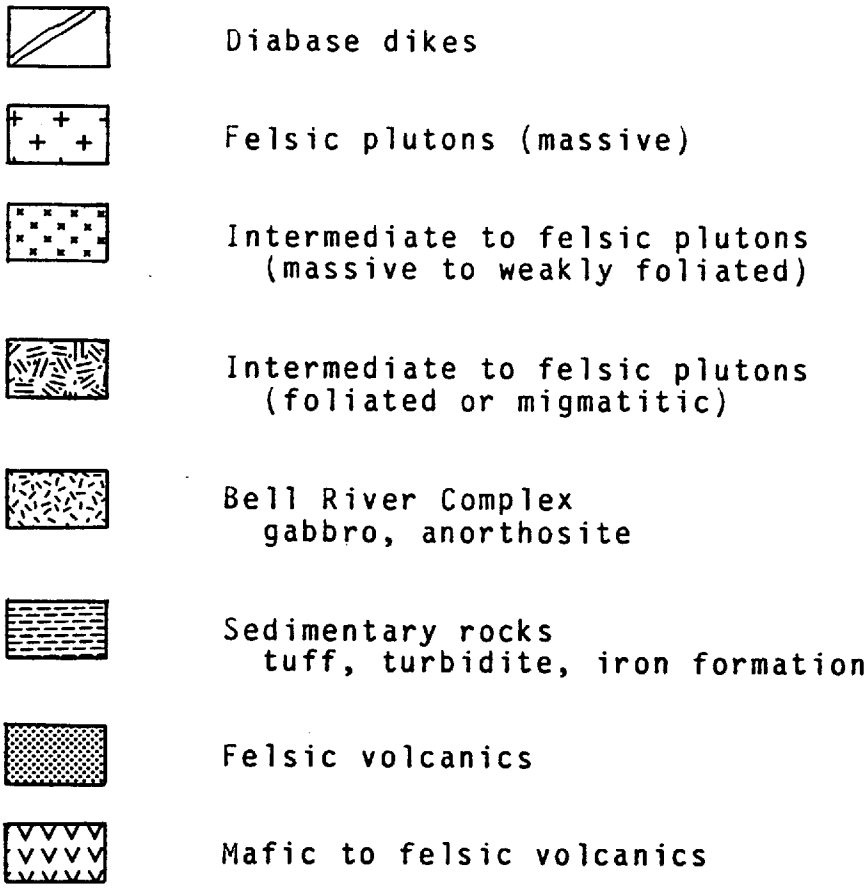
This thesis covers the geology and chemistry of a suite of Archean volcanic rocks located in Daniel township, fifteen kilometers west of Matagami, Quebec (figure 1). The rocks in the thesis area were previously described as dacitic and rhyolitic flows (Sharpe, 1964, 1968; MER, DP-636). This study demonstrates, however, that the area is underlain by a basic to acidic volcanic suite composed mostly of high-alumina basalts and andesites with some dacite and rhyolite flows restricted to the eastern and western parts of the map area.

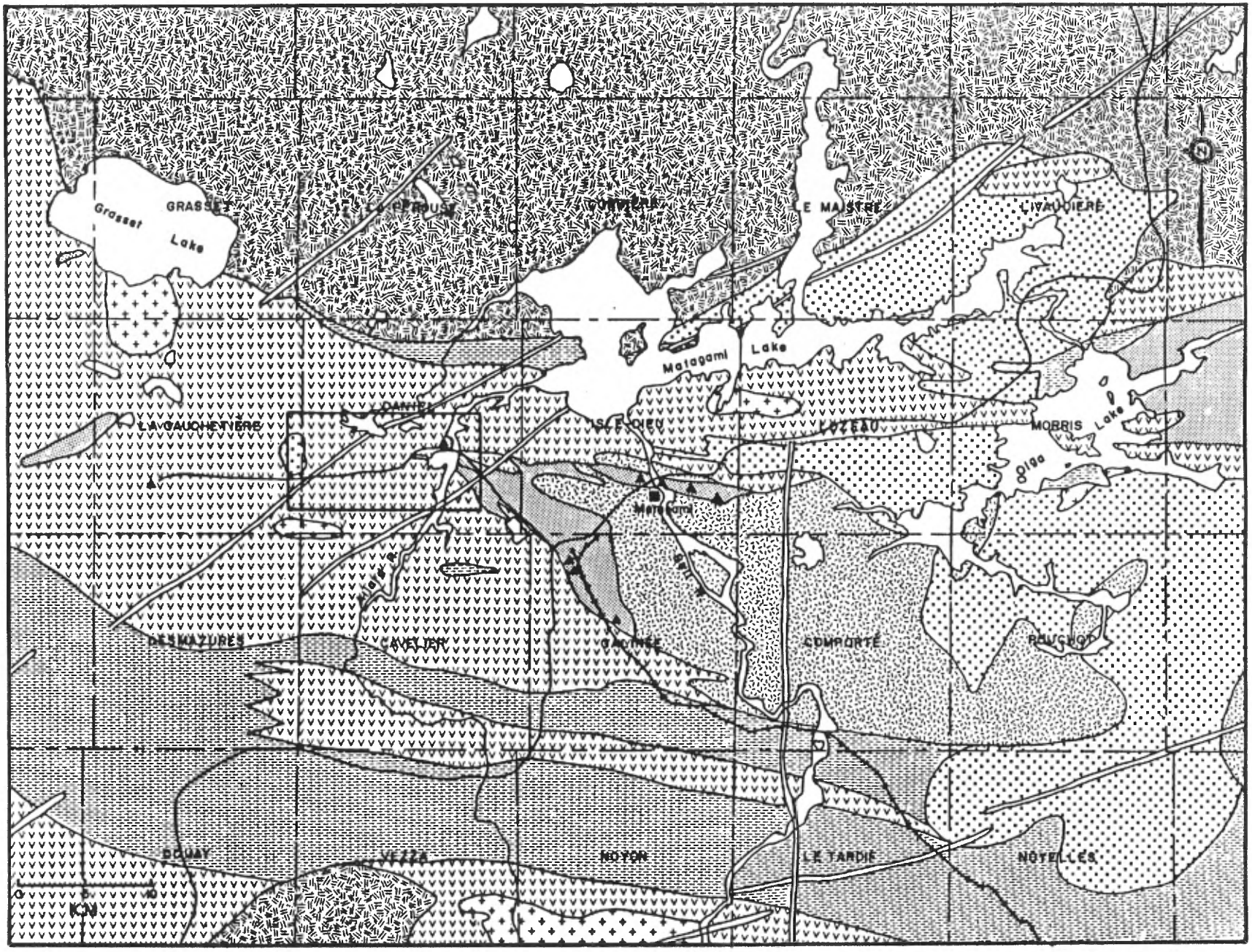
1.2 LOCATION, ACCESS AND PHYSIOGRAPHY

The town of Matagami, Quebec, is situated about 800 kilometers north of Montreal and 300 kilometers north of Val d'Or, Quebec (figure 1). The region is accessible all year by paved road and by air. Travel time overland is approximatly three hours from Val d'Or and eight to nine hours from Montreal. The town of Matagami is serviced daily by Creebec airlines from Val d'Or.

A rail line between Matagami and Lebel sur Quevillon is maintained and operated by Canadian National Railways. No passenger service is offered on this route, however, which is used for transport of mill concentrate and more recently of

Figure 1: Regional geology, Matagami district, Quebec




Grasset Lake
GRASSET
LA PERRAUSE
LE MAISTRE
LIVAUDIERE
Matagami Lake
DAMIEN
LA GAUCHETIERE
ISLE-DIEU
LOZEAU
MORRIS
Lake
Gilda
DESMAZURES
CAVELIER
GAUVREAU
COMPORTE
REUCHON
DOUAY
VEZZA
NOYON
LE TARDIF
NOYELLES
0
10
KM

various supplies for the large James Bay development project.

The thesis area is easily accessible from the townsite. A paved road is provided up to the Allard River opposite the abandoned New Hosco mine. A steel and concrete bridge spans the river at that point. From there to the western extremity of the area an all weather gravel road was built in 1976-78 by Noranda Mines Ltd. for access to the Phelps Dodge mine prospect, and is maintained by forestry companies. In addition, narrow logging roads can be used during the summer. These, however are not maintained and some were found to be impassible a year after the main part of the mapping was performed.

The physiography of the Matagami region is typical of the Abitibi clay belt. A flat to gently undulating surface topography is underlain by clay and silt deposits of glacial lake Barlow-Ojibway (Douglas, 1972). Hills composed of volcanic or intrusive rock locally overlain by a thin veneer of till protrude up to 300 meters above the plain (plates 1,2). Lakes and rivers are generally very shallow and extremely silt laden. Vegetation alternates between dense black spruce forest and open, wet peat bogs. Most of the thesis area has been logged by forestry companies and new growth consists of alders and Labrador Tea.

1.3 SUMMARY OF GEOLOGY AND PREVIOUS WORK

The geology of the Matagami region consists of a volcano-plutonic complex of tholeiitic affinity (MacGeehan, 1978,1979; MacGeehan and MacLean, 1980). The Bell River Complex, a shallow, layered, igneous pluton composed predominantly of gabbro and anorthosite intrudes and is overlain by volcanic flows and sills of the tholeiitic Watson Lake Group (MacGeehan, 1978,1979), and the mixed tholeiitic-calc alkaline Wabassee Group. The region has been folded into a broad anticlinorium with a steeply dipping, westward striking axial plane and a gently westward plunging fold axis (Sharpe, 1968). The Bell River Complex occupies the core of the anticlinorium while the volcanic rocks form the limbs. The thesis area is situated in the Wabassee Group, in the vicinity of the fold hinge. The anticlinal axis can be observed in the field.

Several generations of intrusions postdate the observed volcanism in the district. Dioritic to tonalitic plutons intrude the Bell River Complex around Olga lake and northeast of the town of Matagami (figure 1). A small stock of similar composition and possibly related to them occurs in the western extremity of the thesis area. Granitic plutons occur at Dunlop Bay on Matagami Lake and are thought to occur south of the thesis area. These rocks are considered by Sharpe (1968) to post-date the Bell River complex and diorite-tonalite plutons. Two swarms of diabase dykes, one trending northeast and the other north, occur throughout the district. These are easily detected on regional aeromagnetic maps due to their

anomalous magnetic signature. The dykes are undeformed and transect all other rock units thus representing the last episode of magmatism in the region.

A total of 45 million tons of zinc and copper ore have been extracted from the Matagami mining district. All the deposits except maybe the Phelps-Dodge occur within the lower Watson Lake Group of volcanics. On the southern limb of the regional anticline the Mattagami Lake (Latulippe, 1959; Jenney, 1961; Roberts, 1966, 1975; Roberts and Reardon, 1978), Orchan (Sharpe, 1964, 1968), and Bell Allard (Sharpe, 1964, 1968; Davidson, 1977) mines occur at the base of a single tuffaceous horizon called the Key Tuffite (Davidson, 1977). On the north limb, the New Hosco (Graham, 1960; Sharpe, 1968), Norita (Sharpe, 1968; MacGeehan, 1979; MacGeehan et. al., 1981), Garon Lake (Joklik, 1960; Sharpe, 1968; MacLean and MacGeehan, 1976; MacGeehan, 1979), Bell Channel (Sharpe, 1968; MacGeehan, 1979), and Radiore (MacGeehan, 1979; Bonavia, 1982) mines occur within several stratigraphic horizons.

The geology of the Matagami area has been studied for almost a century. The region was first investigated by Bell (1895,1900) during his stops at Matagami Lake on a trip down the Nottaway river system. Bancroft (1912) subsequently mapped the area and recognized the existence of the Bell River Complex. Freeman (1936) refined the mapping and outlined the principal geological elements of the district. This was followed by more detailed mapping (1 inch= 1 mile) by Longley (1943), Freeman and Black (1944), and Beland (1953).

Subsequent to the discovery of the Mattagami Lake deposit

in 1957 and most of the other deposits shortly thereafter, a large amount of economically oriented research was undertaken (Latulippe, 1959; Miller, 1960; Graham, 1960; Jenney, 1961). Sharpe in a remarkable feat of sientific investigation (1964, 1968) produced an excellent synthesis of the geology of the region. At this point the volcanic rocks overlying the complex were subdivided into a lower Watson Lake Group and an upper Wabassee Group.

A detailed study of the Watson Lake Group rocks on the north limb, east of the townsite was undertaken by MacGeehan and MacLean (MacLean and MacGeehan 1976; MacGeehan, 1978, 1979; MacGeehan and MacLean, 1981a,b). They established that the volcanic rocks in the group consist of a bimodal tholeiitic suite composed of basalt and rhyolite which manifest pseudo-calc alkaline chemical variation trends when hydrothermally altered. These trends are caused by the chloritization of rhyolites and silicification of basalts in the vicinity of volcanogenic massive sulfide deposits. They also demonstrated that the volcanic rocks and Bell River Complex are contemporaneous and probably co-magmatic.

1.4 NATURE AND PURPOSE OF STUDY

This study is undertaken as a research topic for a Master of Science degree and is part of an on-going research project on the geology of the Matagami district by the Department of Geological Sciences at McGill University. Field investigations were carried out during the summer of 1981 with

minor follow-up in 1982 and 1983. The work consisted of mapping part of Daniel township (see box in figure 1) around and to the west of the New Hosco mine. The area was chosen for several reasons: the rocks were thought to belong predominantly to the Wabassee Group which needed investigation on its stratigraphy and chemistry similar to that done on the Watson Lake Group by MacLean and MacGeehan; geological mapping westward from Matagami would tie in the geological setting of the Phelps Dodge deposit with the rest of the Mining district; recent lumbering operations over most of the area west of New Hosco mine permitted easy access for mapping; finally, the area contains up to twenty percent outcrop, which is exceptionally high for the Matagami district.

Geologic mapping was performed at a scale of 1:10000 and the final map has been printed at 1:20000. Most outcrops were visited and more than 200 rock specimens were collected. Over 125 thin sections were prepared of all the various rock types encountered in the field. In addition a total of 58 samples were powdered and pelletized, and chemically analyzed by X-ray fluorescence spectroscopy. Appendix 1 describes the sample preperation procedures and analytical techniques.

The goals of this study are multiple. The first and probably the most important goal is to produce a geological map of the thesis area. Special emphasis is placed on structural and stratigraphic relationships as seen in the field. No individual flows have been mapped, for instance,

due to insufficient outcrop. This is unfortunate but not serious because as a first step it is more important to get the broad distribution of rock units than to identify each flow. The chemistry of the Wabassee Group volcanic rocks in the thesis area is characterized and compared to that of the other volcanic rocks in the Matagami district and to volcanic rocks of the Blake River Group in Noranda.

Petrogenetic modelling of the Allard river volcanics is attempted using selected trace elements.

CHAPTER 2

GEOLOGY

2.1 GENERAL STATEMENT

The geology of the research area is presented on the map located in the pocket on the back cover of this report. A study of the map shows that the geology consists predominantly of felsic, intermediate, and mafic volcanic rocks of the Wabassee and Watson Lake Groups. The rocks are folded into a broad, upright anticline with east-west striking axial plane and gently westward plunging fold axis. Intrusive rocks comprise spilitic and gabbro-norite sills and stocks, felsic dikes and a diorite-tonalite pluton. Diabase dikes transect the area in a northeasterly direction. Table 1 shows the various lithologic units and their relative temporal position within the stratigraphy.

The rocks of the area have undergone little deformation and the metamorphic grade is often quite low. In the east, within the Watson Lake and Wabassee Groups, the rock units have been chloritized and carbonatized beneath the New Hosco orebody. Above the ore zone in the Wabassee Group, however, the metamorphic grade is in the prehnite-pumpellyite facies or zone 2 as defined by Jolly (1978) and increases gradually to greenschist facies (zone 3) to the west with amphibolite facies (zone 4) attained locally around the McIvor Hills (table 2).

Table 1: Table of Formations

Diabase dikes (north and northeast trending)

Tonalite-granodiorite

Basic dikes

Rhyolitic dikes

Wabassee Group
- Gabbro and gabbro-norite sills and stocks
- Rhyolite flow
- Mafic to intermediate flows and pyroclastic sediments and spilitic sills
- Sulfide-rich pyroclastic unit and New Hosco Deposit

Watson Lake Group
- Gabbro sills
- Pyroclastic sediments (Key tuffite)
- Rhyolitic flows (Watson Lake rhyolite)

In this chapter each rock unit in the area is described in terms of its macro- and microscopic characteristics. In addition, field and petrographic evidence is presented which relates the various units in a relative temporal framework.

2.2 PETROGRAPHY OF ROCK UNITS

Watson Lake Group

The Watson Lake Group is represented in the area by ryolitic flows intruded by gabbroic sills. These rocks are restricted to the eastern extremity of the map area around New Hosco bay. The felsic rocks underly the Wabassee Group and occupy, along with the Bell River Complex, the core of the

Table 2: Metamorphic-alteration mineral assemblages in the Wabassee Group lavas

	Zone 2* sub-greenschist facies	Zone 3* greenschist facies	Zone 4* amphibolite facies
modal color	light blue-green to light blue-grey	medium green	dark green to black
phenocrysts: alteration mineral assemblage	albite, clinozoisite, chlorite	albite, clinozoisite, chlorite, (sericite)	plagioclase, sericite
groundmass: alteration mineral assemblage	albite, clinozoisite, chlorite, prehnite, pumpellyite, calcite, leucoxene, (tremolite)	actinolite, albite, clinozoisite, chlorite, leucoxene, (sericite), (biotite)	hornblende, plagioclase, biotite, chlorite, (sericite)
amygdules: mineral assemblage	clinozoisite, calcite, chlorite, prehnite, pumpellyite, (zeolites in tuff)	clinozoisite, calcite, chlorite, (sericite)	epidote, chlorite, (sericite), (hornblende)
veins: mineral assemblage	clinozoisite, calcite, chlorite, prehnite, pumpellyite	clinozoisite, calcite, chlorite, (sericite)	epidote, (sericite)

* Zonal subdivision from Jolly (1978)
Minerals in parentheses are only occasionally present
All assemblages include quartz

regional anticline (Sharpe, 1968).

The southwestern contact of the Watson Lake Group is virtually unknown for lack of outcrop or drilling information. Along strike, to the southeast in the vicinity of Watson Lake, however, it's upper contact is known from drilling to correspond closely to the Key Tuffite (Sharpe, 1964, 1968). It is possible that this horizon extends as far northwest as the thesis area.

To the west the Watson Lake Group is seperated from the overlying succession by an interpreted north-south fault with considerable displacement. An actual fault surface has been identified by drill data and by sub-surface mapping only to the east of the New Hosco mine, beneath the Allard River (Sharpe, 1968). Elsewhere the interpretation of dip-slip faults is required by the orientation of flows and the trace of the fold hinge in the Wabassee Group.

The northern contact of the Group is not exposed but drill information shows that the rhyolite is bounded to the overlying group by an intervening tuffaceous horizon. This horizon may be equivalent to the Key tuffite around the Matagami Lake mine (Sharpe, 1968; Bernard, oral comm., 1983).

The lower or eastern contact of the Watson Lake Group is very poorly exposed but is thought to lie to the southeast, outside the map area. Drilling information and the few outcrops present suggest that gabbroic apophyses of the Bell River Complex are interlayered with rhyolitic rocks and become more and more abundant towards the east until the main body of

the Complex is reached (Sharpe, 1968).

Massive and brecciated rhyolite occurs on the north side of New Hosco bay, on the east shore of the Allard River, and near the intersection of the southeastern diabase dike with the airport highway.

In the latter locality, the rhyolite is exposed next to the dike. Here the rhyolite is fresh except for moderate shearing in one of two samples studied. Up to 15 percent quartz and plagioclase phenocrysts generally less than 2 mm in length are set in a fine grained matrix composed of quartz and albite. Spherulitic growth on quartz and plagioclase phenocrysts, granophyric grains, and common centers occurs in one sample (plate 3). Further to the southeast, adjacent to the road, samples collected indicate the common occurence of spherulitic development. Substantial alteration is limited to shear zones and consists of red or green biotite, sericite, and quartz in less than 0.5 mm wide veinlets which form an interlocking network between 2 to 4 mm sized "islands" of fresh rhyolite. Hornblende occurs in one section but the common metamorphic assemblage is sericite-biotite-albite-quartz.

To the northwest, in New Hosco Bay, the rhyolitic rocks are similar to those described above in terms of primary mineral assemblage, but have been moderatly chloritized and carbonatized (ferrodolomite). The outcrops are massive or brecciated and locally appear tuffaceous. In one sample inverted beta-quartz phenocrysts are mantled by thin platelets

of tridymite (plate 4). Granophyric grains are sometimes present but not abundant. Perlitic glass was found in one sample (plate 5). Plagioclase phenocrysts are slightly to completely altered to ferrodolomite or quartz. The groundmass is altered to an equigranular mosaic of quartz, chlorite, and ferrodolomite with local sericite development. Veins up to 5 mm in size of the above composition are present in one sample. Closely associated with the rhyolite is an equigranular, massive, siliceous rock of uncertain nature (possibly a tuff). The rock consists of a mosaic of quartz, albite, and chlorite grains less than one millimeter in size with abundant fine grained disseminated sericite. The distinctive character of this alteration is thought to be related in some way to the New Hosco ore deposit.

Wabassee Group

This group of rocks which includes lava flows and their associated sills and stocks overlie and may be locally interlayered with the Watson Lake Group. It forms a distinct chemical suite here called the Allard River Volcanics. Predominant presence of pillows are witness to its sub-marine origin.

At the base of the Wabassee Group near the eastern edge of the map, outcrop and drilling information around the New Hosco mine provides evidence that the mineralized, pyroclastic horizon containing the New Hosco deposit is interlayered with pillowed and massive spilitic andesite. In addition an

outcrop in New Hosco Bay (81c-169) composed of chloritized and carbonatized mafic lava and occuring stratigraphically below the ore zone is probably part of the Wabassee Group.

It is not known however if the mineralized horizon represents interlayering of the Watson Lake and Wabassee Groups or if the horizon represents a seperate hydrothermal event that occured during Wabassee volcanism. Absence of exhalative sediments elsewhere in the thesis area argues in favor of the former hypothesis. Alternately the mineralization could be derived from exhalations emanating from a seperate but laterally correlated volcanic edifice located in the Wabassee Group to the east of the thesis area around the Bell River.

Allard River Volcanics

In this category are included pillowed and massive, mafic to intermediate (i.e. basalt to dacite) flows and their associated hyaloclastic sediments derived by the process of emplacement of the volcanic rocks. In addition the fine-grained spilitic sills are included because they are difficult to distinguish from the volcanic flows except where the sills are thicker and their grain size larger.

The predominant lithology consists of pillow lava. The rock is generally light greyish-blue to green in color except in the west where it is black. Pillows are usually well developped and vary in size from a few tens of centimeters to lobes 3 to 5 m wide and 1 or 2 m high. Hollow pillow cores

partly filled with quartz (geopetals) are occasionally present. Chilled pillow margins are about 1 to 3 cm wide (plate 6). Interpillow material is mainly hyaloclastic tuff and breccia (plate 7) with angular pillow fragments of variable size. The hyaloclastic matrix to the breccia and tuff consists of angular glass shards generally less than a few mm in size but which may locally attain cm sizes.

Pillow breccia also occurs intercalated with the pillow lava. Here the breccia is composed of rounded to angular chilled pillow fragments (of varying size and abundance) set in a hyaloclastic or rarely tuffaceous matrix (plate 8). The exact relation of the pillow breccia to the pillow lava is not generally known due to lack of outcrop. Where outcrop is more abundant, however, the pillow breccia occurs at the top of the flow. On the south side of McIvor Lake for example, three entire flows are observed. The lower one-half of each flow is composed of massive basalt. The upper part of the flow is either all pillow basalt or pillow basalt overlain by up to an equal thickness of hyaloclastic breccia.

The pillowed facies is separated from the massive facies in the field on the basis of dominant lithology within a given area. It may be that areas of predominant massive facies simply contain thicker flows. More detailed mapping in specific areas should help to elucidate this problem.

The pillow lava is often aphyric but usually contains up to 5 percent plagioclase, and locally clinopyroxene or altered orthopyroxene phenocrysts less than 1 mm in size. These are set in a fine grained groundmass composed of albite microliths

and devitrified glass. Spilitization of the rock precludes proper identification of the plagioclase phenocrysts. Quartz is invariably present in the groundmass but rarely can it be shown to be primary.

Amygdules are usually present, especially close to the rim of pillows. These vary in size (0.3 to 10 mm) and abundance (1 to 20 %). The usual amygdular phases are quartz, chlorite, calcite, and clinozoisite, but pyrite (or pyrrhotite), prehnite, and pumpellyite are common in the eastern part of the map (plate 9).

The rock is generally altered to a spilitic assemblage. Plagioclase phenocrysts are replaced by epidote, chlorite, sericite, and quartz (plate 10); clinopyroxene is altered to actinolite (locally hornblende), epidote, chlorite, and leucoxene (plate 11); and the groundmass is a fine-grained, randomly oriented sub-assemblage of the following minerals: amphibole, albite, chlorite, epidote, quartz, sericite, biotite, prehnite, pumpellyite, and calcite.

Although the mineralogy of the rock is very different from the primary or volcanic assemblage, and significant hydration has occured (see LOI's in appendix 2), the primary volcanic textures of the rocks have been preserved. The outlines of altered phenocrysts are generally sharp. In addition, the groundmass often contains abundant swallow tailed albite microliths suggesting that alteration did not involve appreciable migration of components. Where obviously altered, as for instance in some of the hyaloclastic breccias, the rock

turns to an apple-green colour, and most of the volcanic textural components have been altered to a granular aggregate of quartz and epidote.

The massive facies of flows and the thin sills known to intrude the pillow lava are petrographically identical to the pillowed rocks. Amygdules up to 3 millimeters in diameter may even be present in the sills suggesting shallow emplacement and water depth.

A definite pro-grade metamorphic zonation is observable from east to west in the Wabassee Group. Throughout most of the area these rocks are metamorphosed in the subgreenschist (zone 2) facies (Jolly, 1978) (see table 2). In the vicinity of the McIvor Hills, at the western end of the map area, however, the rocks are in the greenschist (zone 3) and amphibolite (zone 4) facies. The highest metamorphic grades are recorded adjacent to the gabbro-norite stock and to the southwest in the dacitic and rhyolitic flows.

Good evidence exists in thin-section showing that zone 3 and zone 4 assemblages were overprinted on that of zone 2. Close to the assumed southern margin of the gabbro-norite stock, prehnite bearing amygdules have been altered to chlorite and clinozoisite (plate 12). The prehnite has been obliterated but its crystal form is preserved and its sweeping extinction, a characteristic of prehnite bundles, is still visible. Jolly (1978) considers that zone 3 and zone 4 assemblages are almost invariably related to contact metamorphism around igneous plutons. This is perhaps too broad a generalization, as the amphibolite facies in the Mont

Laurier area northeast of Matagami appears to be unrelated to any intrusion (MacLean, pers. commun.). Evidence for contact metamorphism can be found on the north side of North McIvor Hill where lava flows, which are correlative with flows containing zone 3 and 4 assemblages located on the south side of the mountain close to the gabbro-norite stock, contain prehnite and are therefore in the subgreenschist (zone 2) facies. These rocks are located on either side of the hinge of the regional anticline and are consequently eroded to the same structural level. It seems likely in this case that the higher metamorphic grades here were caused by syn-volcanic plutonism.

In the northeastern sector of the map, on both sides of the Allard River, variolitic lavas are present. These lavas are mostly pillowed and resemble pillowed flows found elsewhere in the thesis area except for the abundance of circular to oval, light green coloured varioles 0.5 to 3 cm in size set in a dark green matrix. The varioles may be scattered randomly through the rock or concentrated close to the pillow margins. They range in concentration from a few percent to more than three quarters of the rock.

It is interesting to note that these variolitic rocks are associated with the only tholeiitic flows in the Wabasee Group in the map area (MacLean, unpublished data). This is probably not fortuitous and may reflect a fundamental relationship between variolitic lavas and tholeiitic volcanism.

Pyroclastic Sediments

Pyroclastic sedimentary rocks are generally rare in the Wabassee Group within the map area. They are present, however, in the central and north-central part of the map in the vicinity of McIvor Lake. Also, thin beds of fine-grained tuff and chert are locally intercalated with the pillow lavas.

The best exposed horizon occurs in the center of the map, north of the Phelps-Dodge road. The pyroclastic flow is about 200 m thick and discontinuously exposed over a distance of two km (see map in back pocket and figure 2). At its northeast end the flow is composed of breccia with angular mafic to intermediate volcanic fragments generally less than 30 cm in size in a matrix of lithic tuff. Fragment boundaries are sharp and rarely if ever chilled.

Towards the southwest the breccia gives way to a lapilli tuff. Here the rock is composed of rounded accretionary lapilli less than 2 mm in size set in fine-grained palagonitic groundmass (plate 13). Amygdule-like structures filled with well crystallized plagioclase suggest some lithic volcanic fragments may be present.

The rock has been strongly hydrated and alteration phases include albite, clinozoisite, calcite, prehnite, pumpellyite, and palagonite. In addition, zeolite minerals, in a unique occurence in the thesis area, are abundant in a thin-section of the lapilli tuff.

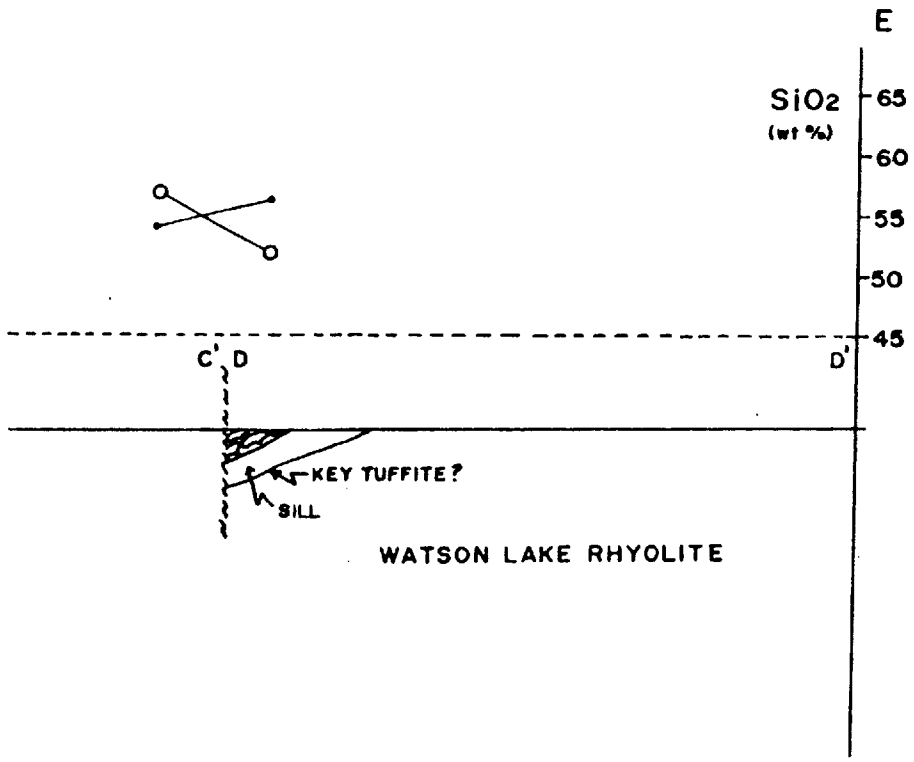
Although the pyroclastic rocks tend to be hydrous, the plagioclase phenocrysts have undergone only minor alteration.

ONALITE INTRUSION

ORPHYRITIC SILL

YROCLASTIC FLOW

ILLOWS



These tend to be slightly turbid but original twinning planes are preserved.

Deformation has produced a weak penetrative schistosity. In thin-section, however, no deformation is visible: no tectonic fabric was observed and the accretionnary lapilli and amygdules are circular.

The unit as a whole is not well exposed but those outcrops which have been studied indicate a southwestward decrease in fragment size suggesting that the source of the volcanic material was to the northeast.

Pyroclastic sediments are fairly abundant, but not well exposed around McIvor Lake. They look a lot like the sediments described above, but differ mainly by the presence of a moderate to well developed schistosity.

Acid Volcanic Rocks

Acid volcanic rocks including rhyolite and agglomerate are exposed on the southeastern slope of north McIvor Hill. These rocks are distinguished from the mafic to intermediate lavas by quartz phenocrysts. The unit which occurs in two outcrops is roughly 25 m thick, strikes northwest and is probably offset by a northwest striking fault. Although contacts are not well exposed the unit appears to be conformable with underlying and overlying pillowed flows. It is bounded on the west by a gabbro-norite stock and to the east by a major north-south dextral fault.

The agglomerate occurs in close proximity to the massive facies and is composed of angular to sub-rounded, mixed mafic and felsic volcanic fragments generally less than 30 cm in size, set in a tuffaceous matrix comprising 20 to 40 % of the rock (plate 14, 15). Pyroclastic textures in the groundmass have been obliterated during contact metamorphism related to the emplacement of the gabbro-norite stock. The matrix is presently an aggregate of hornblende, biotite and quartz. The mafic clasts possess similar mineralogy and texture to the mafic and intermediate lavas. The rhyolite fragments on the other hand comprise 10 % beta-quartz and albite phenocrysts less than 1 mm in size set in a fine-grained equigranular matrix composed of quartz and feldspar (plate 16).

Gabbro-Norite and Gabbro Intrusions

Quartz bearing gabbro-norite intrudes all the volcanic rocks of the Wabassee Group. Intrusions occur to the south of Wabassee Lake and in the vicinity of North and Middle McIvor Hills. The intrusive bodies are generally sill-like in form with sub-concordant attitudes and range in thickness up to 100 m. One intrusion on the southeast slope of North McIvor Hill is stock shaped with a sill-like extension to the northwest. The size of the stock is estimated between 1 and 2 km in diameter; paucity of outcrop precludes a better estimate. Another stock occurs on the eastern slope of Middle McIvor Hill; the size of the intrusion is not known because only the western contact is exposed. The gabbro-norite ranges in

colour from light blue-green south of Wabassee Lake to medium green around McIvor Hill. The colour is darker in the west of the map where the metamorphic grade is higher.

In thin-section the rock is very massive and equigranular with a grain size of about 1 to 2 mm. Phenocrysts of orthopyroxene, clinopyroxene, and plagioclase ranging in size from 2 to 4 mm form up to 25 or 30 % of the rock (plate 17). Quartz and granophyre are common as interstitial phases and sphene is present in minor amounts (less than 3%). The groundmass is intensely altered to actinolite, epidote, sericite, and quartz. Plagioclase phenocrysts are strongly to totally altered to sericite while orthopyroxene crystals are replaced by fibrous antigorite, chlorite and actinolite. The clinopyroxene phenocrysts in the sill close to Wabassee Lake are generally fresh but may be weakly altered to chlorite, epidote and quartz and often rimmed by pale green actinolite (plate 17). In contrast, the clinopyroxenes in the intrusions close to North McIvor Hill are invariably pseudomorphed by actinolite (plate 18); only in a sample from a chilled margin of the stock is primary clinopyroxene observed.

Tholeiitic gabbro sills intrude the Watson Lake Group and the eastern or lower part of the Wabassee Group. These sills are absent from the rest of the thesis area. A good example of this rock type occurs on the east side of the Allard River near the bridge. In outcrop the gabbro is dark green to black, massive, and equigranular with a mean grain size of 2 to 3 mm. The rock presently contains 20 %

hornblende, 30 % plagioclase, 15 % chlorite, 15 % pistacite or clinozoisite, 10 % carbonate, 5 % quartz, and 5 % altered skeletal magnetite crystals (visual estimate from thin-sections).

Rhyolite dikes

Rhyolite dikes intrude intermediate flows south of the main road in the western part of the map area. South McIvor Hill contains several dikes ranging in thickness from a few m to about 10 m. Grey in color, the rhyolite consists of beta-quartz (5%) and albite (25%) phenocrysts less than 2 mm in size distributed throughout a fine-grained groundmass. Metamorphic hornblende is randomly distributed in the groundmass. Thin prehnite-clinozoisite bearing veinlets transect the rhyolite.

A 3 m thick rhyolite dike cuts pillowed andesite about 100 m south of the main road southeast of North McIvor Hill (outcrop 82c-02). The dike rock is equigranular and composed of quartz and albite grains about 1 mm in size. The dike is chilled against the andesite and at the contact, in a zone about 5 mm thick micrographic intergrowth of quartz and feldspar is apparent indicating eutectic crystallization. Chemical evidence will be presented in the next chapter to show that this dike is not related to the dikes on South McIvor Hill or the rhyolite flow close to North McIvor Hill.

Thin Basic Dikes

Two varieties of black, fine-grained gabbro dikes intrude the volcanic rocks and the gabbro-norite. The dikes range in thickness from a few cm to a few m. In one variety, 10 % clinopyroxene and altered plagioclase phenocrysts 1 to 2 mm in size occur in a felted, fine-grained groundmass composed of albite, clinopyroxene, and actinolite (plate 19). The clinopyroxene is pristine while the plagioclase is altered to an assemblage of chlorite and albite. The altered grounmass of the rock contains calcite, sericite, chlorite, quartz, and clinozoisite.

The second type of mafic dike contains clinopyroxene and plagioclase phenocrysts in an equigranular matrix composed of euhedral, brown pleochroic hornblende crystals less than 0.4 mm in length, generally overgrown by actinolite (plate 20). The plagioclase phenocrysts are altered to chlorite, calcite, epidote, and quartz. Clinopyroxene is weakly altered to calcite and epidote.

The relationship between the two types of mafic dikes is not known. They are classified together because of their similar field characteristics.

These basic dikes have not been identified on the geologic map (figure 2) because of their rarety and small size. They were observed at stations 81c-043, 81c-047, 81c-077, 81c-114, and on the north slope of North McIvor Hill.

Basic dikes are also observed on South McIvor Hill where they intrude the rhyolitic dikes.

Tonalite Intrusions

An oval shaped stock of tonalite (quartz-diorite) is present on the western slope of North McIvor Hill and extends beyond the western limit of the map. Estimated size of the intrusion is 0.5 by 1.0 km but this estimate is a minimum due to the absence of outcrops on the western side. A fine-grained pink rock interpreted to be a chilled margin suggests that the tonalite is younger than the volcanic rocks.

The tonalite is variable in appearance in the two principal outcrops studied indicating that more than one intrusive phase may be present. In one example (81c-181) the rock consists of an equigranular mosaic of interlocking plagioclase crystals up to 2 mm in size with interstitial quartz, hornblende, biotite, and minor pistacitic epidote and sphene (plate 21). Graphic intergrowth of quartz and plagioclase is common. Where this occurs the granophyre is located in interstices between plagioclase crystals.

Alteration in the rock is restricted to sericitization of the more calcic cores of the plagioclase, and partial chloritization of biotite (plate 22). Clinopyroxene when present may be rimmed by hornblende.

Mafic xenoliths up to 30 cm in size may form up to 5 % of the rock (plate 23). These are composed of equigranular clinopyroxene, plagioclase and hornblende with minor biotite and quartz and a trace of apatite. No volcanic textures are preserved so that the origin of the xenoliths is uncertain.

There are no contact relationships between the tonalite and the gabbro-norite so the relative ages of the two units is unknown. The tonalite is very similar petrographically, however, to the dioritic phase of a granodiorite pluton located northeast of the town of Matagami (MacGeehan, 1979). The intrusion in question is known to truncate both the volcanic rocks and gabbro dikes and sills and hence is younger. As shown later, geochemical evidence indicates the gabbro-norite is co-magmatic with the mafic to intermediate lavas. If this is the case then the tonalite represents a later phase of intrusion and is consequently younger than the gabbro-norite intrusions.

Diabase Dikes

Three northeast striking, steeply dipping diabase dikes are present in the map area. The dikes range in thickness from 10 to 200 m but average 30 m. The dikes are magnetic and prominent on aeromagnetic maps. These maps suggest that the dikes which, like the other units, are poorly exposed are nonetheless continuous over many tens of kilometers. The dikes transect all other rock types and possess a 1 to 2 m chilled margin wherever the contacts are exposed. These dikes represent the last phase of magmatism in the area.

In outcrop the rock is black and weathers brown and grey. Grain size is quite uniform and averages 3 to 4 mm except in the chilled margins where the diabase is fine-grained. The central part of the dike consists of interlocking plagioclase crystals with interstitial clinopyroxene and magnetite (plate

24). Quartz and granophyre are usually present as an interstitial phase. Plagioclase crystals are well zoned and range in composition from An52 to An58 in the cores, to An40 in the rims. Zoning is also present but not as well developed in the clinopyroxene. The rock is very magnetic due to the abundance (5 to 10 %) of skeletal magnetite grains. The modal composition of the rock is presented in Table 3.

Table 3: Mean modal composition of diabase (visual estimate)

	pl	cpx	hb+bio	mag	qtz	granophyre
%	50-55	30-35	5-10	5	3	2

Alteration of the rock is generally very weak. Clinopyroxene is locally altered (especially along cleavage) to biotite, hornblende and chlorite. Plagioclase cores are occasionally sericitized. In one sample from a chilled zone, the plagioclase is completely altered to sericite.

2.3 STUCTURAL GEOLOGY

The rocks located within the thesis area have undergone one phase of ductile deformation and at least three phases of faulting. The whole stratigraphy has been folded into an upright anticline with an east-west striking axial surface and gently westward plunging fold axis. The rock units were subsequently displaced by northeast, northwest, and north trending faults.

Evidence for folding comes from direct field observation because bedding measurements taken on pillows are so imprecise as to give a random distribution when plotted on a stereonet.

Faults are infered from topographic lineaments and stratigraphic requirements. On regional scale air photographs a number of lineations are present incating discrete fault structures.

East of the Allard River, the position of the anticlinal hinge line is not known due to lack of outcrop but is inferred to be half way between the north and southwest contacts of the Watson Lake and Wabassee Groups. This is also the location where Sharpe (1968) puts the hinge zone.

West of New Hosco Bay all the volcanic flows are oriented east-west, face north, and dip steeply towards the north. This interpretation is in contradiction with Sharpe (1968) who interpreted these flows as south facing. Recent lumbering and consequent improvement in outcrop quantity and quality permit a confident interpretation to be made. These rocks have

therefore been displaced in a left-lateral motion across a fault located at the west end of New Hosco Bay (see map in back pocket).

Very shallow dipping flows in the central sector of the map close to outcrops 81c-017 and 81c-135 suggest that the hinge line is near. In outcrop 81c-135 pillows face straight upward on several different surfaces. Also, a few geopetals observed as open cavity fillings in the center of pillows are nearly horizontal.

Close to the McIvor Hills, in the west end of the map area, good field evidence suggests that the hinge line has been displaced to the north by approximatly 2 km. Around North McIvor Hill all the rocks strike northwest, face southwest, and dip towards the southwest at about 60 degrees. On the north side of the hill about one kilometer north of 82c-18, pillows are definitly facing north (figure 3), and a little further south the pillows are oriented north-south, face west, and dip westerly at intermediate angles.

Several generations of faulting appear to be present in the thesis area although the relative ages of only three are known. The oldest faults are located in the east, are oriented towards 010 degrees, and are sinistral or dextral. Vertical displacement cannot be estimated but may be significant.

In the central sector a 010 degree fault is displaced sinistrally by about 1.5 km by a northwest striking fault. This fault is thought to be of the same age as the major dextral fault located to the east of North McIvor hill but no

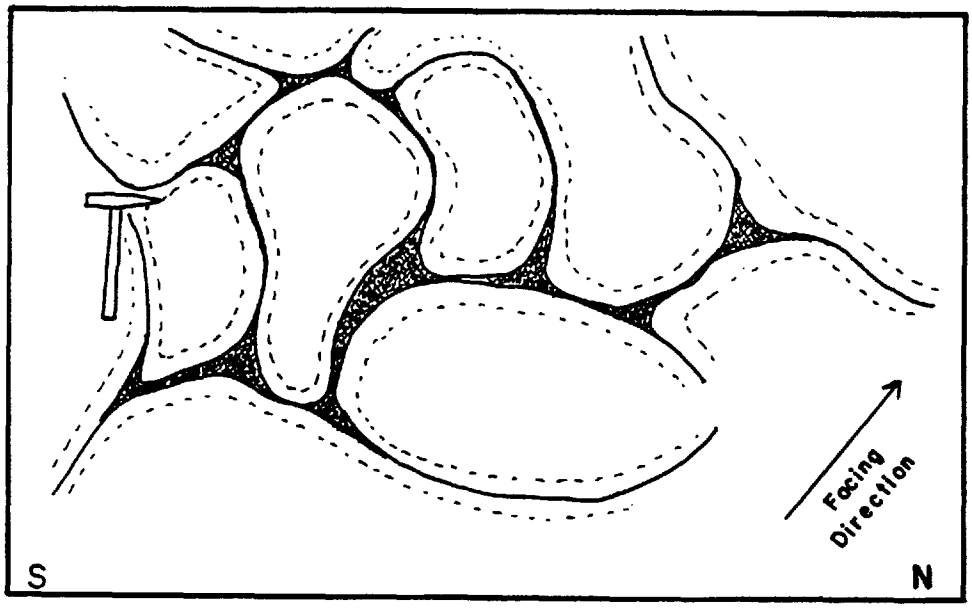


Figure 3: Sketch of vertical outcrop looking towards west. Site located north of North McIvor hillnear station 82c-18.

field evidence confirms this hypothesis.

Finally, on the south shore of McIvor Lake a north striking (350 degrees) dextral fault with a displacement of about 100 m cuts a diabase dike. This dike is not offset by the dextral fault on the east of North McIvor Hill implying that the 350 degree fault is younger.

Plate 1: Photograph of outcrop 81c-017 looking to the southeast. The Phelps-Dodge road crosses the middle of photograph.

Plate 2: Similar scene as plate 1. Note the extent of deforestation.

Plate 3: Photomicrograph of Watson Lake Group spherulitic rhyolite. Plane light. Grey spherules mantle white beta-quartz phenocrysts. Dark phase is mainly hornblende. Sample 82c-23. Scale in mm.

Plate 4: Photomicrograph of Watson Lake Group rhyolite. Plane light. Thin platelets of tridymite mantle beta-quartz phenocrysts. Groundmass is chloritic. Sample 81c-133. Scale in mm.

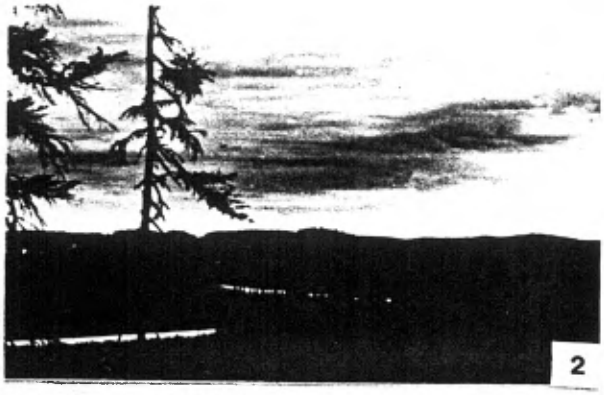
Plate 5: Photomicrograph of Watson Lake Group rhyolite. Plane light. Oval structures represent devitrified perlitic glass. Note the beta-quartz phenocryst at the center of a perlitic structure. Rock has chloritized (dark grey phase) and carbonatized (lower right corner). Sample MAT80-18. Scale in mm.

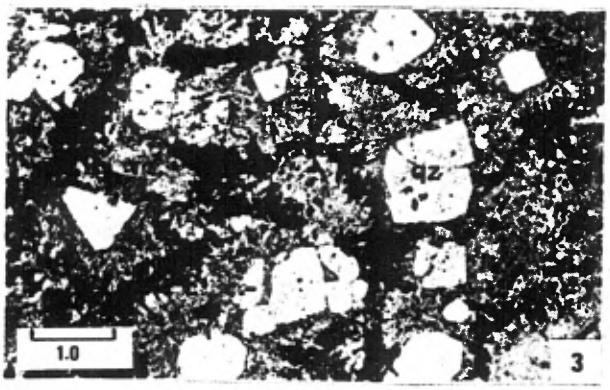
Plate 6: Photograph of pillowed outcrop close to station 81c-004. Pillow selvages are replaced by quartz and epidote and are resistant to weathering.

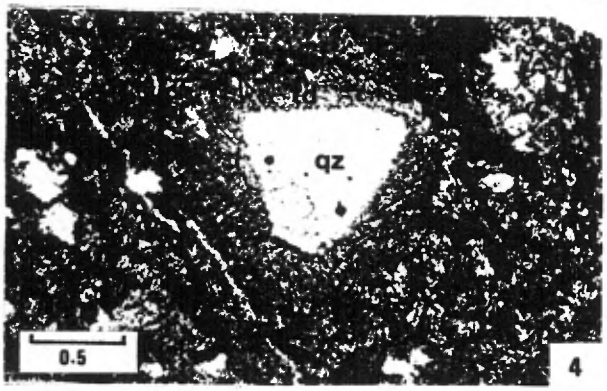
Plate 7: Close-up photograph of hyaloclastic tuff near station 81c-135. Rock consists of angular ,glass' fragments (recessive) surrounded by diagenetic quartz (prominent).

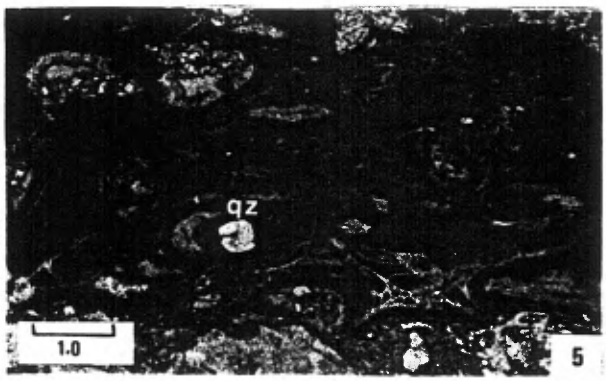
Plate 8: Photograph of pillow breccia outcrop

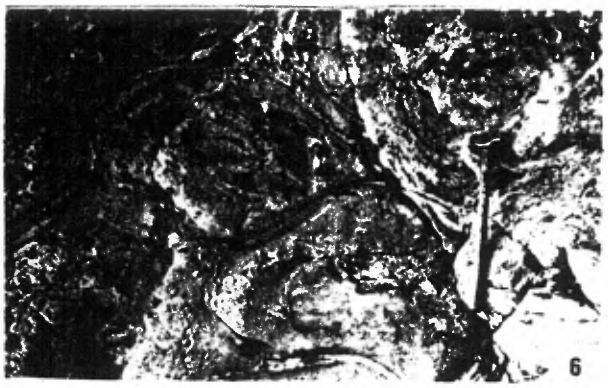

1

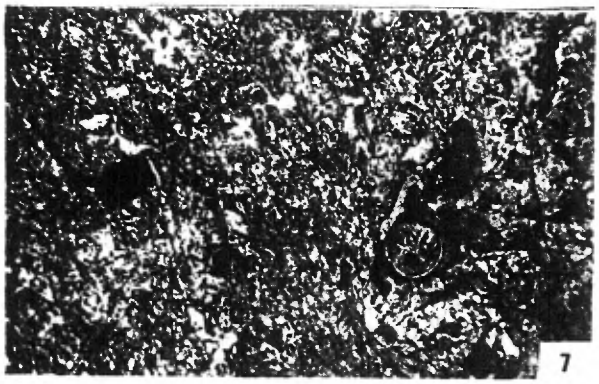

2


qz
1.0
3


qz
0.5
4


qz
1.0
5


6


7


8

Plate 9: Photomicrograph of prehnite-clinozoisite bearing amygdule in andesite. Crossed nichols. Note the characteristic habit and extinction of prehnite rosettes. Sample 81c-056a. Scale in mm.

Plate 10: Photomicrograph of plagioclase phenocrysts in andesite. Plane light. Phenocrysts are typically altered to albite chlorite and clinozoisite. Sample 81c-093. Scale in mm.

Plane 11: Photomicrograph of clinopyroxene in basalt. Plane light. Pyroxene (high relief) has been altered to chlorite and actinolite. Sample 81c-028b. Scale in mm.

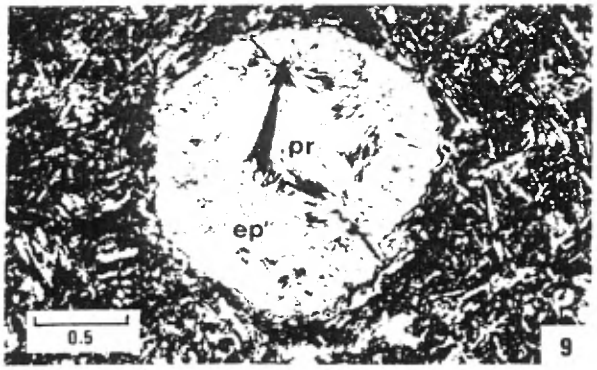
Plate 12: Photomicrograph of altered prehnite bearing amygdule. Plane light. The prehnite has been totally altered to chlorite and clinozoisite but the original radiating habit is preserved proving that high metamorphic grades were overprinted on lower grades. Sample 81c-111. Scale in mm.

Plat 13: Photomicrograph of accretionary lapilli tuff. Plane light. Pyroclastic sediment contains plagioclase phenocrysts, small accretionary granules (see rounded structures with dark-grey cores), and quartz-calcite-zeolite amygdules. Also present but not shown are angular lapilli. Sample 81c-062. Scale in mm.

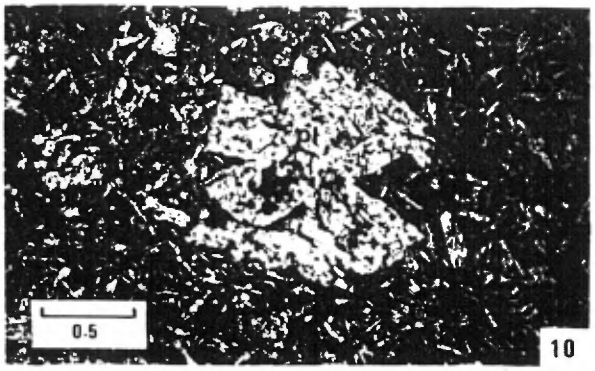
Plate 14: Photograph of Wabassee Group rhyolite breccia. Station 81c-023. Pyroclastic breccia contains both acid and basic volcanic fragments.

Plate 15: Close-up of outcrop shown in plate 14. Note the well defined acidic but poorly defined basic fragments.

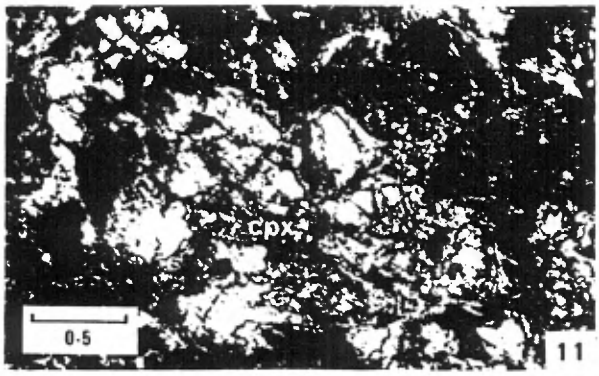
Plate 16: Photomicrograph of acid fragment from outcrop shown in plate 14. Plane light. Beta-quartz phenocryst is set in quatzo-feldspathic groundmass. Fragment boundary is located left of center.



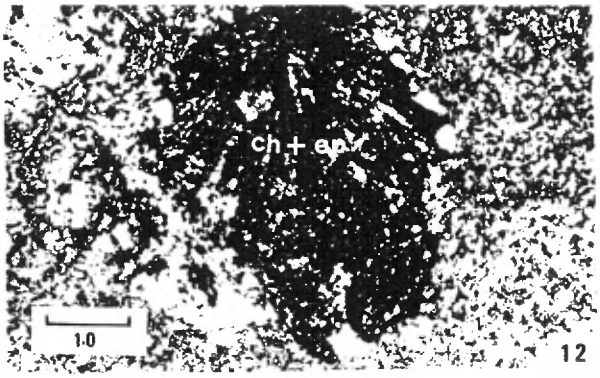
9



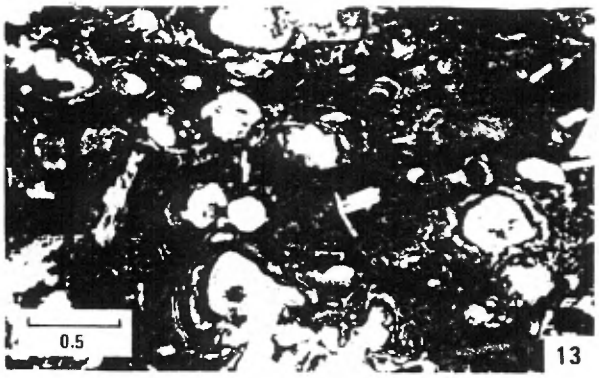
10



11



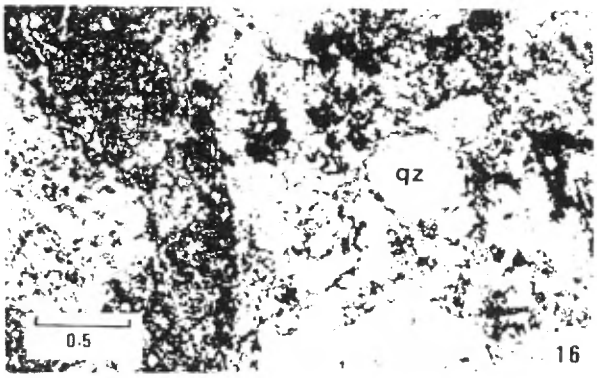
12



13


14


15



16

Plate 17: Photomicrograph of gabbro-norite. Plane light. Rock is altered and hydrated as shown by antigorite pseudomorph after orthopyroxene (top right of center, oriented towards 020 degrees). Clinopyroxene is only slightly altered to tremolite-actinolite (high relief phase left of center). Sample 81c-132. Scale in mm.

Plate 18: Photomicrograph of gabbro-norite metamorphosed to higher grade than in plate 17. Plane light. Orthopyroxene is altered to antigorite and clinopyroxene is almost totally altered to actinolite. Sample 81c-020. Scale in mm.

Plate 19: Photomicrograph of basic dike. Plane light. Rock consists of slightly altered clinopyroxene phenocrysts (center) in a very fine-grained felted groundmass. Plagioclase phenocrysts (not shown) where present are invariably altered to chlorite. Sample 81c-043. Scale in mm.

Plate 20: Photomicrograph of hornblende-rich basic dike. Plane light. High relief phase in center of field is remnant clinopyroxene. Dark, stubby crystals in groundmass are brown pleochroic hornblende. Sample 81c-114b. Scale in mm.

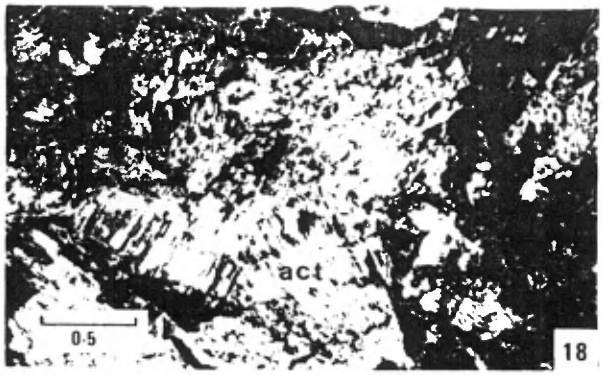
Plate 21: Photomicrograph of tonalite. Plane light. Rock composed of plagioclase (fresh rims and turbid cores), clinopyroxene (high relief), and quartz (white interstitial phase). Sample 81c-181. Scale in mm.

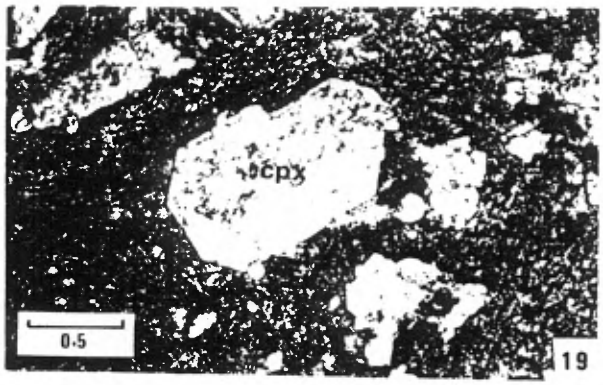
Plate 22: Enlarged view of plate 21. Plane light. Note turbid calcic cores of plagioclase crystals and fresh rims.

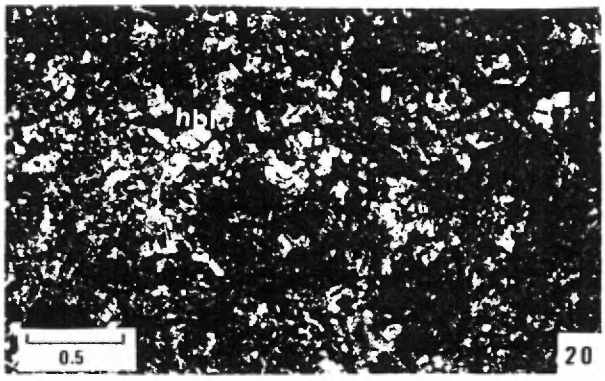
Plate 23: Photograph of outcrop 81c-182. Basic xenolith (basalt ?) in tonalitic host. Outcrop contains about 10% xenoliths.

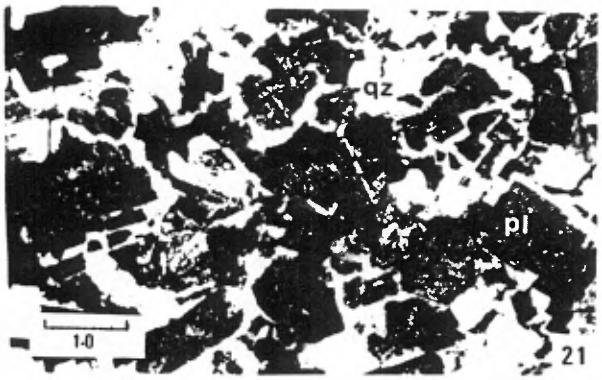
Plate 24: Photomicrograph of diabase. Crossed nichols. Rock composed of plagioclase crystals with interstitial clinopyroxene (high relief) and quartz. Sample 81c-177c. Scale in mm.

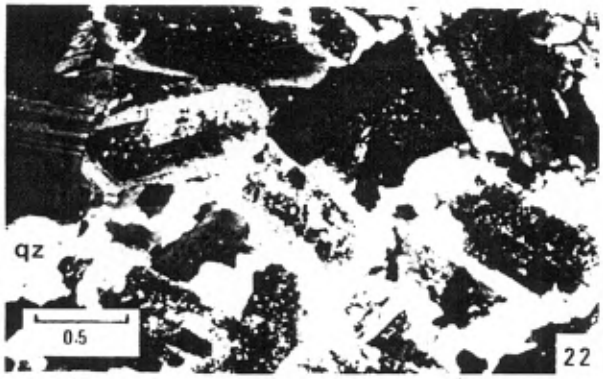

opx
0·5
17

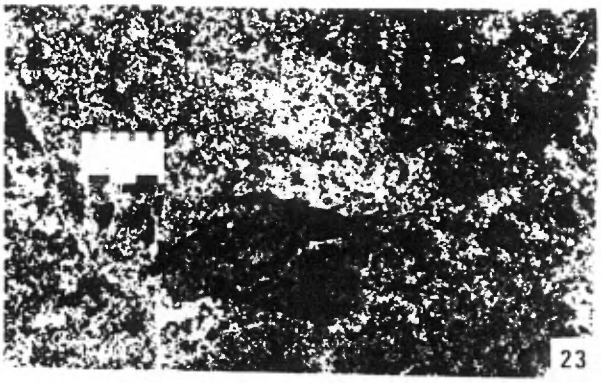

act
0·5
18

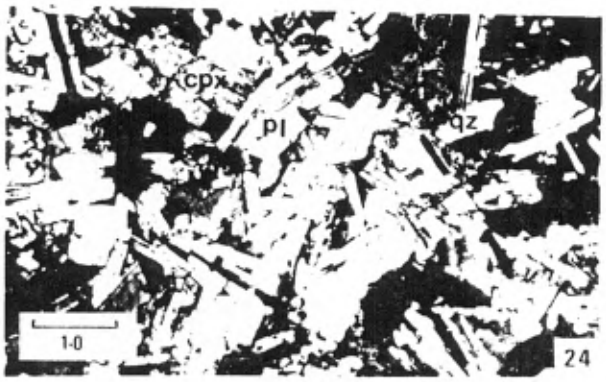

cpx
0·5
19


hbl
0.5
20


qz
pl
1·0
21


qz
0.5
22


23


cpx
pl
qz
1·0
24

CHAPTER 3

GEOCHEMISTRY

3.1 GENERAL STATEMENT

A total of 58 samples chosen among those described in thin-section were crushed and pelletized. These are divided among different rock units as follows:

Allard River volcanics	38
Gabbro-norite	7
Watson Lake rhyolite	3
Diabase	3
Rhyolite dikes	2
Basic dikes	2
Tonalite	1
Tholeiitic gabbro dike	1
Total	58

The chemical analyses were done to obtain a preliminary estimate of the chemistry of all rock units on the one hand and a more detailed view of chemical variations within the Allard River volcanic suite.

Where possible only samples with good preservation of magmatic textures were chosen so as to minimize alteration effects. Sampling of the Allard River volcanics was based on two additional criteria: (1) presence of large stable mineral assemblages and consequent large number of immobile components (Korzinskii, 1957; Gelinas et al., 1982), and (2) absence of secondary volume change (i.e. absence of veins or amygdules).

Samples were analysed for 10 major and 5 minor elements. The results are tabulated in appendix 2. Precision and

accuracy determinations are shown in appendix 3.

Three samples of Allard River volcanics were also selected for rare earth element determinations by instrumental neutron activation analysis at Universite de Montreal. These results are presented in appendix 4.

3.2 Effect of alteration

As shown in the last chapter, the Allard River volcanics frequently contain spilitic mineral assemblages. Their spilitic character suggests that secondary chemical processes may have acted on the rocks to alter their primary magmatic chemical signature. This problem is presently assessed.

A review of available litterature on elemental mobility in spilites indicates that gains and losses of elements are highly variable so that only general conclusions on the relative mobility of specific elements are possible (Table 4). The major oxides most likely to move significantly during spilitisation are -SiO2, -Al2O3, +Fe2O3, -FeO,-CaO, -Na2O, +K2O, and +MnO . Of these K2O is considered particularly mobile. It seems that other components, particularly TiO2, Zr, Y, Nb and the REE are immobile except at high water/rock ratios (Condie et al., 1977; Finlow-Bates and Stumpfl, 1981; MacGeehan, 1979).

The behavior of alkaline, high field strength (HFS) and rare earth elements (REE) during progressive alteration of pillows in the Blake River Group was studied by Ludden et al. (1982). Results of this study are summarized in table 5.

Table 4: Summary of alteration studies on spilitic rocks

	Myashiro et al., 1969	Hart R.A., 1970	Hart and Nalwalk, 1970	Hekinian, 1971	Shido et al., 1974	Hart et al., 1974	Vallance, 1974	Aumento et al., 1976	Condie et al. 1977 Epidote	Condie et al. 1977 Chlorite, carbonate	Gélinas et al., 1982	Generalizations
SiO_2		-		-		-	--	-	-		N.C.	-
Al_2O_3		+/-		-		-	-	-	-			-
Fe_2O_3		++		++	+	++		+Fe	+	-	V.M.	+
FeO	-	-		-	-	-			-	+	M.	-
MgO		-		+/-		+/-			-		M.	+/-
CaO		--		-		-	--	-	+	-	V.M.	-
Na_2O		+	-	-		+/-			-	-	M.	-
K_2O		++		++		++	+	+	-		V.M.	++
TiO_2	+	++	+	-	+	-	N.C.		-		N.C.	+/-
P_2O_5	+	++	-	N.C.	+	+/-			-		N.C.	+/-
MnO	+	+	-	+		++			-	-		+
Zr							N.C.		-	N.C.		N.C.
Y							N.C.			+		N.C.
Sr							+		+	-		+/-
Rb							+		-			+/-
Nb							N.C.		-	+		+/-
LREE									N.C.	+		N.C.
HREE										N.C.		

\+ Gain in rock ++ Large gain in rock
\- Loss in rock -- Large loss in rock
+/- Minor gain or loss in rock
N.C. No change M. Moderatly mobile V.M. Very mobile

Here Zr/Y and Zr/Ti ratios are virtually unnafected by secondary processes even at high water/rock ratios. REE's are immobile at low water/rock ratios but can move at high ratios.

Table 5. Result of alteration of pillows in Blake River Group, Abitibi greenstone belt. From Ludden et al. (1982).

water/rock ratio	alkaline elements	HFS elements	REE
low	mobile	immobile	immobile
medium	Sr less		
high	V.mobile	Mobile Zr/Ti,Zr/Y constant	mobile

Large scattering of points on Na2O, K2O vs SiO2 diagrams, and to a lesser extent on CaO vs SiO2 (figure 4a,b) suggest these elements were mobile during spilitization. Samples are plotted on a Hughes diagram in figure 5 to evaluate alteration. As can be seen, most points fall near or within the igneous spectrum. On the other hand, tie lines joining centers and rims of pillows show that considerable change in K2O and Na2O has taken place.

FeO and CaO are plotted against Zr in figures 6a, and b. Correlation of FeO with Zr is better than CaO with Zr. Tie lines joining center and margin of pillows are longer in CaO vs Zr (figure 6b). Fractionation cannot produce this feature because tie lines in figure 6a are very short. Note also that the tie lines are close to vertical again implying constant degree of fractionation. Diagrams of this type indicate that Na2O, K2O, CaO, Rb, and Sr are mobile.

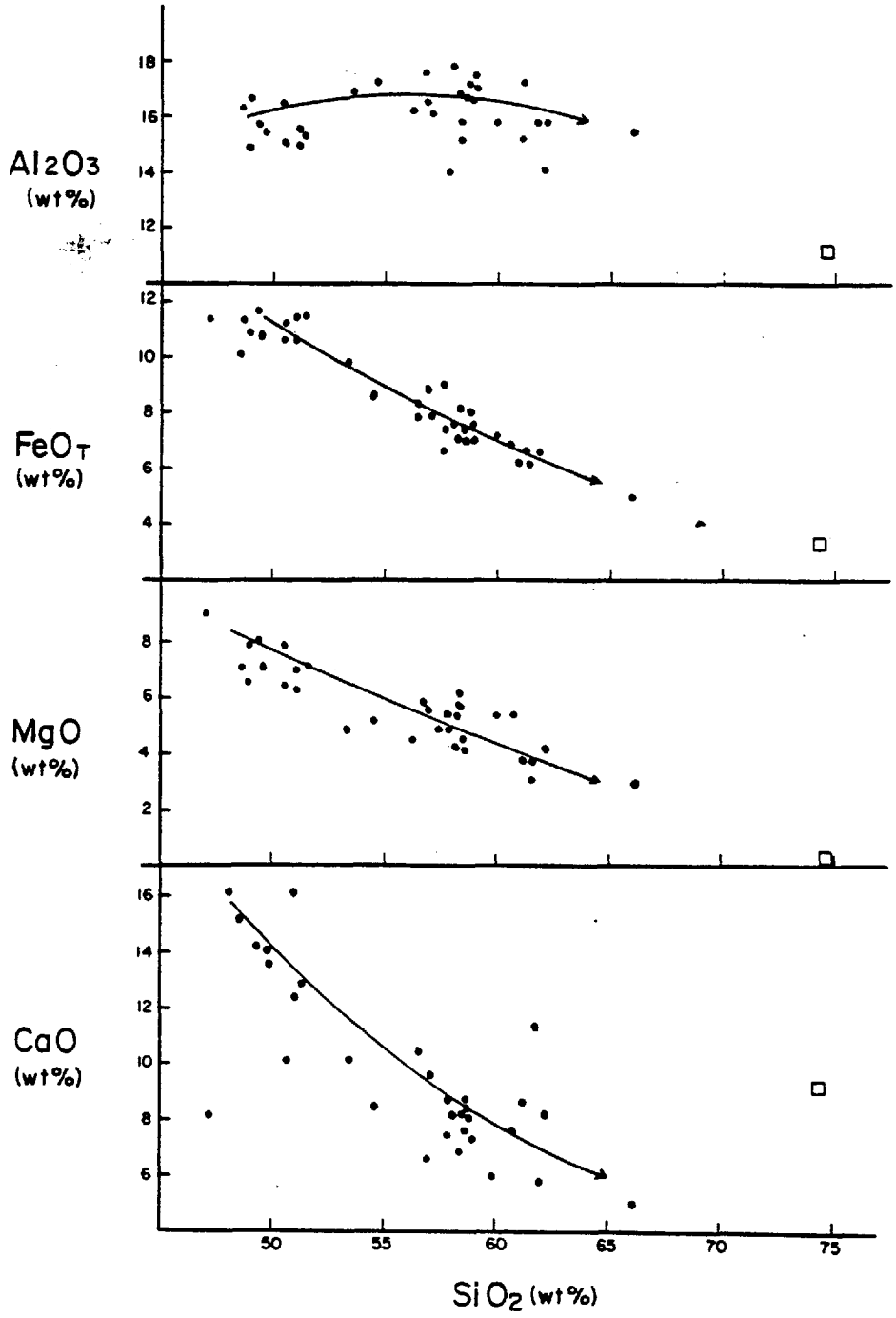


Figure 4a: Harker diagrams of analyses of Allard River volcanics.
dots= basalt, andesite, dacite
square= rhyolite.

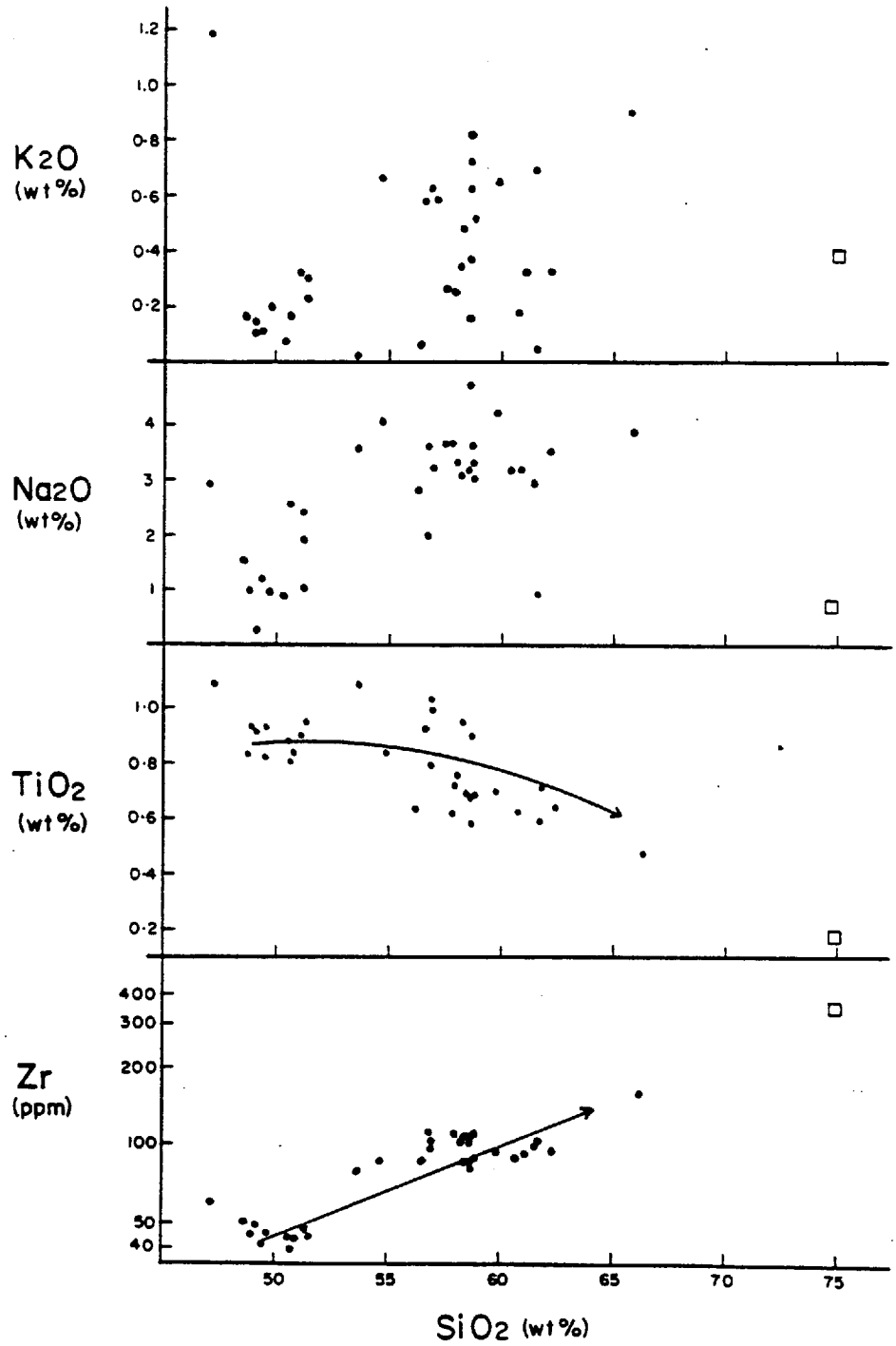


Figure 4b: Harker diagrams of analyses of Allard River volcanics (continued).

Figure 5: Hughes diagram. Note that most samples plot in igneous field. Dots = Allard River Volcanics; Square = Allard River rhyolite; Crosses = Gabbro norite intrusions. Tie lines join centers (circled dots) and margins (dots) of pillows. From Hughes (1973a, b).

Figure 6a,b: FeO and CaO vs Zr. Mobility of CaO reflected in length of pillow-rim tie lines. Symbols as in figure 5.

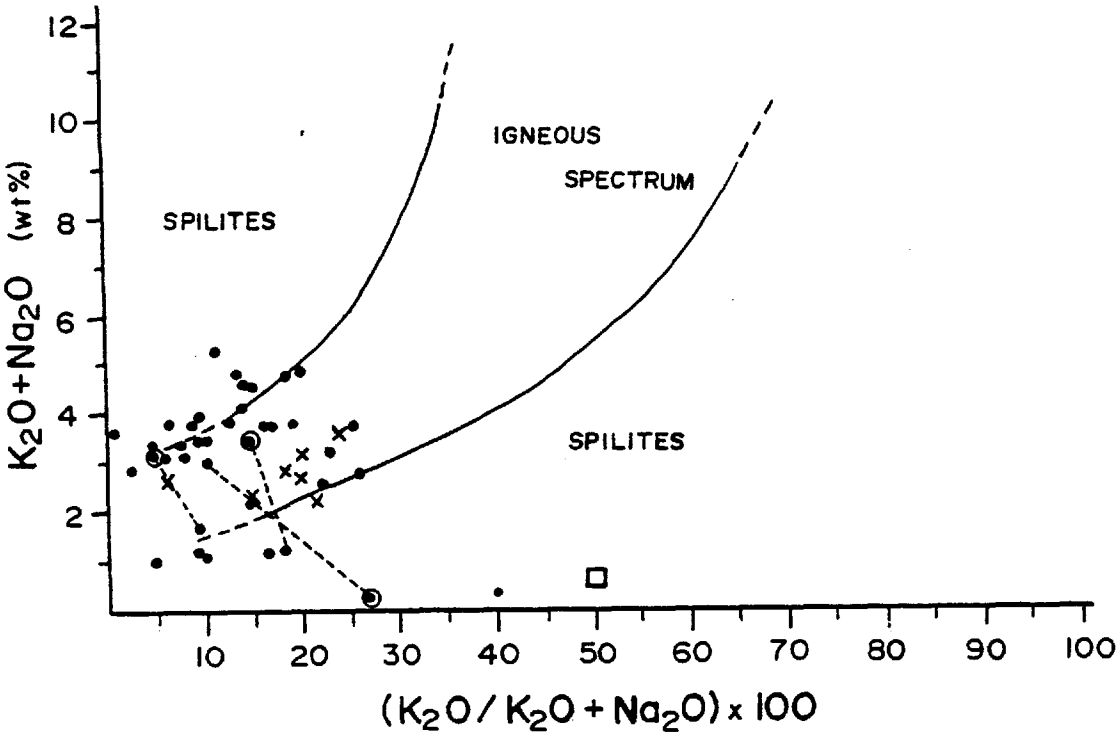


Figure 5

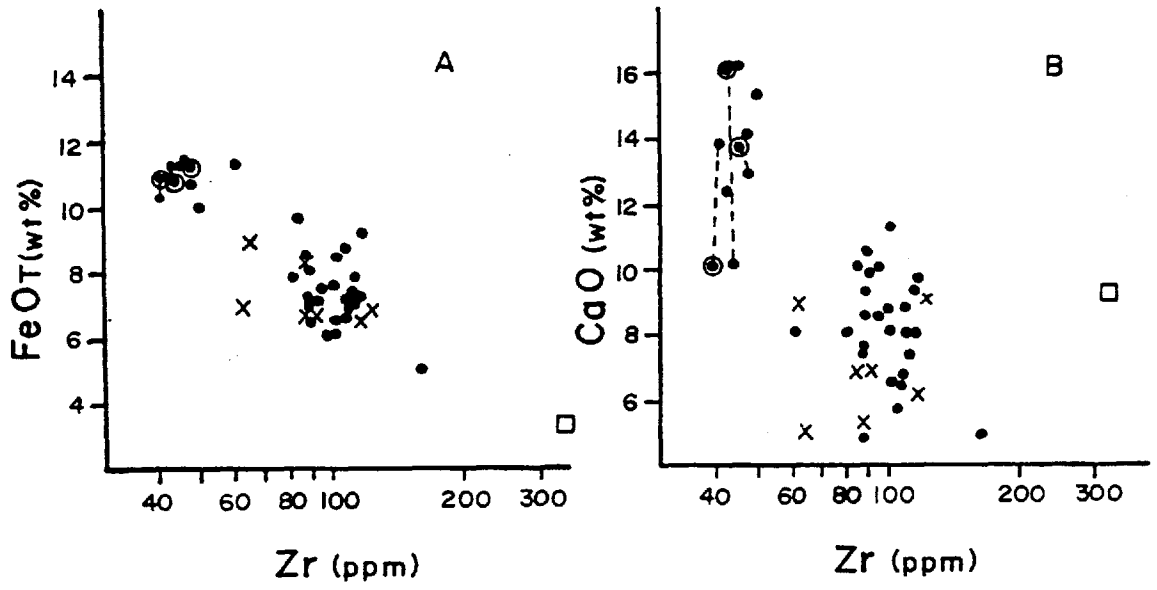


Figure 6

In order to evaluate the relation between CaO, Na2O, and K2O and degree of hydration+carbonation these oxides are plotted against loss on ignition (LOI) (figures 7a, b, and c). The distribution of Wabassee Group data is almost random. Tie lines are sub-parrallel indicating directional alteration. Because tie lines are steep, they suggest increasing Na2O and decreasing CaO with increasing LOI. Alternatly alteration in pillows may occur at constant degree of hydration+ carbonation.

Elements in centers and rims of pillows in figures 5, 6, and 7 are often enriched or depleted in different pillows implying that chemical gradients can be reversed.

Evidence presented here indicates that although certain components have been mobile and therefore do not represent magmatic concentrations (Na2O, K2O, CaO), most can be effectively considered immobile for the purpose of interpreting magmatic chemistry. This assumption is also supported by the preservation of fine textures as shown in the last chapter.

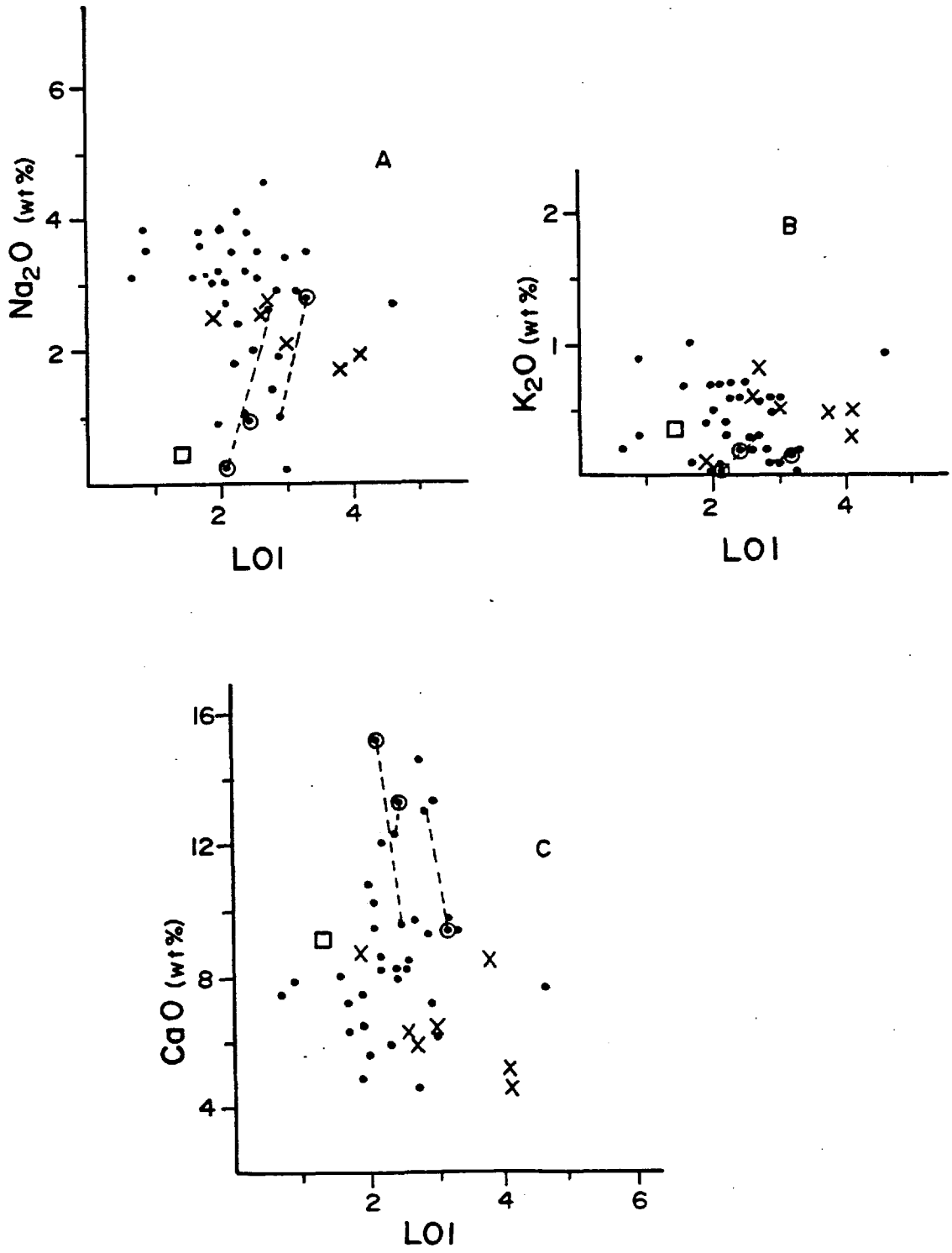


Figure 7a,b,c: Na2O, K2O, and CaO vs loss on ignition (LOI). Large scattering of points indicates poor correlation of alteration with degree of hydration + carbonation. Sub-vertical tie lines suggest spilitization occured at constant degree of hydration + carbonation. Symbols as in figure 5.

3.3 General Geochemistry

In this section the chemistry of the various rock units in the map area is characterized.

Watson Lake Group

Three samples of Watson Lake rhyolite were analysed (table 6). Two samples (82c-22a,82c-23a) are from fresh looking rhyolite close to the diabase dike near the airport and the third sample (81c-133) is from New Hosco bay.

Table 6: Chemical analyses of Watson Lake Group rhyolite.

	1 82c-22a	2 82c-23a	3 81c-133
SiO2	73.0	71.7	72.6
TiO2	0.74	0.60	0.52
Al2O3	11.0	11.6	13.3
FeO	9.9	7.2	3.0
MnO	0.04	0.13	0.1
MgO	1.8	1.1	1.5
CaO	0.71	2.8	3.3
Na2O	0.8	4.7	2.9
K2O	2.0	0.1	2.5
P2O5	0.16	0.10	0.00
Rb	33	44	46
Sr	32	51	61
Y	123	148	136
Zr	356	472	537
Nb	29	37	37

1,2: Fresh rhyolite near airport.
3: Altered rhyolite in New Hosco Bay.
Total iron as FeO

Sample 81c-133 which is silicified and slightly chloritized and carbonatized, is enriched in Al2O3, Zr, and

Sr and depleted in FeO relative to the two fresh rhyolites. A large difference in Na2O and K2O between the two fresh rhyolites precludes any inference about these elements in the altered rhyolite.

Wabassee Group

This group of rocks includes the Allard River lavas and their closely related spilitic sills.

Lavas and spilitic sills are combined in the histograms in figure 8a and b. Major elements and Sr are roughly normally distributed while the other trace elements appear to be log-normal in distribution. Four oxides in this figure show apparent bimodal distribution; these are SiO2, TiO2, FeO, and K2O. The other oxides are either bimodally or unimodally distributed.

Average Allard River basalt and andesite are shown in table 7 along with average gabbro-norite and a gabbro sample. The basalts and andesites are similar except that compatible components (MgO, FeO, CaO) are more abundant and incompatible components (SiO2, Zr, P2O5, Y, Nb) are depleted in the basalts.

On the AFM diagram (figure 9) samples that have low SiO2 and Zr plot in the tholeiitic field while samples enriched in these components plot in the calc-alkaline field. Compared to the differentiation trend of B1 to B7 flows in the Watson Lake Group (MacGeehan, 1979), the Allard River lavas (arrow) have evolved without iron enrichment.

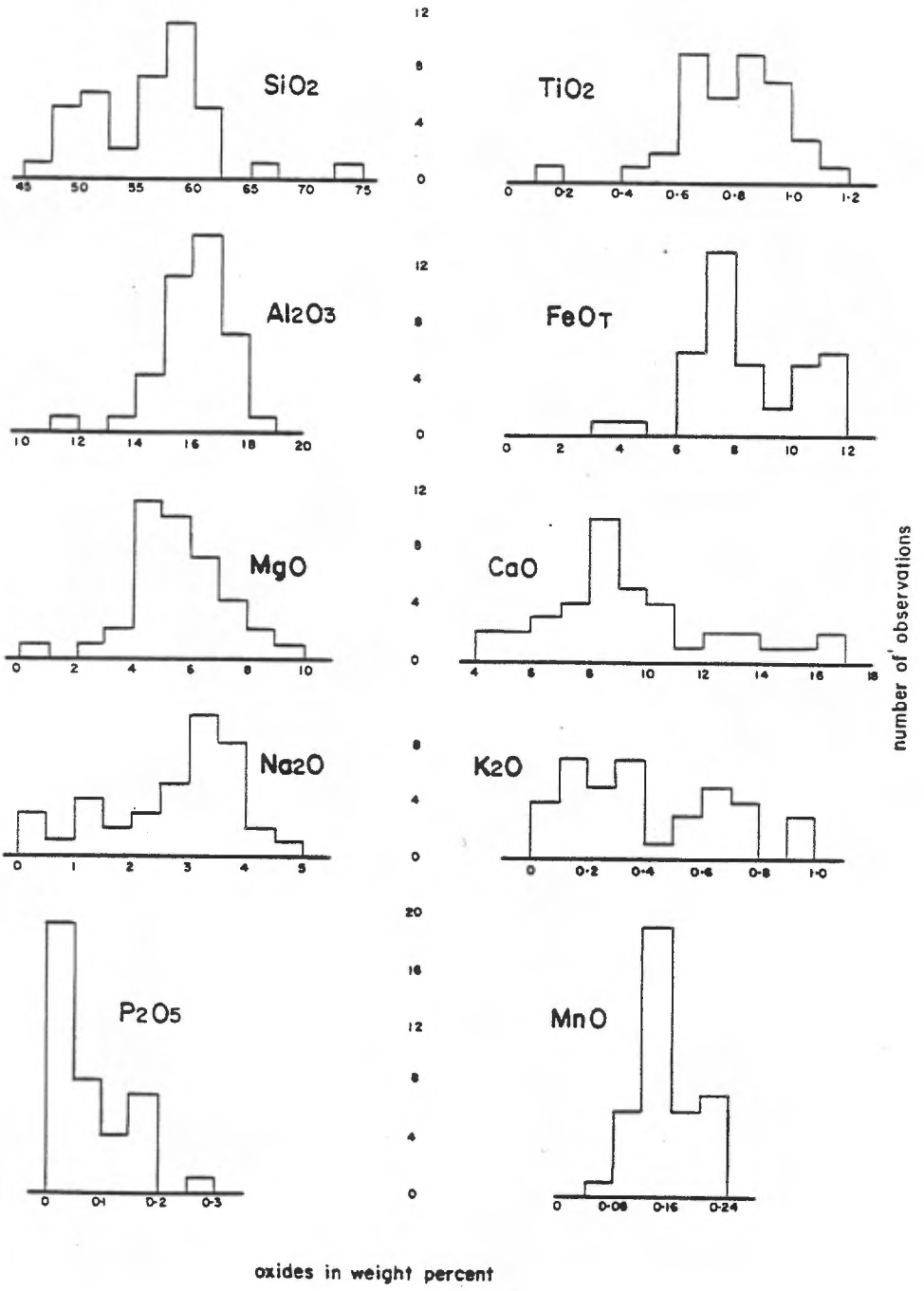


Figure 8a: Histograms of analyses of Allard River Volcanics.

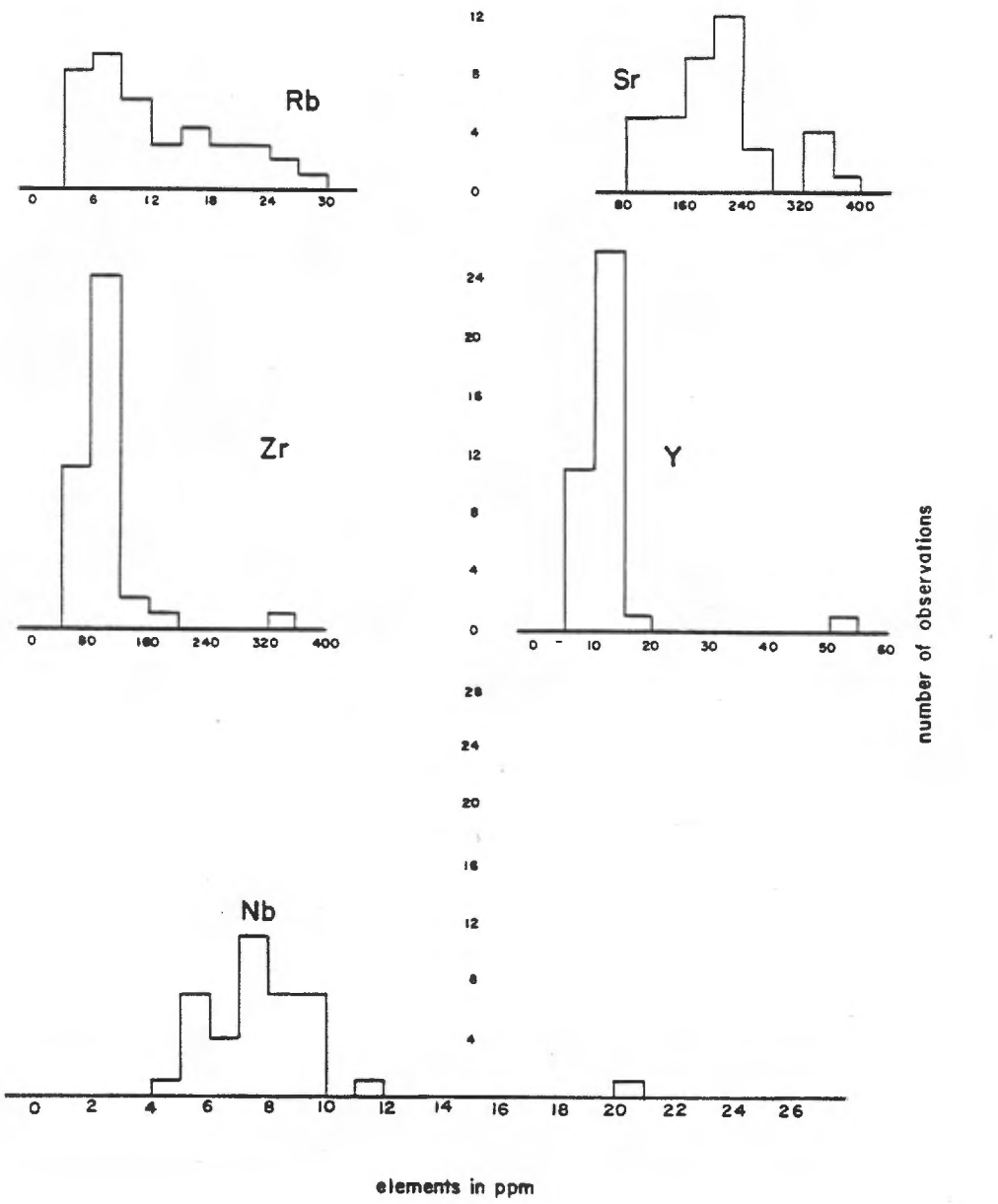


Figure 8b: Histograms of analyses of Allard River Volcanics (continued).

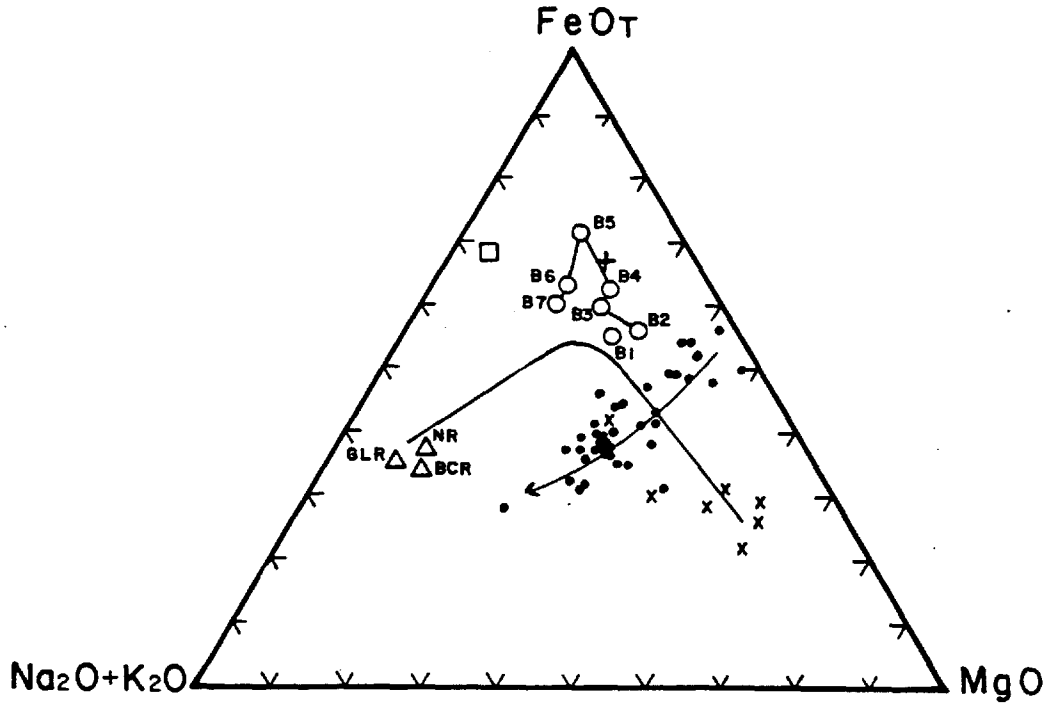


Figure 9: AFM diagram. Tholeiitic-calc-alkaline boundary Irvine and Baragar (1971).
Circles = Watson Lake Group basalts;
Triangles = Watson Lake Group rhyolites;
Plus = Gabbro sill from near New Hosco mine;
Other symbols as in figure 5.
Watson Lake Group data from MacGeehan (1979).

Table 7: Comparison between average chemistry of gabbro-norites and Allard River basalts and andesites.

	Gabbro-norites	Gabbro	Basalts	Andesites
N	7	1	7	26
SiO2	58.6	50.0	50.1	58.0
TiO2	0.46	1.78	0.89	0.78
Al2O3	13.8	13.5	15.6	16.2
FeO	7.3	15.4	10.9	7.2
MnO	0.12	0.23	0.20	0.13
MgO	9.8	5.2	7.0	5.2
CaO	6.8	9.2	13.9	8.4
Na2O	2.3	2.6	1.3	3.2
K2O	0.51	0.22	0.17	0.48
P2O5	0.07	0.14	0.01	0.09
Rb	16	9	15	13
Sr	155	117	169	226
Y	7	27	10	11
Zr	91	99	45	101
Nb	8	9	6	8

This feature is even better shown in MgO against FeO (figure 10). Here the Allard River volcanics follow the Cascade trend indicating calc-alkaline type differentiation.

The Jensen plot in figure 11 provides confirmation of the dual nature of the Allard River volcanics. The samples on this diagram are also strongly bimodally distributed.

Samples are also plotted on the Pearce and Cann-type diagrams in figure 12a, b, and c to add additional proof of magma parentage. In figure 12a (Ti vs Zr) the primitive lavas plot in the mixed field and the more evolved lavas plot in the calc-alkaline field. Samples plot in all fields in figure 12b (Zr-Ti/100-Sr/2) and in the intraplate field in 12c (Zr-

Figure 10: MgO vs FeO (total). Allard River volcanics follow Cascade trend of McBirney (1968) while Watson Lake Basalts show strong Fe-enrichment typical of tholeiitic Thingmuli suite (Carmichael, 1964). Gabbro norites define a trend which intersects the volcanic trend at andesitic compositions. Symbols as in figures 5 and 9.

Figure 11: Jensen diagram. Symbols as in figures 5 and 9. From Jensen (1976). Components in Mole %.

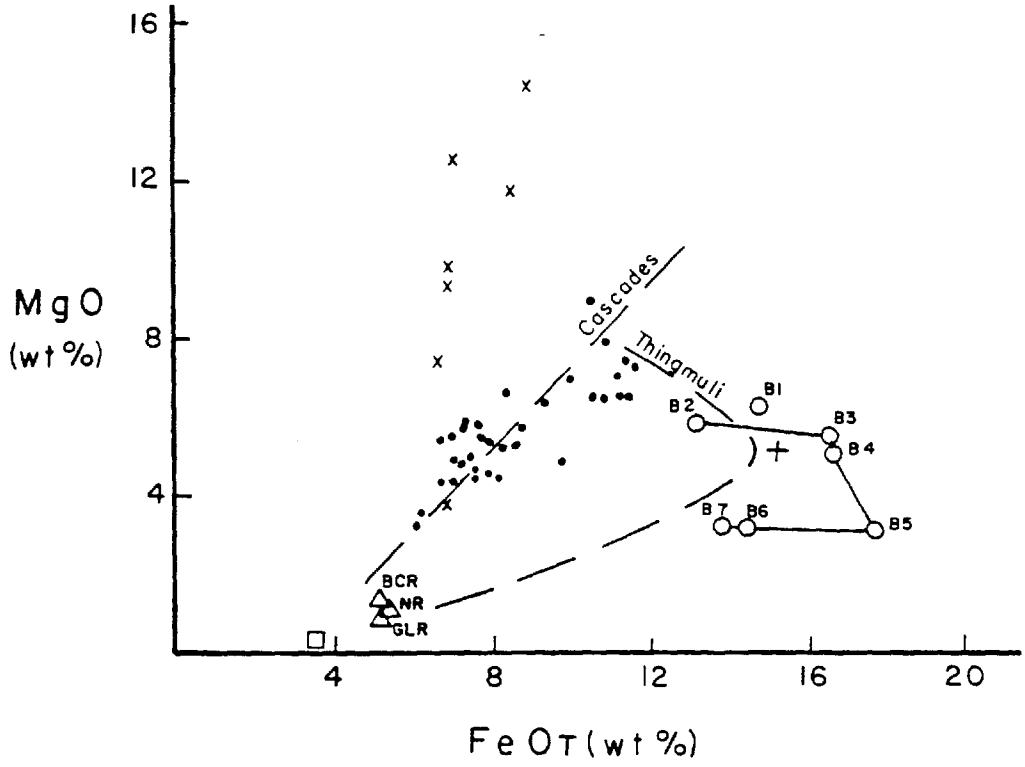


Figure 10

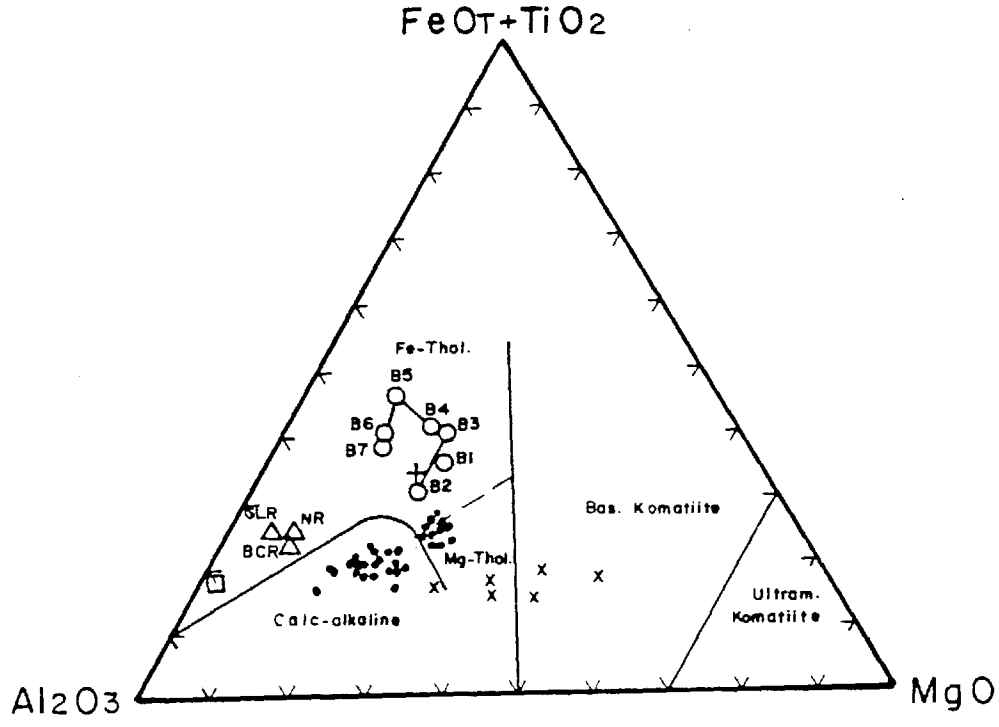


Figure 11

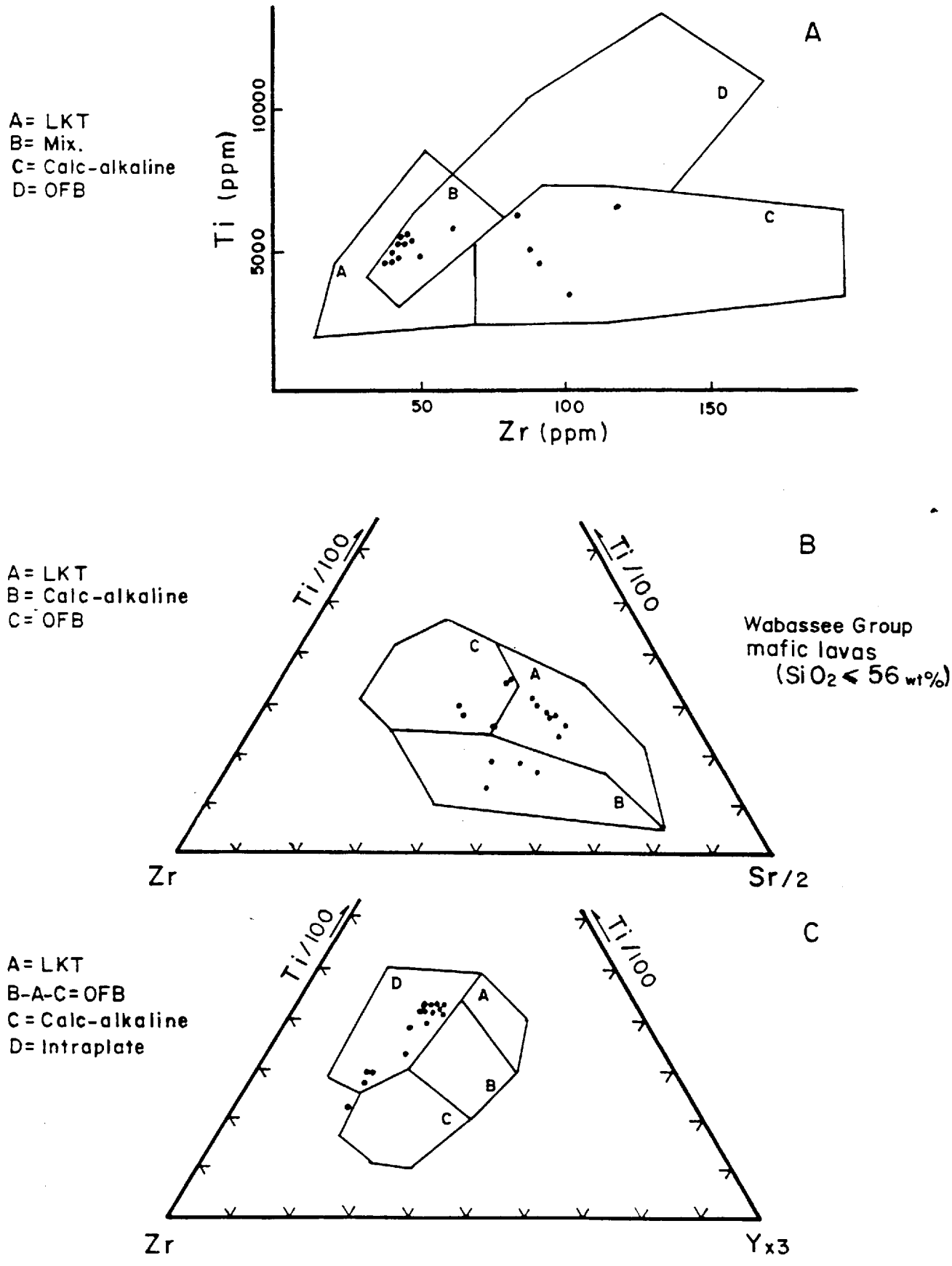


Figure 12a,b,c: Trace element diagrams after Pearce and Cann (1973). Dots = Allard River volcanics with less than 56 % SiO2.

Ti/100- Y*3). It is apparent that the rocks possess unusual chemistry and the source of the missclassification may be related to variable Sr and generally low Y concentrations. The localisation of primitive samples in the mixed field in figure 12a is compatible with low-K tholeiitic parentage.

The tholeiitic and calc-alkaline character of the Allard River lavas is strongly supported by the relative abundances of the rare-earth elements (REE). Chondrite normalized REE profiles for a sample of Allard River basalt (81c-135a) and two samples of andesite (81c-001, 81c-177a) are shown in figure 13. The primitive lava has a flat REE profile and is poor in the sum of REE (only about 9x chondrite). This curve contrasts strongly with the sloping, LREE enriched profiles of the two andesites.

The Allard River lavas appear to be composed of two chemical units. The mafic lavas are tholeiitic (Mg- or low-K tholeiitic) and the andesites are calc-alkaline. It remains to be shown, however, what relation if any there is between the tholeiitic and calc-alkaline lavas. This problem is treated in the section on petrogenetic modelling (section 5.5).

Gabbro-Norites and Gabbro

Average values of 7 analyses of gabbro-norite and 1 gabbro are compared with the Allard River lavas in table 7. The gabbro-norites are enriched in SiO2 and MgO relative to both the average basalt and andesite. Conversely they are depleted

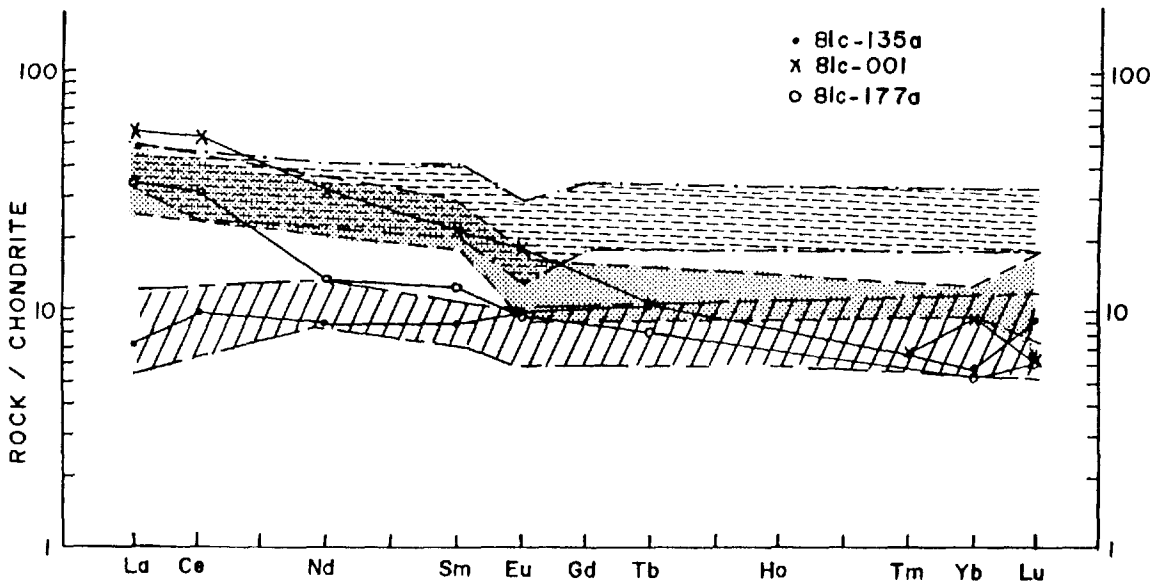


Figure 13: Chondrite normalized rare earth element profiles for 1 basalt (81c-135a) and 2 andesites from Allard River volcanics. Fields for Destor-Dufresnoy, Dufault-Reneault, and Pelletier-Rouyn-Noranda series from Ludden et al. (1982). dashed pattern= Destor-Dufresnoy Fe-tholeiitic series; microdots= Dufault-Reneault calc-alkaline series; Hachured pattern= Pelletier-Rouyn-Noranda Mg-tholeiitic series.

in TiO2, Al2O3, CaO, and Sr. They have similar concentrations of FeO, K2O, P2O5, MnO, Nb, and Zr to the calc-alkaline andesites.

On the AFM diagram (figure 9) the gabbro-norites are more magnesian than the lavas. This feature is also shown in figures 10 and 11. Note also that they form a trend which points towards the andesites suggesting they are cumulates derived from andesitic or more felsic liquids. This interpretation is supported by high SiO2 values in the gabbro-norites.

The gabbro analysis in table 7 is derived from a sill which intrudes the New Hosco formation. Note the low SiO2, Al2O3, and MgO and high FeO, and TiO2 when compared to the G.N. and the lavas. On variation diagrams (see "+" in figures 9, 10, and 11) the gabbro plots invariably within the range of liquids produced during differentiation of Watson Lake Group basalts.

Rhyolitic rocks

Three generations of rhyolitic rocks are present within the Wabassee Group in the thesis area; analyses of these rocks are shown in table 8. Included are a rhyolitic flow from the Allard River lavas, a sample of rhyolite dike from South McIvor Hill, and a small felsic dike intruding andesite close to the largest gabbro-norite stock.

Compare the first two rhyolites in table 8. These contain roughly equal amounts of FeO, K2O, and MnO. Lower compatible

and higher incompatible elements indicate that the rhyolite flow is more evolved than the rhyolite dike.

The chemistry of the felsic dike is highly unusual. This sample (82c-02) has very high SiO2 and very low values of compatible oxides like FeO, MgO, CaO, and Sr. At the same time the sample contains very low values of incompatible elements (i.e. TiO2, P2O5, Zr, and Y). This dike has similar Nb, however, to the other two rhyolite samples. It is highly fractionated and has precipitataed Zr + Y bearing minerals.

Table 8: Chemistry of rhyolitic rocks in Wabassee Group

	Allard River lavas,rhyolite (82c-06)	Rhyolite dike (82c-15a)	Felsic dike (82c-02)
SiO2	74.9	70.0	78.3
TiO2	0.17	0.52	0.07
Al2O3	11.1	14.2	12.9
FeO	3.5	4.3	0.57
MnO	0.06	0.04	0.01
MgO	0.13	1.1	0.03
CaO	9.3	4.7	0.85
Na2O	0.37	4.7	5.4
K2O	0.37	0.32	1.8
P2O5	0.02	0.11	0.02
LOI	1.4	1.5	0.28
Rb	11	11	28
Sr	339	96	71
Y	52	20	7
Zr	356	212	81
Nb	20	14	16
SiO2/Zr *0.001	2.1	3.3	9.7

Basic dikes

As mentioned in the last chapter, two types of basic dikes are observed in the area. One type is porphyritic with clinopyroxene and plagioclase phenocrysts set in a felted plagioclase-rich groundmass. The second type is equigranular and composed of over half of small stubby hornblende grains.

An analysis of each type of dike is presented in Table 9. The equigranular dike is enriched in Al2O3 and FeO, but depleted in MgO, CaO, K2O, Zr, and Rb relative to the porphyriric dike. The two samples have nearly equal SiO2, Na2O, TiO2, P2O5, MnO, Nb, Sr, and Y.

Table 9: Chemistry of basic dikes

	Porphyritic dike (81c-043)	Equigranular dike (81c-114b)
SiO2	54.0	54.8
TiO2	0.72	0.66
Al2O3	13.3	15.4
FeO	7.0	9.3
MnO	0.12	0.14
MgO	9.0	7.5
CaO	10.0	7.8
Na2O	3.3	3.4
K2O	2.0	0.49
P2O5	0.36	0.27
Rb	36	8.9
Sr	284	301
Y	13	14
Zr	151	106
Nb	9	9
SiO2/Zr *0.001	3.6	5.2

Tonalite

One sample of the tonalitic intrusion located on the western edge of the map is presented in table 10. In spite of it's high silica content the rock is poor in incompatible elements like Zr, Y, and Nb. Comparison of alumina and alkaline oxides indicates that the rock is peraluminous (i.e. molar Al2O3 /molar CaO+K2O+Na2O).

Table 10: Analysis of Tonalite (sample 81c-181)

SiO2	68.7
TiO2	0.31
Al2O3	16.2
FeO	2.3
MnO	0.04
MgO	1.7
CaO	3.6
Na2O	5.6
K2O	1.4
P2O5	0.06
Rb	38
Sr	483
Y	6
Zr	113
Nb	9

Diabase dikes

Three analyses of diabase dikes are presented in table 11. High FeO and TiO2 values suggest these are tholeiitic. Note that sample 81c-061b which has the most silica has nonetheless the least FeO and TiO2. In addition this sample has the lowest incompatible element content suggesting it is more primitive than the other two.

Table 11: Analyses of diabase dikes

	81c-061b	81c-066a	81c-096b
SiO2	52.9	49.8	50.3
TiO2	0.63	1.9	1.5
Al2O3	14.9	14.5	14.3
FeO	9.9	15.7	14.3
MnO	0.19	0.24	0.24
MgO	7.1	5.1	6.3
CaO	11.2	9.9	10.5
Na2O	1.9	2.2	1.9
K2O	1.2	0.41	0.26
P2O5	0.00	0.05	0.00
Rb	44	16	10
Sr	120	136	120
Y	15	28	23
Zr	55	119	98
Nb	6	12	11

5.4 Comparison of chemistry of Allard River lavas with Archean lavas from the Abitibi greenstone belt.

To obtain some perspective on the significance of their general chemistry the Allard River lavas are compared with other volcanic suites in the Matagami district on the one hand, and with volcanic suites in other parts of the Abitibi greenstone belt on the other.

Within the Matagami district extensive sampling in lavas has been performed on the Watson Lake Group (MacGeehan, 1979) and on the Wabassee Group in the map area (Allard River lavas), and to the east of the Bell River (MacLean,unpublished data); the latter suite of lavas are here called the Bell River volcanics. Average analyses for the three Matagami suites are presented in table 12. Compared to the other two, the Allard

River basalt contains more Al2O3, MgO, CaO, and Sr but less FeO, TiO2, P2O5, Zr, and Rb. Note also the much higher MgO/MgO+FeO ratio in the Allard River basalt.

Table 12: Comparison of average Allard River basalt and andesite with average Watson Lake and Bell River basalt

	Wabassee Group			Watson Lake Group
	Allard River lavas		Bell River lavas(1)	B1 to B7 (2)
N	7	26	31	31
SiO2	50.1	58.0	50.2	51.4
TiO2	0.9	0.8	1.4	2.0
Al2O3	15.6	16.2	12.8	13.3
FeO	10.9	7.6	15.2	17.3
MnO	0.20	0.13	0.22	0.25
MgO	7.0	5.2	5.8	4.5
CaO	13.9	8.4	9.9	7.5
Na2O	1.3	3.2	2.4	3.0
K2O	0.17	0.48	0.3	0.30
P2O5	0.01	0.09	0.20	0.40
Rb	15	13	30	89
Sr	169	226	137	63
Y	10	11	6.6	12.4
Zr	45	101	93	229
Nb	6	8	---	---
SiO2/Zr *.001	11.1	5.7	5.4	2.2
MgO/ MgO+FeO	0.39	0.41	0.28	0.21

(1) MacLean, unpublished data
(2) MacGeehan, 1979
--= no data

Previous work by MacGeehan (1979) has shown that the Watson Lake basalts are high-iron tholeiites characterized by

high concentrations of incompatible elements. This extreme iron enrichment is shown in figures 9, 10, and 11. These features contrast strongly with the Allard River basalts and even more so the andesites.

Anomalously high FeO and TiO2 and low Al2O3 in the average Bell River basalt suggests a closer parentage of these lavas with the Watson Lake than the Allard River lavas.

Thus the Allard River basalts, although tholeiitic in character bear little resemblance with the other two tholeiitic suites in the Matagami district. The Allard River basalts and andesites are similar except for higher compatible and lower incompatible element concentrations in the basalts.

To better characterize their chemistry the average values for the Allard River basalts and andesites are compared with average values from the Timmins-Kirkland Lake-Noranda regions (Goodwin,1979; Ludden et al.,1982; Gelinas et al., 1977).

In table 13 the Allard River lavas are compared to data compiled by Goodwin (1979). While the andesites are chemically most similar to Goodwin's calc-alkaline andesites, indeed only Al2O3 and CaO appear to be significantly different, the basalts are on the whole intermediate between tholeiitic and calc-alkaline basalts.

Table 13: Comparison between the Allard River lavas and compiled averages for the Timmins-Kirkland lake-Noranda region

	Allard River lavas		Abitibi averages Goodwin, 1979			
			Tholeiitic		Calc-alkaline	
	bas.	and.	bas.	and.	bas.	and.
N	7	26	298	64	139	251
SiO2	50.1	58.0	52.2	57.7	52.9	58.8
TiO2	0.9	0.8	1.3	1.5	1.1	0.9
Al2O3	15.6	16.2	14.7	15.1	17.7	17.1
FeO	10.9	7.6	12.3	10.5	9.4	7.0
MnO	0.20	0.13	0.23	0.21	0.19	0.15
MgO	7.0	5.2	6.4	3.6	6.1	4.7
CaO	13.9	8.4	9.4	6.4	8.6	5.9
Na2O	1.3	3.2	2.6	3.7	3.2	4.1
K2O	0.2	0.5	0.4	0.6	0.5	0.9
P2O5	0.01	0.09	0.13	0.31	0.14	0.17
Rb	15	13	---	---	---	---
Sr	169	226	133	119	169	203
Y	10	11	---	---	---	---
Zr	45	101	88	122	76	107
Nb	6	8	---	---	---	---
SiO2/Zr *.001	11.1	5.7	5.9	4.7	7.0	5.5

--= no data

Similarities between the Allard River basalts and either of Goodwin's tholeiitic or calc-alkaline basalts are not so evident. In the Allard River basalts silica is at least 2 % lower than both types. MgO is somewhat higher than both, although a 1 % difference may not be significant. CaO on the other hand is clearly higher and Na2O and K2O are lower in the Allard River basalts. These three oxides may not reflect magmatic values due to the effects of spilitization. Other

elements which appear to be lower than either tholeiitic or calc-alkaline basalts are TiO2, P2O5, and Zr. Al2O3, FeO, and MnO are intermediate between the two magma types.

The SiO2/Zr*10 ratio is quite high in the Allard River basalts. This suggests that silica is enriched relative to a differentiation index.

The three rare earth element (REE) analyses from the Allard River lavas are compared to confidence bands of certain volcanic suites from the Noranda district (Ludden et al.,1982) in figure 13. The basalt plots completely within the range computed for the high-magnesium tholeiitic Pelletier series (equivalent to Rouyn-Noranda series of Gelinas et al.,1977). The andesite profiles resemble the band produced by the Dufault-Reneault calc-alkaline series. HREE's may be slightly lower however in the Wabassee Group andesites.

The similarity in REE pattern between the Allard River basalt and the Pelletier-Rouyn-Noranda series is further investigated by a comparison with the series average major element composition (Gelinas et al., 1977) in table 14. The basalts are strikingly similar except for higher CaO and lower TiO2 in the Allard River basalts. Likewise the Wabassee Group andesites contain more MgO and less TiO2.

In summary, the Allard River lavas are different than either the Watson Lake Group or the Bell River basalts. Compared to other suites in the Abitibi belt they are primitive with high compatible and low incompatible element content but also have high silica. Striking chemical resemblance is found with the basalts and andesites of the

Pelletier-Rouyn-Noranda series.

Table 14: Comparison between Allard River lavas and the Pelletier-Rouyn-Noranda series

	Allard River lavas		Pelletier-Rouyn-Noranda series(1)	
	bas.	and	bas.	and.
N	7	26	11	4
SiO2	50.1	58.0	51.0	58.0
TiO2	0.9	0.8	1.3	1.2
Al2O3	16.6	16.2	15.9	16.7
FeO	10.9	7.6	11.8	8.3
MnO	0.20	0.13	---	---
MgO	7.0	5.2	6.3	3.6
CaO	13.9	8.4	10.9	7.9
Na2O	1.3	3.2	2.2	3.1
K2O	0.2	0.5	0.1	0.7
P2O5	0.01	0.09	0.09	0.20

(1) data from Gelinas et al.,(1977).

5.5 Petrogenetic modelling of Allard River volcanics

As demonstrated earlier, the Allard River volcanics often contain plagioclase and occasionally clino- and orthopyroxene phenocrysts. They are characterized by high compatible and low incompatible element concentrations except that silica is high.

It was noted above that although the basalts and andesites are markedly different in certain chemical parameters, other characters suggest they are more similar to each other than to any other volcanic suite sampled to date in the Matagami district. Study the Harker diagrams in figures 14a and b. It

is apparent that the Allard River lavas are roughly bimodal. A visual best fit line passing through the centers of the clusters, however, suggests that the samples may be related by a proccess of differentiation. This is especially true for Al2O3, FeO, MgO, and Zr vs SiO2.

The progressive decrease in compatible and increase in incompatible element concentrations with SiO2 is a strong indication that simple fractional crystallization is producing the elemental variations within the suite of lavas. The observed trends on the Harker diagram are compatible with the extraction of plagioclase, clino- and orthopyroxene from a mafic Mg-tholeiitic magma.

This hypothesis is considered from the point of view of the high field stength (HFS) elements (Pearce and Norry, 1979). The vectors outlined by the Allard River lavas (figure 14) can be considered as the result of the crystallization of certain minerals in specific proportions. Each extracted phase then can be represented as a vector in Ti, Y and Nb vs Zr space. These mineral vectors are also shown in figure 14. Differentiation trends in figures 14b and c are compatible with a three phase (pl, opx, cpx) as well as a four phase (+mt) extraction assemblage. Figure 14a, however, shows that the four phase assemblage is required.

However, no magnetite phenocrysts were observed in the Allard River volcanics. Moreover, the differentiation trend of the gabbro-norites exclude magnetite as a cummulus phase (compare figure 14a with b and c). This ambiguity in the data cannot be resolved at present.

Figure 14a,b,c: TiO2, Nb, and Y vs Zr. From Pearce and Norry (1979). Symbols as in figure 5. Mineral extraction vectors are shown as rose diagrams next to each figure.

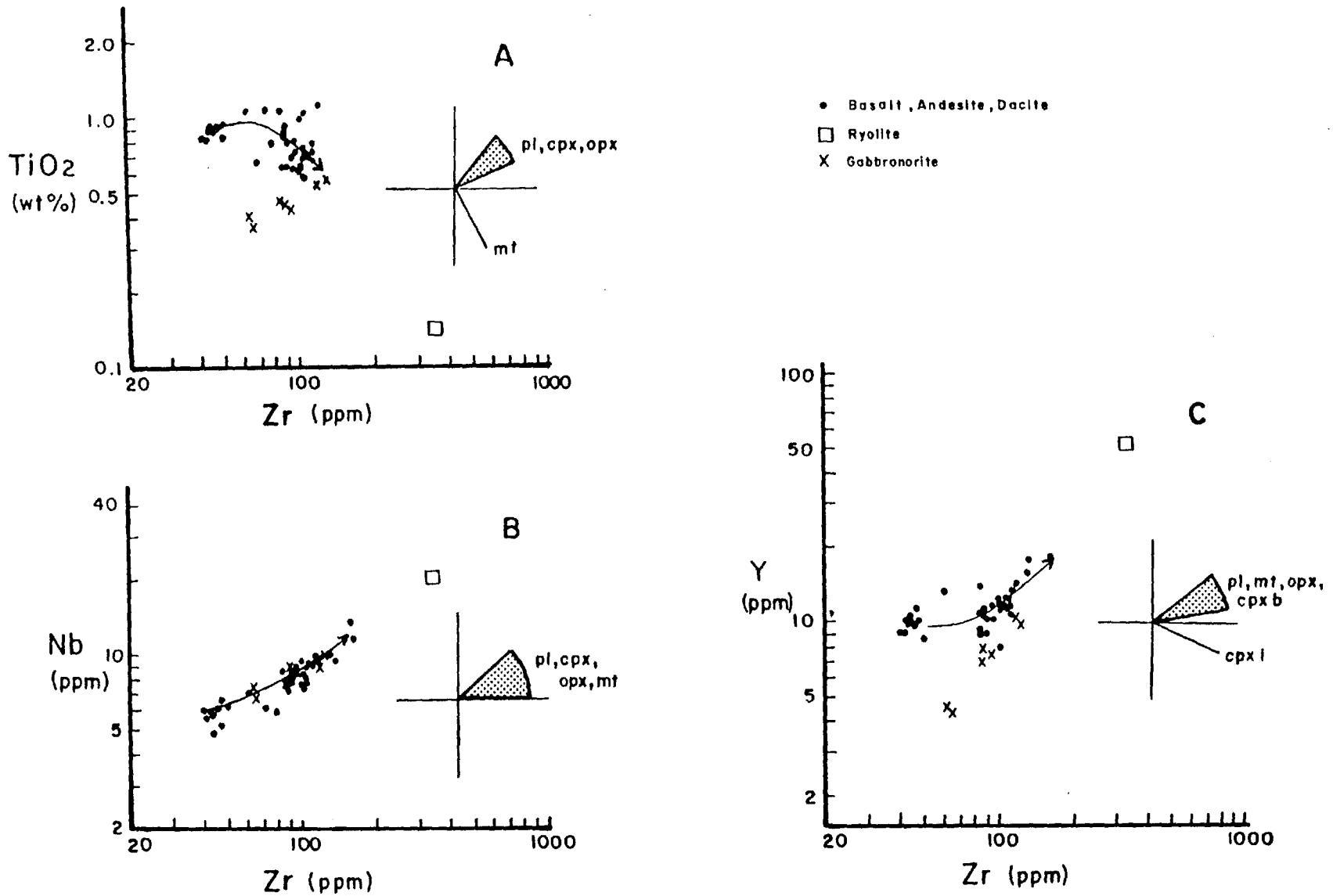

A
2.0
1.0
TiO2
(wt%) 0.5
0.1
20
100
1000
Zr (ppm)
pl,cpx,opx
mt
B
40
Nb
(ppm) 10
5
2
20
100
1000
Zr (ppm)
pl,cpx,
opx,mt
• Basalt, Andesite, Dacite
□ Ryolite
X Gabbronorite
C
100
50
Y
(ppm) 10
5
2
20
100
1000
Zr (ppm)
pl,mt,opx,
cpx b
cpx i

Figure 14

Zr/Nb and Zr/Y ratios vary little during fractional crystallization (Pearce and Norry, 1979). In other words liquid evolution by crystallization produces sub-horizontal lines in Figures 15a and b. In practice however limited substitution of Y in clinopyroxene implies that the Zr/Y ratio should increase slightly during differentiation. This is reflected in the shallow positive slope of the Watson Lake Group crystallization trend in Figure 15b.

In Figure 15c a positive slope in fractionation vector could be the result of extraction of magnetite and/or clinopyroxene.

The slopes of the differentiation trends in the Allard River lavas (Figures 15a and b) are apparently too steep to be explained by simple fractional crystallization. These curves could be the result of contamination of the magma by a source with high Zr/Y,and Zr/Nb ratios.

Light REE enrichment in the calc-alkaline Dufault-Reneault series andesites in the Noranda district is considered by Ludden et al. (1982) to be the result of contamination of a tholeiitic magma by a source enriched in large ion lithophile elements (including the HFS elements). LREE enrichment in the two Wabassee Group andesites may be due to the same process.

In summary, major and some trace element variations in the Allard River lavas and associated gabbro-norite sills can be explained by the crystallization of certain proportions of plagioclase, clino-,and orthopyroxene, and possibly magnetite. Zr/Y and Zr/Nb ratios as well as LREE enrichment in the

Figure 15a,b,c: Zr over Nb, Y, and TiO2*0.01 vs Zr. From Pearce and Norry (1979). Symbols as in figure 5. Arrows with C3 (chondrite value) represent presumed range of liquid compositions derived from mantle. Mineral extraction vectors shown as rose diagrams next to each figure.

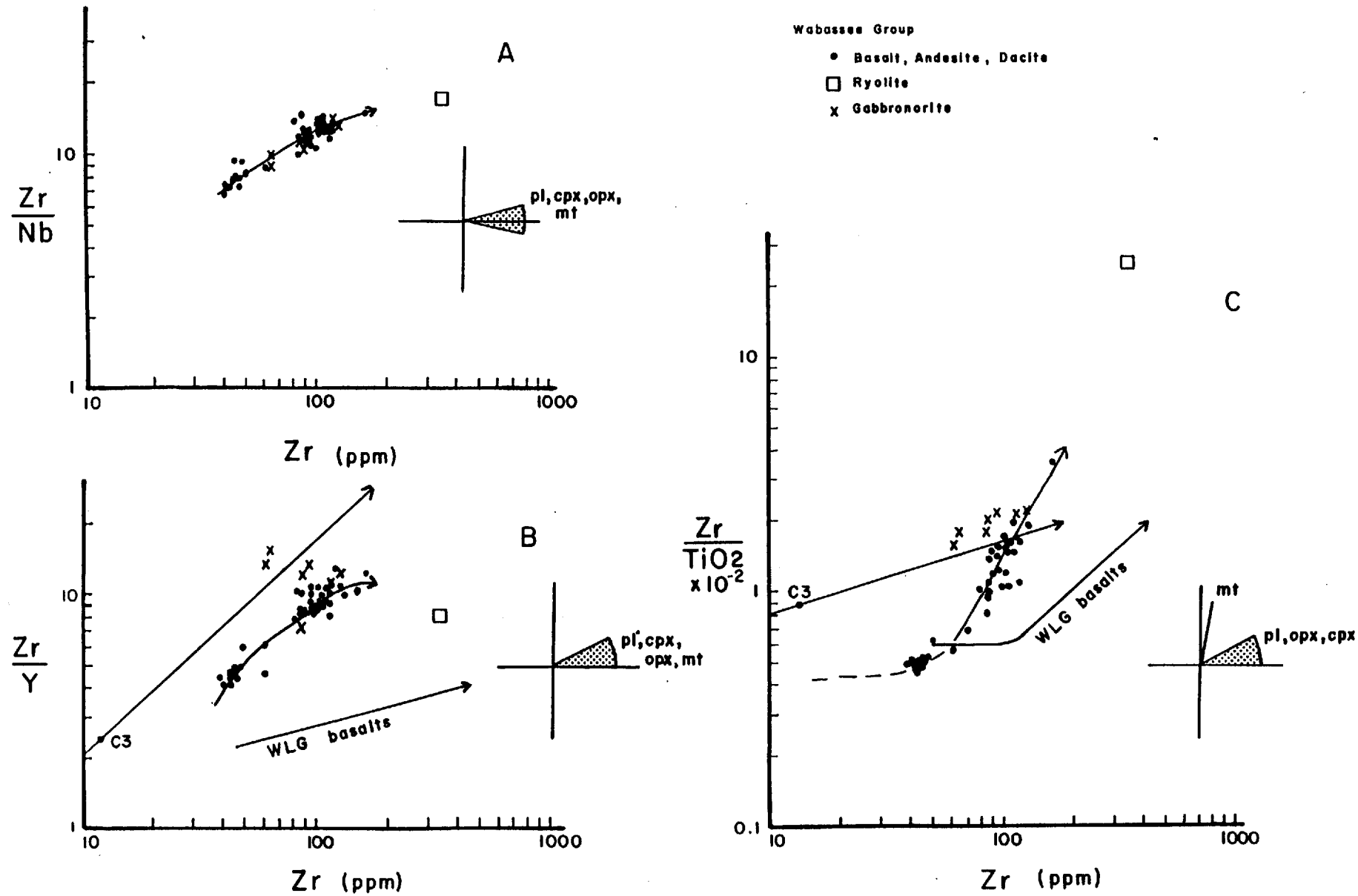

Wabassee Group
Basalt, Andesite, Dacite
Rhyolite
Gabbronorite
A
B
C
Zr/Nb
Zr/Y
Zr/TiO2 x10-2
Zr (ppm)
10
100
1000
1
0.1
C3
WLG basalts
pl,cpx,opx, mt
pl,cpx, opx, mt
mt
pl,opx,cpx

Figure 15

andesites suggests the liquids were contaminated by a source enriched in large ion lithophile elements.

The presence of large volumes of granitic gneiss within and surrounding the Abitibi greenstone belt argues in favor of a sialic contaminant. Indeed, Archean crust is characterized by high La/Yb ratios and REE profiles (La= 40x chondrite; Yb= 7x chondrite) resembling the Allard River andesite and dacite samples (Taylor and McLennan, 1981). Likewise, high Zr/Nb and Zr/Y ratios in Allard River andesites and dacites is attributed to contamination by a source with high ratios of these elements. Figure 15 shows that the Zr/Nb ratio of average Archean crust is compatible with this interpretation. The Zr/Y ratio of average Archean crust however is too low to explain the high Zr/Y ratios in the Allard River andesites and dacites. This is true also with the Zr/TiO2 ratios.

3.6 Discriminant Analysis

A representative suite of Allard River lavas and basalts from the Bell River lavas (MacLean, unpublished data) and the Watson Lake Group (MacGeehan, 1979) have been used to calculate 3 discriminant functions (table 15). The methodology and results of the computation are presented in appendix 5.

Table 15: Discriminant functions for the Matagami area lavas.

Group	function		
Allard R. 1	F1	=	156*SiO2+77*TiO2+124*Al2O3+161*FeO+ 135*MgO+167*CaO+162*Na2O+244*K2O+ 16*P2O5-33*MnO-7331.
Bell R. 2	F2	=	158*SiO2+81*TiO2+122*Al2O3+165*FeO+ 136*MgO+169*CaO+165*Na2O+246*K2O+ 7*P2O5+31*MnO-7520.
Watson L. 3	F3	=	160*SiO2+100*TiO2+126*Al2O3+166*FeO+ 136*MgO+169*CaO+166*Na2O+239*K2O+ P2O5+105*MnO-7713.

Mahalanobis D-square index = 927.

Degrees of freedom = 20

The three functions are plotted as F1/F2 vs F3/F2 in figure 16. This diagram is good at separating the Allard River lavas from the other series. Similarly, F3/F2 ratios separate well the Bell River basalts from the Watson Lake Group. Some overlap is present however, indicating similarity of chemistry between the two groups.

More elaborate interpretation is not attempted because of the difficulty in determining the factors responsible for the differences in chemistry between Groups. In particular note that the efficacy of the functions has not been verified with a test sample. It is suggested therefore that Groups of samples of known parentage be used to test the functions before they are utilized in a systematic fashion.

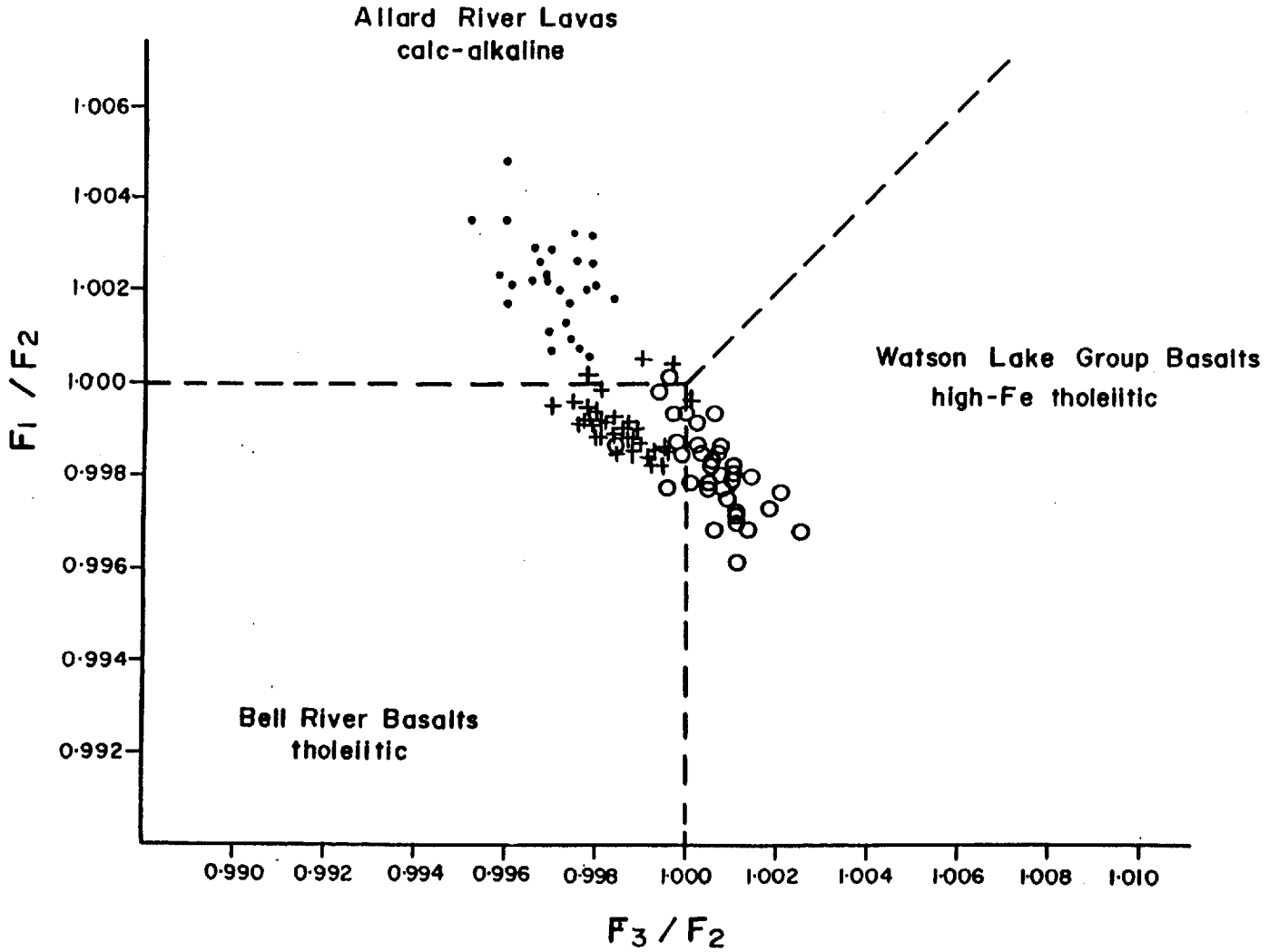


Figure 16: Discriminant diagram. See appendix 5 for method.
Dots = Allard River volcanics;
Plus = Bell River basalts (MacLean, unpublished data);
Circles = Watson Lake Group basalts (MacGeehan, 1979).

CHAPTER 4
DISCUSSION

4.1 GENERAL STATEMENT

The Wabassee Group in the thesis area consists of a mafic to felsic submarine volcanic cycle. The mafic rocks are Mg-tholeiitic in character and these differentiate towards calc-alkaline compositional trends in the more felsic rocks. In this section the evidence will be synthesized into a generalized model on the origin of these rocks.

4.2 GEOLOGICAL RECONSTRUCTION

The common presence of pillows and amygdules throughout most of the thesis area indicates that the Wabassee Group lavas were extruded in a relatively shallow marine environment. Volcanism must have been continuous because pyroclastic or epiclastic horizons are rare except around McIvor Lake. One thick pyroclastic flow located in the center of the map shows an eastward increase in fragment size implying the source was to the east. Contact relations between the Wabassee and Watson Lake Groups were not observed in the thesis area, but elsewhere in the Matagami district there is good evidence that the two groups interfinger. Around the Matagami Lake, Orchan, and Bell Allard Mines, Sharpe (1968) describes spherulitic rhyolite interlayered with pillowed andesites at the base of the Wabassee Group. Compare the

local stratigraphy around the Matagami Lake Mine with the stratigraphy around the New Hosco deposit (Table 16).

Table 16: Comparison of stratigraphy around Matagami Lake and New Hosco mines. Modified after Sharpe (1968).

Mattagami Lake Mine	meters	New Hosco Mine	meters
Wabassee Group		Wabassee Group	
andesite-basalt lava, some sills	140	pillowed dacitic lava	700
		andesitic lava and tuff	100
upper tuffite	10	coarse and fine tuffs	110
andesite-basalt	50	andesite lava	35
spherulitic rhyolite	180		
dacitic lava	160		
Key tuffite	3	basal tuffite (1)	3
Watson Lake Group		Watson Lake Group	
rhyolite, silicified rhyolite	+300	spherulitic rhyolite, intermediate lava	+300

(1)= Bernard, P., personal communication.

In contrast, no rhyolitic horizons are present at the base of the Wabassee Group around the New Hosco Mine. Sharpe (1968) does report, however, the presence of numerous thin intersections of siliceous spherulitic rocks in drill cores. Also, siliceous shards and fragments found in the pyroclastic horizon host to the deposit may be of rhyolitic composition (Sharpe, 1968). Finally, rhyolite horizons are reported in drill core to the east of the mine at about the same stratigraphic level as the deposit (Sharpe, 1968).

The rocks in the Watson Lake Group and near the base of the Wabassee Group (i.e. around New Hosco Bay) are intruded by mafic, tholeiitic gabbro sills. Their source is not known but chemical similarity with a gabbro-granophyre sill to the east (MacGeehan, 1979) suggests that the tholeiitic gabbro sills in

the thesis area are co-magmatic with the Bell River Complex.

A number of syn-volcanic gabbro-norite intrusions are emplaced to the Allard River Volcanics. Similarity in metamorphic grade with the surrounding rocks indicates the gabbro-norite were intruded shortly after extrusion of the lavas. The chemistry of the intrusions are generally similar to the enclosing lavas and their compatible element variations indicates these were derived partly by crystal sorting in an andesitic or dacitic magma.

On the basis of these data it is possible to infer the events which occured in the area. In this scenario the Wabassee volcanic suite was extruded beneath the ocean surface and probably developed as a shield volcano in view of the lack of sediments. At first, andesitic flows alternated with rhyolite and tuffaceous horizons. During one such "felsic eruption" the New Hosco orebody was deposited as a sulfide-rich tuff (Sharpe, 1968).

Rhyolite volcanism eventually stopped and andesite flows built up, unabated, about one kilometer of section. Volcanism suddenly changed to abasaltic composition. From here, a succession of progressively more felsic eruptions built up the volcanic pile to several kilometers of thickness.

While volcanism was active, tholeiitic gabbro sills intruded the base of the Wabassee Group and gabbro-norite intrusions, the middle and possibly the top part (figure 17).

After volcanism stopped, the volcanic flows and sills were intruded by amphibole-rich and clinopyroxene-plagioclase

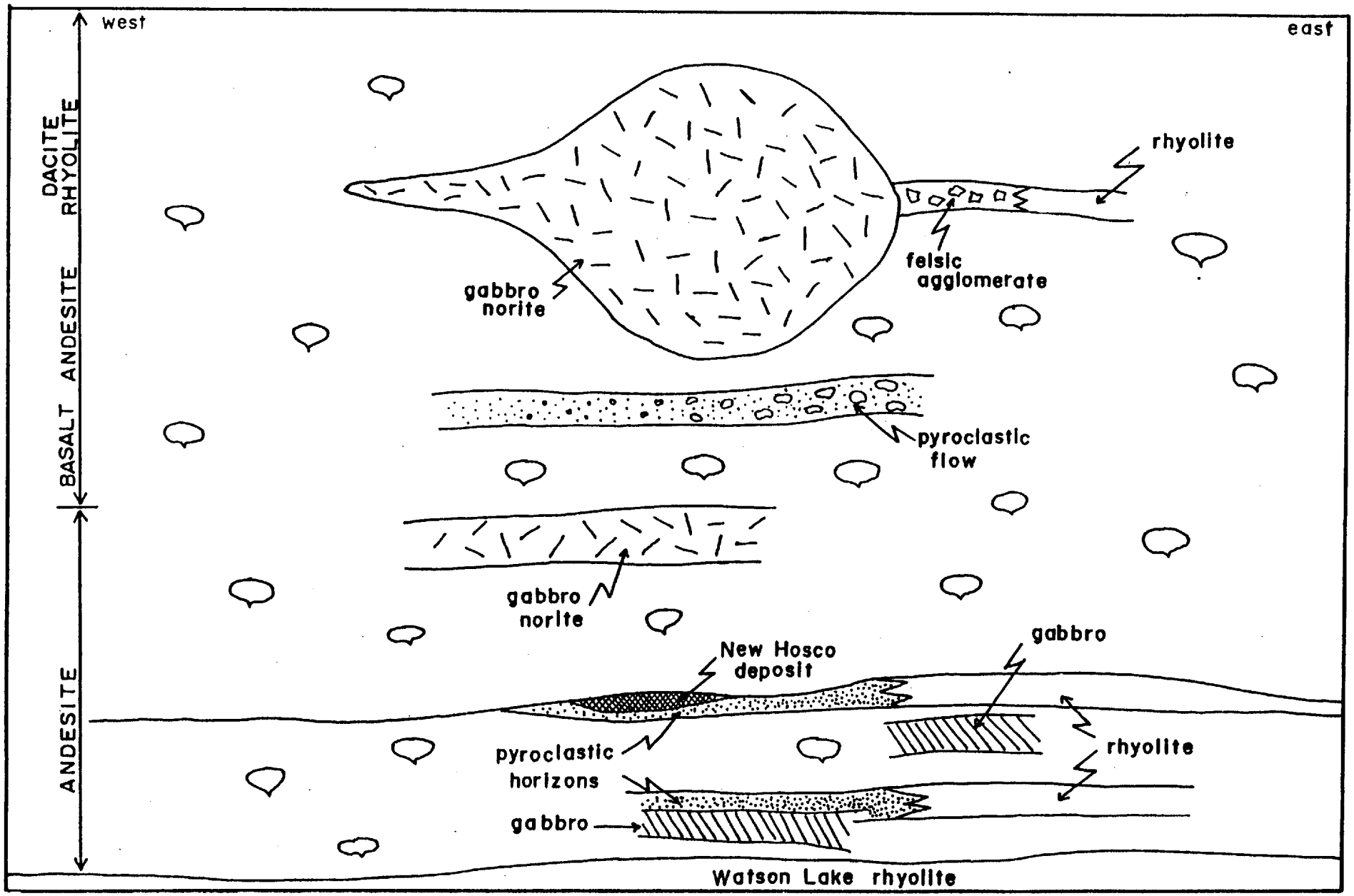


Figure 17: Cartoon model of geology of map area. Not to scale

phyric basic dikes, by a tonalitic pluton, and by various granitic dikes.

The whole area was then deformed into an east-west, upright anticline with concomittant faulting in northwest, northeast, and north-south directions. These faults may be related to the same stress field which produced the folding in the rocks.

A series of diabase dikes were intruded into northeast striking sub-vertical fractures. Minor faulting followed which locally offset the dikes in a dextral fashion.

4.3 PETROGENESIS OF THE ALLARD RIVER VOLCANICS

The Wabassee Group in the thesis area is composed of a mafic to felsic volcanic suite. The most basic lavas (50% SiO2) are Mg-tholeiitic in character while the more differentiated lavas (58% SiO2) are calc-alkaline.

The various major element variation diagrams presented in the last chapter show that the Allard River Volcanics define a magmatic differentiation trends that can be attributed to crystal fractionation. Although bi-modal distributions are present with certain elements, this is thought to be the result of sampling bias because basaltic flows are geographically restricted and were oversampled to get better resolution of their chemistry. Compare sampling density for the area containing basalts with the rest of the map (map in back pocket and figure 2). Moreover, no field evidence was obtained which would indicate the basalts were different than

the andesites and dacites. In fact, the special character of the basalts was only discovered in the laboratory on chemical and subsequently on petrographical evidence.

It may seem unusual to suggest that a Mg-tholeiitic magma can evolve through a calc-alkaline differentiation trend. There is nonetheless ample evidence in the literature to show that this can happen. Kuno (1950) in his classic study of the Hakone volcano in Japan demonstrated that calc-alkaline and tholeiitic flows are present on the same volcanic edifice and suggests they were derived from the same magma chamber. He concludes that the two magmas were derived from a common tholeiitic precursor and that the calc-alkaline suite was caused by the contamination of the magma by crustal rocks. He later revised his opinion (Kuno, 1968) and proposed that only water was required as a contaminant.

The number of models proposed to explain calc-alkaline magmatism are witness to a general lack of understanding of the genesis of this family of rocks. In his review, Kuno (1968) outlines 4 principal models to explain calc-alkaline magmatism: 1) calc-alkaline rocks are due to contamination of a tholeiitic magma by sialic material; 2) experiments show that calc-alkaline trends occur in basaltic liquids at high fO2 but not at low fO2; 3) partial melting of crust can produce liquids of calc-alkaline andesite composition; 4) melting of quartz-eclogite at high pressures produces mainly an andesitic liquid. Green (1980) in a review of petrogenetic models for island arc and continental margin magma genesis proposed that calc-alkaline magmas can be produced by 1)

melting of eclogite in a subduction zone, 2) melting of contaminated peridotite, or 3) shallow level, hydrous, amphibole dominated fractionation. He also points to the possibility of magma mixing of primitive liquids with earlier, fractionated batches, partial melting of the volcanic pile, and contamination by the volcanic pile as altenative models to explain calc-alkaline magmas.

Kuno's models 3 and 4 and Green's model 1 are ruled out as potential processes because the primary magma that produced the Allard River volcanics is thought to be tholeiitic basalt. Green's third model is also rejected because there is no evidence to suggest that amphibole was a fractionating phase. Of these, there remains Kuno's first and second and Green's second models to explain the observed chemical variations.

From thermodynamic considerations the process of assimilation can be regarded as an addition of major components and trace elements to a magma. It is because this process requires large amounts of energy to consume minerals that Bowen (1928) concluded that a superheated primary magma (more than 300 degrees above liquidus) is required to cause melting of wallrock. Since magmas are invariably at or near the liquidus superheating never occurs. Assimilation, to Bowen, was therefore impossible except on a very local scale. McBirney (1979) argued that the large amounts of energy required by assimilation is supplied by the crystallization of the magma itself. Assimilation results in changes in the proportion of crystallizing phases but does not cause

crystallization of wholly different phases. This means chemical variations during assimilation will still be controlled by liquidus relations. Thus, major element variations in magmas which have undergone assimilation should reflect the role of fractional crystallization.

In practice, the lack of iron enrichment, a long recognized characteristic of calc-alkaline magmas, could be due to the early appearance of magnetite on the liquidus. The reason for this is not certain but high oxygen fugacity as a result of assimilation of water has been suggested (Kuno, 1968).

This dual approach (fractionation-assimilation) to the generation of calc-alkaline magmas is taken by O'Hara (1980). Indeed he argues in favor of assimilation of wallrock on the grounds that the emplacement of intrusive rocks, especially those of mafic composition, is impossible unless assimilation occurs because density considerations does not permit mafic magmas to displace felsic crustal rocks. He also points out the contrasting behavior of the major and trace elements; because of liquidus relations, major elements are unlikely to record the effects of assimilation. Incompatible trace elements however, act passively during fractional crystallization, and so are very sensitive to assimilation processes.

DePaolo (1981) modelled the combined effect of assimilation and fractional crystallization on trace and isotopic element distribution and concluded that a whole range of different scenarios is possible. If the rate of

assimilation is equal to the fractional crystallization rate a process similar to zone refining is obtained; if the rate is lower, zone refining is combined with fractional crystallization; and if the rate is much larger, binary mixing curves are approached.

In a comprehensive experimental and geochemical study of the calc-alkaline lava series at Medicine Lake Highland, California, Grove et al. (1982) concluded that a combination of fractionation, assimilation, and magma mixing processes are required to explain elemental and isotopic variations. They note in particular that fractional crystallization is sufficient to explain major element variations.

The chemical variations in the Allard River volcanics are compatible with the fractionation-assimilation model outlined above. Major element variations can be modelled by the extraction of opx+cpx+pl+mt suggesting that fractional crystallization is the principal process involved in these rocks. Variations in selected trace element ratios (Zr/Y, Zr/Nb in figure 15) and large change in slope of rare earth element profiles (figure 13), however, cannot be produced by the fractionation of the phases listed above. The most likely cause of these variations is considered to be assimilation by a Mg-tholeiitic magma of a crustal (?) source enriched in Zr and light rare earth and depleted in Y, Nb, and heavy rare earth elements.

The Zr/Nb and Zr/Y ratio of the calc-alkaline volcanics range from 7 to 15 and 4 to 15 respectively. We may assume therefore that the contaminant will have Zr/Nb and Zr/Y ratios of 15 or greater. Average Archean crust as inferred from sedimentary rocks (Taylor and McLennan, 1981) has a Zr/Nb ratio of 20. On the other hand the Zr/Y ratio of Archean crust is only 7, which is too low for our contaminant. A La/Yb ratio of 4.7 was obtained by Taylor and McLennan (1981). In view of the high La/Yb ratios obtained in the calc-alkaline volcanics (6.2 and 6.5) it is doubtful that Taylor and McLennan's Archean crust was the contaminant. It is also possible that the granitoid gneisses within and surrounding the Abitibi Greenstone belt have a different composition than that estimated by Taylor and McLennan (1981). This needs to be verified by local sampling around Matagami.

CHAPTER 5

CONCLUSIONS

The geology of the Wabassee Group comprises a mafic to felsic calc-alkaline, submarine volcanic cycle. The group overlies and is interfingered with the rhyolitic rocks of the Watson Lake Group. At the east end of the area, near the base of the Wabassee Group, the New Hosco deposit is thought to be related to exhalations caused by the final episodes of Watson Lake Group volcanism. The rest of the Wabassee Group is composed of the Allard River volcanics, a group of variably spilitized pillowed and massive lavas which form a comagmatic suite describing fractional crystallization and assimilation in rocks that range in composition from Mg-tholeiitic basalt, through calc-alkaline andesite and dacite, to rhyolite. The volcanics are intruded by unrelated tholeiitic gabbro sills, and by synvolcanic gabbro-norite sills and stocks. These latter rocks were derived at least partly as accumulations of minerals in an andesitic or dacitic magma.

Unequivocal interpretation is impossible but the evidence indicates that the Allard River volcanics were formed by the combined processes of fractional crystallization and assimilation. Major element variations can be ascribed to extraction of two pyroxenes, plagioclase and magnetite. Variations in ratios of certain incompatible elements (Zr/Y, Zr/Nb, La/Yb) suggest on the other hand that the crystallizing magma was simultaneously assimilating its host.

Following volcanism the area was intruded by various mafic to felsic rocks, folded and faulted, and transected by a swarm of northeast striking diabase dikes.

CONTRIBUTIONS TO KNOWLEDGE AND RECOMMENDATIONS FOR FURTHER STUDIES

Two principal contributions to the understanding of the geology of the Matagami area are the result of this research. The Wabasee Group in the thesis was previously thought to be composed of dacitic and rhyolitic volcanics has been shown to consist of a mafic to felsic, calc-alkaline volcanic suite with associated synvolcanic intrusions. The volcanic rocks form a comagmatic suite related by the combined processes of fractional crystallization and assimilation.

At this point there remains several problems which warrant investigation. To the east the Wabassee volcanics are tholeiitic in character suggesting that this Group of rocks needs to be redefined. To the west, forestry operations are exposing new areas and mapping towards the Phelps-Dodge mine will soon be practical. Within the thesis area itself it would be usefull to look for field or petrographic evidence of assimilation. Finally, the geology around New Hosco mine is so poorly known that detailed mapping and systematic drilling are required to properly evaluate the area for it's massive sulfide potential.

REFERENCES

Abbey, S., 1980. Studies in "Standard Samples" for Use in the Analysis of Silicate Rocks and Minerals. Part 6. 1979 Edition of Usable Samples. Geological Survey of Canada, Paper 80-14, 30 p..

Anderson, T.W., 1958. An Introduction to Multivariate Statistical Analysis. John Wiley and Sons Inc., New York, 374 p..

Bancroft, J.A., 1912. A Report on the Geology and Natural Resources of Certain Parts of the Drainage Basins of the Harricanaw and Nottaway Rivers, to the North of the National Transcontinental Railway in Northwest Quebec. Quebec Bureau of Mines, Report on Mining Operations, pp. 131-198.

Beland, R., 1953. Allard River Area. Quebec Department of Mines, Geological Report 57, 30 p..

Bell, R., 1895. Geological Survey of Canada, Annual Report, Vol. III, Part A, pp. 74-85.

--------, 1900. Geology of the Basins of the Nottaway River. Geological Survey of Canada, Vol. XIII, Part K.

Bonavia, F.F., 1981. The Geology and Geochemistry of Radiore 2 Mine, Matagami, Quebec. Unpublished M.Sc. Thesis McGill University, Montreal.

Bowen, N.L., 1928. The Evolution of the Igneous Rocks. Princeton University Press, 332 p..

Carmichael, I.S.E., 1964. The Petrology of Thingmuli, a Tertiary Volcano in East Greenland. Journal of Petrology, Vol. 5, pp. 435-460.

Condie, K.C., Viljoen, M.J., and Kable, E.J.D., 1977. Effects of Alteration on Element Distributions in Archean Tholeiites from the Barberton Greenstone Belt, S.A.. Contributions to Mineralogy and Petrology, Vol. 64, pp. 65-89.

Davidson, A.J., 1977. Petrography and Chemistry of the Key Tuffite at Bell Allard, Matagami, Quebec. Unpublished M.Sc. Thesis, McGill University, Montreal, 131 p..

Davis, J.C., 1973. Statistics and Data Analysis in Geology. John Wiley and Sons Inc., New York, 550 p..

DePaolo, D.J., 1981. Trace Element and Isotopic Effects of Combined Wallrock Assimilation and Fractional crystallization. Earth and Planetary Science Letters, Vol. 53, pp. 189-202.

Douglas, R.J.W., 1972. Geology and Mineral Resources of Canada. Geological Survey of Canada, Economic Geology Series, No. 1, 934 p..

Freeman, B.C., 1936. Matagami Lake. Geological Survey of Canada, Map 571A.

----------, and Black, J.M., 1944. The Opaoka River Area. Quebec Department of Mines, Geological Report 16.

Gelinas, L., Brooks, C., Perrault, G., Carignan, J., Trudel, P., and Grasso, F., 1977. Chemo-Stratigraphic Subdivisions Within the Abitibi Volcanic Belt, Rouyn-Noranda, Quebec. In Baragar, W.R.A., Coleman, L.C., and Hall, J.M., (eds.), Volcanic Regimes in Canada. Geological Association of Canada,Special Paper 16, pp. 297-310.

----------, Mellinger, M., and Trudel, P., 1982. Archean Mafic Metavolcanics from Rouyn-Noranda District, Abitibi Greenstone Belt, Quebec. 1: Mobility of Major Elements. Canadian Journal of Earth Sciences, Vol. 19, pp. 2258-2275.

Goodwin, A.M., 1979. Archean Volcanic Studies in the Timmins-Kirkland Lake-Noranda Region of Ontario and Quebec. Geological Survey of Canada, Bulletin 278, 51 p..

Gordon, M., 1977a. MUSIC/STATPAK User Manual. McGill University Computing Center, 23 p..

----------, 1977b. MUSIC/STATPAK Reference Manual, 2nd Edition. McGill University Computing Center, 141 p..

Graham, R.B., 1960. Geology of the New Hosco Mines Ltd., Copper-Zinc Deposits, Matagami Area. (Abstract), Canadian Mining Journal, Vol. 81, p. 94.

Green, T.H., 1980. Island Arc and Continent-Building Magmatism. A Review of Petrogenetic Models Based on Experimental Petrology and Geochemistry. Contributions to Mineralogy and Petrology, Vol. 63, pp. 367-385.

Grove, T.L., Gerlach, D.C., and Sando, T.W., 1982. Origin of Calc-Alkaline Series Lavas at Medicine Lake Volcano by Fractionation, Assimilation and Mixing. Contributions to Mineralogy and Petrology, Vol. 80, pp. 160-182.

Hart, R.A., 1970. Chemical Exchange Between Sea Water and Deep Ocean Basalts. Earth and Planetary Science Letters, Vol. 9, pp. 269-279.

----, S.R., Erlank, A.J., and Kable, E.J.D., 1974. Sea Floor Basalt Alteration. Some Chemical and Sr Isotopic Effects. Contributions to Mineralogy and Petrology, Vol. 44, pp. 219-230.

----------, and Nalwalk, A.J., 1970. K, Rb, Cs, and Sr Relationships in Submarine Basalts from the Puerto Rico Trench. Geochemica Cosmochemica Acta, Vol. 34, p. 145.

Hekinian, R., 1971. Petrological and Geochemical Study of Spilites and Associated Rocks from St-John, U.S. Virgin Islands. Geological Society of America Bullitin, Vol. 82, pp. 659-681.

Hughes, C.J., 1973a. Spilites, Keratophyres, and the Igneous Spectrum. Geological Magazine, Vol. 109, No. 6, pp. 513-527.

------------, 1973b. Late Precambrian Volcanic Rocks of Avalon, Newfoundland. A Spilite/Keratophyre: Recognition and Implications. Canadian Journal of Earth Sciences, Vol. 10, pp. 272-282.

Irvine, T.N., and Baragar, W.R.A., 1971. A Guide to the Chemical Classification of the Common Volcanic Rocks. Canadian Journal of Earth Sciences, Vol. 8, pp. 523-548.

Jenney, C.P., 1961. Geology and Ore Deposits of the Matagami Area, Quebec. Economic Geology, Vol. 56, pp. 740-757.

Jensen, L.S., 1976. A New Cation Plot for Classifying subalkalic Volcanic Rocks. Ontario Ministry of Natural Resources, Miscellaneous Paper 66, 22 p..

Korzhinskii, D.S., 1957. Physicochemical Basis of the Analysis of the Paragenesis of Minerals. Chapman and Hall, London, 142 p..

Kuno, H., 1950. Petrology of Hakone Volcano and Adjacent Areas, Japan. Geological Society of America, Bulletin 61, pp. 957-1020.

Kuno, H., 1968. Origin of Andesite and its Bearing on the Island Arc Structure. Bulletin Volcanologique, Vol. 32, pp. 141-176.

Jolly, W.T., 1978. Metamorphic History of the Archean Abitibi Belt. In Fraser, and Heywood (eds.), Metamorphism in the Canadian Shield. Geological Survey of Canada, Paper 78-10, pp. 63-78.

Latulippe, M., 1959. The Matagami Area of Northwestern Quebec. Geological Association of Canada, Proceedings 11, pp. 46-54.

Longley, W.N., 1943. Kitchigama Lake Area. Quebec Department of Mines, Report 12, 34p..

Ludden, J.N., Gelinas, L., and Trudel, P., 1982. Archean Metavolcanics from the Rouyn-Noranda District, Abitibi Greenstone Belt. 2: Mobility of Trace Elements and Petrogenetic Constraints. Canadian Journal of Earth Sciences, Vol. 19, pp. 2276-2287.

MacLean, W.H., and MacGeehan, P.J., 1976. Garon Lake Mine, Matagami, Quebec. Case History. Mineral Exploration Research Institute, Dept. Geol. Sci., McGill University, Montreal.

MacGeehan P.J., 1978. The Geochemistry of Altered Volcanic Rocks at Matagami, Quebec: A Geothermal Model for Massive Sulfide Genesis. Canadian Journal of Earth Science, Vol. 15, No. 4, pp. 551-570.

----------, 1979. The Petrology and Geochemistry of Volcanic Rocks at Matagami, Quebec, and their Relationship to Massive Sulfide Mineralization. Unpublished Ph.D. Thesis, McGill University, Montreal, 414 p..

----------, and MacLean, W.H., 1980a. An Archean Sub-Seafloor Geothermal System, Calc-Alkaline Trends, and Massive Sulfide Genesis. Nature, Vol. 286, No. 5775, pp. 767-771.

----------, 1980b. Tholeiitic Basalt-Rhyolite Magmatism and Massive Sulfide Deposits at Matagami, Quebec. Nature, Vol. 283, No. 5743, pp. 153-157.

McBirney, A.R., 1968. Petrochemistry of the Cascade Andesite Volcanoes, Oregon. Department of Geology Mineralogy Ind., Bulletin 62, pp. 101-107.

----------, 1979. Effects of Assimilation. In Yoder H.S. Jr. (ed.), Evolution of the Igneous Rocks. Princeton University Press.

Miller, R.J., 1960. Geology of the Matagami Lake Area (Abstract). Canadian Institute of Mining and Metallurgy Bulletin 53, No. 575, p. 194.

Miyashiro, A., Shido, F., and Ewing, M., 1979. Diversity and Origin of Abyssal Tholeiites from the Mid-Atlantic Ridge near 24 and 30 Degrees Latitude. Contributions to Mineralogy and Petrology, Vol. 23, pp. 38-52.

O'Hara, M.J., 1980. Nonlinear Nature of the Unavoidable Long-lived Isotopic, Trace and Major Element Contamination of a Developing Magma Chamber. Philosophical Transactions of the Royal Society of London, A 297, pp.215-227.

Pearce, J.A., and Cann, J.R., 1973. Tectonic Setting of Volcanic Rocks Determined Using Trace Element Analyses. Earth and Planetary Science Letters, Vol. 19, pp. 290-300.

----------, and Norry, M.J., 1979. Petrogenetic Implications of Ti, Zr, Y, and Nb Variations in Volcanic Rocks. Contributions to Mineralogy and Petrology, Vol. 69, pp. 33-47.

Roberts, R.J., 1966. The Geology of the Matagami Lake Mine. Unpublished Ph.D. Thesis, McGill University, Montreal, 224 p..

----------, 1975. The Geological Setting of the Matagami Lake Mine, Matagami, Quebec. A Volcaniclastic Massive Sulfide Deposit. Economic Geology, Vol. 70, pp. 115-129.

----------, and Reardon, E.J., 1978. Alteration and Ore-Forming Processes at Matagami Lake Mine, Quebec. Canadian Journal of Earth Sciences, Vol. 15, pp. 1-21.

Sharpe, J.I., 1964. Precambrian Geology and Massive Sulfide Deposits of the Matagami Area, Quebec. Unpublished Ph.D. Thesis, McGill University, Montreal, 202 p..

----------, 1968. Geology and Sulfide Deposits of the Matagami Area, Abitibi East County, Quebec. Quebec Department of Natural Resources. Geological Report 137, 122p..

Shido, F., Miyashiro, A., and Ewing, M., 1974. Compositional Variation in Pillow Lavas from the Mid-Atlantic Ridge. Marine Geology, Vol. 16, pp. 177-190.

Taylor, S.R. and McLennan, S.M., 1981. Evidence from Rare-Earth Elements for the Chemical Composition of the Archean Crust. in Glover, J.E. and Groves, D.I. (eds.), Archean Geology, Geological Society of Australia, Special Publication No. 7, Second International Symposium, Perth, Australia, pp. 255-261.

Vallance, T.G., 1974. Spilitic Degredation of a Tholeiitic Basalt. Journal of Petrology, Vol. 15, pp. 79-96.

APPENDIX 1

SAMPLE PREPERATION PROCEDURES AND ANALYTICAL TECHNIQUES

Over 200 fist-sized samples of the various rock types in the thesis area were collected from accessible parts of outcrops. From these, approximatly 120 thin sections were made by Mr. Weiss of McGill University. Thin sections were described in detail prior to chosing specimens for chemical analysis in order to minimize alteration effects and thus ensure that the analyses represented primary magmatic features.

A total of 58 texturally fresh looking samples were powdered in a 2 or 3 step process outlined in table 2-1. Samples were analyzed at McGill University for major, minor and trace elements and at the University of Ottawa for major and minor elements. Pellet making procedures and XRF equipment are slightly different and are described seperatly.

Table 2-1: Crushing and grinding procedures. The three step procedure was used up to January, 1982, and the two step procedure thereafter.

	jaw crusher (steel jaws)	Beco grinder (ceramic plates)	Shatter box (Cr-steel puck)
	max. grain size	max. grain size	
3 step	2 cm	5 mm	3 min. minus 200 mesh
2 step	1 cm	---	40 sec. minus 200 mesh

University of Ottawa

Fused pellets were prepared by adding 4.500 g Li2B407 and 0.500 g Li2C03 to 1.500 g of rock powder. Samples were fused in platinum crucibles using a Claisse fluxer and subsequently cast in platinum molds. Loss on ignition was determined by measuring weight loss after heating about 1 g of rock powder for 20 minutes at 1050 degrees C.

Samples were analyzed on a Phillips PW 1410/20 X-ray fluorescence spectrometer using a rhodium tube. One standard (BCR-1) was analyzed in each run as a control on accuracy and precision.

Data were reduced to weight percent oxides on a main frame computer using a locally written program.

McGill University

Major and minor element chemistry was determined on fused pellets while trace elements were measured on pressed powder pellets. Fused pellets were made from a mixture of 5.0000 g Li2B407, 0.3000 g LiF, 0.01 g ammonium nitrate, 0.015 g lithium bromide, and 1.0000 g of sample rock powder. The mixture was fused in platinum crucibles using a Claisse fluxer and subsequently poured in platinum molds. Pressed pellets were prepared by compressing about 6 g of rock powder (plus a few drops of mowiol as a binding agent) in small aluminium cups to a load of 20 tons in a hydraulic press for 3 minutes.

The sample pellets were analyzed on a Phillips model PW-1400 X-ray spectrometer. Analytical techniques are summarized in XRF procedures, circular #1, McGill University (1983).

APPENDIX 2

RESULTS OF XRF ANALYSES

In the following pages (5) are listed the results of analyses made on the XRF spectrometers at McGill University and the University of Ottawa. Abbreviations are as follows: PL- pillow lava; ML- massive lava; c- center of pillow; m- margin of pillow; SL- sill; CM- chilled margin; por.- porphyritic; eq.- equigranular. Values on the first line of each sample are as determined using XRF techniques. Values on the second line are recalculated to 100 %, volatile-free with Fe2O3 converted to FeO.

Allard River lavas

	SiO_2	Al_2O_3	Fe_2O_3	FeO	MgO	CaO	Na_2O	K_2O	TiO_2	P_2O_5	MnO	LOI	SUM	Zr	Sr	Rb	Y	Nb
81c-001	49.78	16.86	10.28	----	6.01	9.36	2.76	0.24	1.05	0.24	0.16	3.31	100.05	119.	414.	5.8	13.7	9.4
PL	52.23	17.69	-----	9.28	6.31	9.82	2.90	0.25	1.11	0.25	0.17							
81c-004	54.02	15.75	8.47	----	5.52	9.54	2.00	0.70	0.75	0.00	0.12	2.51	99.38	96.	354.	25.	10.3	8.8
ML	56.44	16.45	----	7.64	5.77	9.97	2.09	0.73	0.78	0.00	0.12							
81c-005	56.66	16.01	8.09	----	4.22	7.91	3.16	0.16	0.55	0.15	0.10	2.36	99.57	111.	211.	5.7	11.4	8.9
ML	58.92	16.65	----	7.55	4.39	8.22	3.28	0.16	0.57	0.15	0.10							
81c-011b	52.49	16.41	9.16	----	4.97	8.11	3.84	0.63	0.80	0.17	0.15	2.35	99.09	88.	232.	22.	10.5	7.5
ML	54.80	17.13	----	8.58	5.19	8.47	4.01	0.66	0.83	0.18	0.16							
81c-012b	54.41	16.68	9.39	----	6.44	6.33	3.80	0.96	0.59	0.03	0.14	1.74	100.51	101.	212.	24.	11.1	7.3
PL	55.72	17.09	----	8.46	6.60	6.48	3.89	0.98	0.60	0.03	0.14							
81c-013a	53.85	15.99	8.13	----	4.72	9.48	2.95	0.70	0.75	0.04	0.13	2.11	98.85	91.	198.	21.	10.2	8.3
SL	56.31	16.72	----	7.33	4.94	9.91	3.09	0.73	0.78	0.04	0.14							
81c-013b	57.50	14.96	8.74	----	5.15	8.04	3.14	0.65	0.79	0.06	0.14	1.63	100.82	81.	237.	17.	10.5	5.9
PL	58.57	15.24	----	7.88	5.26	8.19	3.19	0.66	0.80	0.06	0.14							
81c-017	44.65	17.15	12.74	-----	8.46	7.65	2.68	0.91	1.02	0.09	0.20	4.64	100.79	61.	108.	29.	12.9	7.0
PL	47.35	18.82	-----	11.54	8.92	8.11	2.85	0.97	1.08	0.09	0.21							
81c-021	54.80	15.60	8.84	----	4.32	10.18	2.73	0.07	0.87	0.18	0.12	2.13	99.84	89.	242.	3.3	10.8	7.3
ML	56.61	16.12	----	8.20	4.46	10.52	2.82	0.07	0.90	0.18	0.12							
81c-024a	47.99	15.44	11.93	-----	7.33	9.52	2.92	0.15	0.77	0.00	0.20	3.15	99.42	40.	108.	6.1	9.0	6.0
PL-c	50.94	16.38	-----	10.50	7.78	10.11	3.10	0.16	0.82	0.00	0.21							
81c-024b	46.61	14.57	11.91	-----	7.59	13.01	1.00	0.10	0.77	0.00	0.19	2.92	98.67	41.	135.	5.8	9.0	5.5
PL-m	49.60	15.50	-----	10.79	8.07	13.85	1.06	0.11	0.82	0.00	0.20							
81c-026	47.30	14.01	12.20	-----	6.27	15.51	0.97	0.11	0.89	0.07	0.19	2.90	100.43	45.	208.	5.4	9.7	4.8
ML	49.14	14.55	-----	11.37	6.51	16.11	1.01	0.11	0.91	0.07	0.19							
81c-028b	46.50	15.64	11.92	-----	7.47	13.30	0.20	0.13	0.88	0.00	0.18	2.95	99.17	48.	181.	6.3	9.9	5.3
SL	49.20	16.55	-----	10.79	7.91	14.08	0.21	0.14	0.93	0.00	0.19							
81c-030a	47.63	14.02	11.96	-----	5.98	15.13	0.18	0.07	0.83	0.00	0.18	2.05	98.03	44.	168.	4.2	9.7	5.7
PL-c	50.55	14.88	-----	10.83	6.35	16.06	0.19	0.07	0.88	0.00	0.19							
81c-030b	49.37	14.65	12.33	-----	6.99	9.73	2.60	0.30	0.91	0.08	0.20	2.67	99.81	44.	115.	9.7	10.5	5.6
PL-m	51.49	15.28	-----	11.54	7.29	10.15	2.71	0.31	0.95	0.08	0.21							

Allard River lavas (cnt'd)

	SiO_2	Al_2O_3	Fe_2O_3	FeO	MgO	CaO	Na_2O	K_2O	TiO_2	P_2O_5	MnO	LOI	SUM	Zr	Sr	Rb	Y	Nb
81c-036	60.19	15.31	7.28	----	4.51	5.58	3.80	0.68	0.68	0.06	0.12	2.02	100.23	106.	168.	23.	10.2	7.8
ML	61.84	15.73	----	6.56	4.64	5.73	3.91	0.70	0.70	0.06	0.12							
81c-038	49.15	14.39	12.43	----	6.71	11.95	1.82	0.31	0.85	0.00	0.21	2.18	100.00	43.	119.	10.6	10.1	5.9
PL	51.08	14.96	-----	11.23	6.98	12.42	1.89	0.32	0.89	0.00	0.22							
81c-041	46.60	15.52	11.16	-----	6.60	14.65	1.43	0.15	0.79	0.00	0.18	2.78	99.86	50.	210.	6.9	8.5	6.1
PL	48.76	16.24	-----	10.08	6.91	15.33	1.50	0.16	0.83	0.00	0.19							
81c-056a	56.99	16.57	8.05	----	5.57	4.63	4.60	0.60	0.86	0.12	0.12	2.69	100.80	89.	242.	3.3	10.8	7.8
PL	58.70	17.07	----	7.26	5.74	4.76	4.73	0.61	0.88	0.12	0.12							
81c-056b	57.93	15.24	7.80	----	5.27	5.78	4.06	0.64	0.67	0.06	0.12	2.30	99.87	96.	183.	14.	11.3	8.3
SL	60.00	15.78	----	7.03	5.46	5.99	4.20	0.66	0.69	0.06	0.12							
81c-068	54.81	15.42	8.23	----	5.30	8.25	3.12	0.60	0.94	0.18	0.12	2.64	99.61	100.	199.	11.4	12.2	9.4
PL	57.02	16.04	----	7.69	5.51	8.58	3.24	0.62	0.98	0.19	0.12							
81c-069	54.60	16.91	8.40	----	4.28	9.20	1.94	0.56	0.76	0.15	0.10	2.89	99.80	116.	254.	18.	13.0	9.9
SL	56.85	17.61	----	7.85	4.46	9.58	2.02	0.58	0.79	0.15	0.10							
81c-072	56.60	16.56	7.84	----	4.17	8.51	2.38	0.71	0.67	0.03	0.12	2.28	99.87	110.	230.	16.	12.0	9.0
ML	58.61	17.15	----	7.07	4.32	8.81	2.46	0.73	0.69	0.03	0.12							
81c-074	54.60	15.64	9.38	----	5.57	6.21	3.41	0.57	1.00	0.18	0.15	3.04	99.74	107.	182.	15.8	12.3	7.6
ML	57.03	16.33	----	8.79	5.82	6.48	3.56	0.59	1.04	0.19	0.16							
81c-077	59.29	15.71	6.71	----	3.40	8.22	3.12	0.33	0.61	0.13	0.10	2.63	100.26	96.	154.	8.2	9.2	7.9
ML	61.17	16.21	----	6.21	3.51	8.48	3.22	0.34	0.63	0.13	0.10							
81c-085	56.86	15.26	8.91	----	5.07	7.42	3.04	0.35	0.92	0.19	0.14	1.92	100.09	88.	202.	9.9	10.9	6.2
ML	58.48	15.69	----	8.22	5.21	7.63	3.13	0.36	0.95	0.19	0.14							
81c-093	56.18	16.28	8.03	----	4.76	7.82	3.47	0.23	0.69	0.14	0.12	2.62	100.34	115.	215.	6.0	11.0	9.2
ML	57.98	16.80	----	7.44	4.91	8.07	3.58	0.24	0.71	0.14	0.12							
81c-097	58.34	14.87	6.61	----	3.05	10.80	0.90	0.05	0.55	0.00	0.09	2.03	97.29	102.	386.	3.0	7.8	7.4
ML	61.80	15.76	----	6.10	3.23	11.44	0.96	0.05	0.59	0.00	0.09							
81c-101a	57.48	16.92	7.82	----	4.85	7.13	2.91	0.51	0.67	0.08	0.11	2.85	101.33	113.	247.	19.	10.8	9.0
ML	59.00	17.36	----	7.06	4.88	7.32	2.99	0.52	0.68	0.08	0.11							
81c-135a	49.17	14.74	12.71	-----	6.26	12.32	1.02	0.23	0.90	0.00	0.21	2.37	99.93	47.	192.	8.7	11.3	6.6
PL	51.29	15.38	-----	11.48	6.53	12.85	1.07	0.24	0.94	0.00	0.22							

Allard River lavas (cnt'd)

	SiO_2	Al_2O_3	Fe_2O_3	FeO	MgO	CaO	Na_2O	K_2O	TiO_2	P_2O_5	MnO	LOI	SUM	Zr	Sr	Rb	Y	Nb
81c-135b	48.40	15.10	12.82	-----	6.98	13.29	0.99	0.20	0.89	0.00	0.22	2.44	101.33	46.	153.	7.2	9.6	5.9
PL	49.73	15.51	-----	11.57	7.17	13.66	1.02	0.20	0.92	0.00	0.22							
81c-140a	56.02	13.45	7.22	----	9.39	7.14	3.47	0.24	0.60	0.10	0.13	1.72	99.48	90.	351.	5.7	8.9	7.3
ML	57.85	13.89	----	6.51	9.69	7.37	3.59	0.25	0.62	0.10	0.13							
81c-142b	60.97	13.73	7.43	----	4.16	7.92	3.39	0.32	0.63	0.03	0.12	0.93	99.63	102.	103.	9.0	11.6	8.3
ML	62.33	14.03	----	6.69	4.26	8.10	3.46	0.33	0.64	0.03	0.12							
81c-158	51.20	15.95	10.81	----	4.52	9.59	3.47	0.03	1.02	0.01	0.17	3.30	100.07	85.	192.	3.0	13.9	8.5
PL	53.74	16.74	-----	9.78	4.75	10.07	3.64	0.03	1.07	0.01	0.18							
81c-177a	56.69	16.35	8.23	----	5.73	6.54	3.22	0.47	0.73	0.06	0.13	1.99	100.14	109.	216.	18.	11.1	9.0
PL	58.38	16.83	----	7.42	5.90	6.73	3.31	0.48	0.75	0.06	0.13							
81c-179	64.92	15.02	5.51	----	2.91	4.89	3.81	0.88	0.46	0.04	0.09	0.93	99.46	166.	206.	18.	14.	11.4
ML	66.34	15.35	----	4.96	2.97	4.99	3.89	0.90	0.47	0.04	0.09							
81c-184	59.99	14.98	7.57	----	5.27	7.47	3.14	0.19	0.61	0.04	0.12	0.68	100.06	89.	207.	6.2	8.9	7.5
PL	60.89	15.21	----	6.81	5.35	7.58	3.20	0.19	0.62	0.04	0.12							

Gabbro-Norite

81c-020	54.82	10.00	9.33	----	13.60	4.55	1.92	0.33	0.34	0.08	0.17	4.09	99.23	65.	65.	8.4	4.3	6.7
	58.21	10.62	----	8.89	14.44	4.83	2.04	0.35	0.36	0.08	0.19							
81c-114a	56.84	13.28	7.68	----	8.90	6.51	2.08	0.52	0.41	0.00	0.13	2.98	99.33	93.	197.	21.	7.2	8.1
	59.65	13.94	----	6.93	9.34	6.83	2.18	0.54	0.43	0.00	0.14							
81c-116	56.47	14.99	7.35	----	6.87	5.87	2.65	0.83	0.53	0.07	0.11	2.73	98.47	119.	162.	27.	10.5	9.0
	59.65	15.84	----	6.64	7.25	6.20	2.80	0.88	0.56	0.07	0.12							
81c-132	51.72	13.44	7.75	----	11.83	8.48	1.72	0.47	0.38	0.00	0.13	3.76	99.68	63.	238.	16.	4.6	7.3
	54.56	14.17	----	7.00	12.48	8.94	1.81	0.49	0.40	0.00	0.14							
81c-151b	58.31	15.60	7.35	----	3.82	8.77	2.48	0.16	0.54	0.12	0.10	1.89	99.16	123.	216.	6.2	9.9	9.7
CM	60.43	16.17	----	6.84	3.96	9.09	2.57	0.16	0.56	0.12	0.10							
81c-152a	56.74	13.31	7.29	----	9.15	6.31	2.46	0.62	0.42	0.09	0.09	2.55	99.03	88.	123.	22.5	7.5	7.9
	59.27	13.90	----	6.84	9.56	6.59	2.57	0.65	0.44	0.09	0.09							
82c-18	55.88	11.77	8.97	----	11.16	5.13	2.24	0.50	0.46	0.10	0.13	4.05	100.39	88.	84.	13.7	7.1	8.5
	58.57	12.34	----	8.44	11.70	5.38	2.35	0.52	0.48	0.10	0.13							

Allard River Rhyolite

	SiO_2	Al_2O_3	Fe_2O_3	FeO	MgO	CaO	Na_2O	K_2O	TiO_2	P_2O_5	MnO	LOI	SUM	Zr	Sr	Rb	Y	Nb
82c-06	72.93	10.77	3.83	----	0.13	9.08	0.36	0.36	0.17	0.02	0.06	1.36	99.07	356.	339.	10.6	51.6	20.3
	74.94	11.07	----	3.53	0.13	9.33	0.37	0.37	0.17	0.02	0.06							
Rhyolite dike																		
82c-15a	68.65	13.96	4.74	----	1.05	4.59	4.57	0.32	0.51	0.11	0.04	1.49	100.03	212.	96.	10.8	20.2	13.7
	70.02	14.24	----	4.34	1.07	4.68	4.66	0.32	0.52	0.11	0.04							
Felsic dike																		
82c-02	76.91	12.71	0.62	----	0.03	0.84	5.28	1.81	0.07	0.02	0.01	0.28	98.57	81.	71.	28.	7.3	16.0
	78.30	12.94	----	0.57	0.03	0.85	5.37	1.84	0.07	0.02	0.01							
Tonalite intrusion																		
81c-181	67.16	15.83	2.52	----	1.65	3.51	5.46	1.36	0.30	0.06	0.04	0.99	98.88	113.	483.	38.	5.8	8.7
	68.73	16.20	----	2.34	1.69	3.59	5.59	1.39	0.31	0.06	0.04							
Basic dikes																		
81c-043	52.69	13.00	7.57	----	8.79	9.72	3.17	1.93	0.70	0.35	0.12	2.22	100.26	151.	284.	36.	12.7	8.9
por.	54.04	13.33	----	7.04	9.02	9.97	3.25	1.98	0.72	0.36	0.12							
81c-114b	53.03	14.93	9.89	----	7.26	7.57	3.28	0.47	0.64	0.26	0.14	3.51	100.98	106.	301.	8.9	14.4	9.3
eq.	54.81	15.43	----	9.27	7.50	7.82	3.39	0.49	0.66	0.27	0.14							
Watson Lake Group rhyolite																		
81c-133	69.33	12.68	3.20	----	1.41	3.17	2.81	2.40	0.50	0.00	0.13	4.48	100.17	537.	61.	46.	136.	37.
	72.62	13.28	----	3.03	1.48	3.32	2.94	2.51	0.52	0.00	0.14							
82c-22a	70.43	10.58	10.58	----	1.71	0.68	0.76	1.91	0.71	0.15	0.04	1.96	99.51	356.	32.	33.	123.	29.
	72.99	10.97	-----	9.87	1.77	0.71	0.79	1.98	0.74	0.16	0.04							
82c-23a	71.00	11.43	7.93	----	1.08	2.72	4.66	0.12	0.59	0.10	0.13	0.43	100.19	472.	51.	4.4	148.	37.
	71.74	11.55	----	7.21	1.09	2.75	4.71	0.12	0.60	0.10	0.13							
Chloritized Allard River lava																		
81c-169	51.29	12.92	7.13	----	4.35	10.37	3.23	0.11	0.58	0.00	0.14	10.7	100.86	68.	71.	5.7	3.8	6.2
	57.24	14.42	----	7.22	4.85	11.57	3.60	0.12	0.65	0.00	0.16							

Tholeiitic Gabbro sill

	SiO_2	Al_2O_3	Fe_2O_3	FeO	MgO	CaO	Na_2O	K_2O	TiO_2	P_2O_5	MnO	LOI	SUM	Zr	Sr	Rb	Y	Nb
82c-04	48.45	13.09	16.65	-----	5.05	8.90	2.55	0.21	1.73	0.14	0.22	2.86	99.85	99.	117.	9.1	27.	8.8
	49.95	13.50	-----	15.42	5.21	9.18	2.63	0.22	1.78	0.14	0.23							

Diabase dikes

81c-061b	51.07	14.38	10.48	----	6.82	10.77	1.87	1.13	0.61	0.00	0.18	1.60	98.91	55.	120.	44.	15.	6.2
	52.88	14.89	-----	9.85	7.06	11.15	1.94	1.17	0.63	0.00	0.19							
81c-066a	49.18	14.30	17.01	-----	4.99	9.79	2.19	0.40	1.83	0.05	0.24	0.88	100.86	119.	136.	16.	28.	11.6
	49.84	14.49	-----	15.65	5.06	9.92	2.22	0.41	1.85	0.05	0.24							
81c-096b	50.08	14.19	15.62	-----	6.31	10.41	1.91	0.26	1.52	0.00	0.24	0.49	101.03	98.	120.	9.9	23.	11.1
CM	50.34	14.26	-----	14.30	6.34	10.46	1.92	0.26	1.53	0.00	0.24							

APPENDIX 3

PRECISION AND ACCURACY OF XRF ANALYSES

Samples were analyzed on two XRF spectrometers: at McGill University and at the University of Ottawa. Consequently, precision and accuracy are calculated seperatly for each data set.

University of Ottawa

The mean and standard deviation calculated from 23 analyses made at the University of Ottawa are shown in table 3-1.

Table 3-1: Mean and standard deviation of BCR-1 as calculated from determinations made at the University of Ottawa and published value for BCR-1 by Abbey (1980). N=23.

	mean	standard deviation	Abbey (1980)
SiO2	54.5	0.4	54.53
TiO2	2.20	0.02	2.26
Al2O3	13.64	0.09	13.72
Fe2O3	13.4	0.19	13.41
MnO	0.19	0.00	0.18
MgO	3.46	0.06	3.48
CaO	7.00	0.05	6.97
Na2O	3.3	0.1	3.30
K2O	1.70	0.02	1.70
P2O5	0.33	0.03	0.36

Precision of analyses is indicated by standard deviation. For silica precision is 0.4 wt%, for Fe2O3, 0.19, and for Na2O, 0.1. All other oxides are better than 0.1 wt%.

For accuracy compare mean values for BCR-1 with the published value by Abbey (1980).

Table 3-2 lists the samples which were analyzed for major elements at the University of Ottawa.

Table 3-2: Identification numbers of samples analyzed for major elements at the University of Ottawa.

81c-001	81c-004	81c-012b
-013a	-013b	-017
-024a	-024b	-028b
-029	-030a	-036
-038	-041	-043
-056a	-056b	-061b
-066a	-072	-096b
-097	-101a	-114a
-114b	-116	-132
-133	-135a	-135b
-140a	-142b	-158
-169	-177a	-179
-181	-184	

McGill University

Precision of XRF analyses at McGill University are shown in table 3-3. Standard deviations for major and minor elements are better than 0.1 %; trace elements are better than 1.1 ppm.

Compare measured values (A) with published values (B) from Abbey (1980) for major, minor and trace elements in tables 3-4a and b. Note the great similarity in values for various rock compositions.

Table 3-3: Precision of XRF analyses at McGill University. N=10. Sample number 81c-093.

	mean	standard deviation
SiO2	56.36	0.09
TiO2	0.69	0.004
Al2O3	16.26	0.02
Fe2O3	8.02	0.007
MnO	0.12	0.001
MgO	4.79	0.04
CaO	7.83	0.006
Na2O	3.49	0.06
K2O	0.23	0.002
P2O5	0.13	0.003
Rb	18.0	0.5
Sr	249.2	0.5
Y	11.4	0.8
Zr	110.9	0.7
Nb	9.1	1.1

Table 3-4a: Accuracy of Major and minor element analyses at McGill University.

	MRG-1 III gabbro		GS-N II granite	
	A	B	A	B
SiO2	39.28	39.32	65.99	65.98
TiO2	3.58	3.69	0.67	0.68
Al2O3	8.49	8.50	14.88	14.71
Fe2O3	17.60	17.82	3.74	3.76
MnO	0.17	0.17	0.05	0.056
MgO	13.53	13.49	2.33	2.31
CaO	14.94	14.77	2.46	2.51
Na2O	0.78	0.71	3.70	3.78
K2O	0.19	0.18	4.66	4.64
P2O5	0.062	0.06	0.277	0.28

	NIM-D III dunite		NIM-N I norite	
	A	B	A	B
SiO2	39.21	38.96	52.29	52.64
TiO2	0.02	0.02	0.19	0.20
Al2O3	0.31	0.30	16.63	16.50
Fe2O3	16.89	16.96	8.88	8.91
MnO	0.22	0.22	0.17	0.18
MgO	43.96	43.51	7.60	7.50
CaO	0.28	0.28	11.46	11.50
Na2O	0.03	0.04	2.42	2.46
K2O	0.01	0.01	0.24	0.25
P2O5	0.007	0.01	0.02	0.03

A= Measured at McGill University
B= From Albey, 1980

Table 3-4b: Accuracy of trace element analyses at McGill University.

	BR		QMC-2		DRN	
	A	B	A	B	A	B
Rb	49.2	47.	284.2	310.	73.7	75.
Sr	1318.4	1300.	187.0	185.	384.7	400.
Y	27.8	30.	55.8	60.	23.6	N.D.
Zr	277.6	250.	92.2	100.	133.7	125.
Nb	118.3	100.	9.5	N.D.	10.2	N.D.

	SY-2		BCR-1		BM (N=4)	
	A	B	A	B	A	B
Rb	194.0	220.	49.6	47.	9.4	12.
Sr	240.1	275.	326.4	330.	217.2	230.
Y	131.5	130.	32.6	40.	23.5	26.
Zr	283.8	280.	186.7	185.	104.5	105.
Nb	30.0	23.	15.2	19.	7.5	N.D.

A= Measured at McGill University
B= From Albey, 1980.
N.D.= No data available

APPENDIX 4

RESULTS OF RARE EARTH ELEMENT ANALYSES

Three samples of Allard River volcanics, one basalt and two andesites were analyzed by instrumental neutron activation analysis at l'Universite de Montreal. Analyses are shown in table 4-1 in ppm and normalized to chondrite abundances.

Table 4-1: Rare earth element determinations on Allard River volcanics.

	81c-001		81c-135a		81c-177a	
	ppm	/chon	ppm	/chon	ppm	/chon
La	17.70	56.19	2.30	7.30	10.90	34.60
Ce	43.0	52.89	8.00	9.84	25.00	30.75
Nd	19.60	32.83	5.20	8.71	7.90	13.23
Sm	4.10	21.35	1.70	8.85	2.40	12.50
Eu	1.30	18.01	0.70	9.70	0.70	9.70
Tb	0.50 ?	10.20 ?	0.50 ?	10.20 ?	0.40	8.16
Tm	0.20	6.67	0.20	6.67	0.10 ?	3.33 ?
Yb	1.90	9.13	1.20	5.77	1.10	5.29
Lu	0.20	6.19	0.30	9.29	0.20	6.19

/chon= values divided by chondrite abundance
?= uncertain values (Ludden, pers. comm.)

APPENDIX 5

DISCRIMINANT ANALYSIS

Outline of theory

Discriminant analysis is a mathematical procedure that optimizes the criteria for the classification of a sample population into two or more groups. Two principle methods have been devised which can be called discriminant: the single function and the multiple functions methods. In the first technique, all groups are defined in terms of ranges of value of a single function, the result defining seperate domains on a bar graph as in figure B-1. In this figure, X1 and X2 each occupy a domain with their mutual boundary at half the distance between the means of each group. Although this method is easier to compute than the next procedure, the geometry of a bar graph makes it almost impossible to study the interelationships between more than two groups. In contrast, however, the second method does not suffer from this limitation because one function is generated for each group and these functions can be used as coordinate axes in binary and ternary diagrams (figures B-2a,b).

A multi-function discriminant procedure was executed on MUSIC/STATPAK, a large, multi-purpose, interactive computer program written at McGill University containing numerous standard statistical routines. An outline of the various procedures available on STATPAK can be found in Gordon (1977a,1977b) both of which are published by the McGill University computing center. For an introduction to the subject of discriminant analysis, the reader is referred to Davis (1973). A more rigorous treatment of the subject can be found in Anderson (1958).

Simply stated, discriminant analysis is a procedure which consists of finding the linear combination of variables from a set of observations that has the largest distance in N-dimensional space between the group means and the smallest variances within each group. In the present application, observation points comprising ten variables representing chemical concentrations in weight percent are subdivided into three groups. The groups are defined a priori on the basis of geographical position and field relationships.

As a first step in the procedure a pooled dispersion matrix is constructed as follows:

$$P = \sum_{K=1}^{g} S_K \div \sum_{K=1}^{g} N_K - g \qquad (1)$$

where G= number of groups
Nk= sample size of k-th group

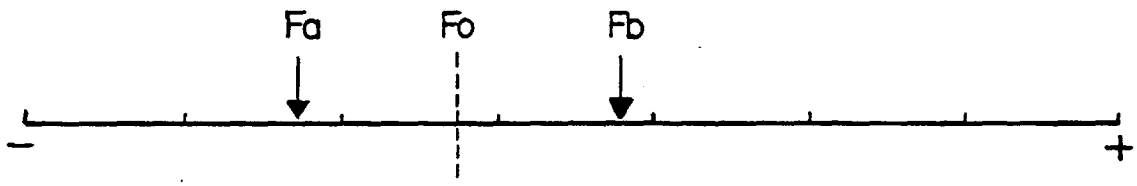


Figure B-1: Projection of two groups of samples onto a discriminant function represented by a bar graph. Fa and Fb are the multivariate means of groups a and b respectively. Fo is the discriminant index and the boundary between domains a and b. The difference between Fa and Fb is the Mahalanobis index (D2). From Davis (1973, p.450).

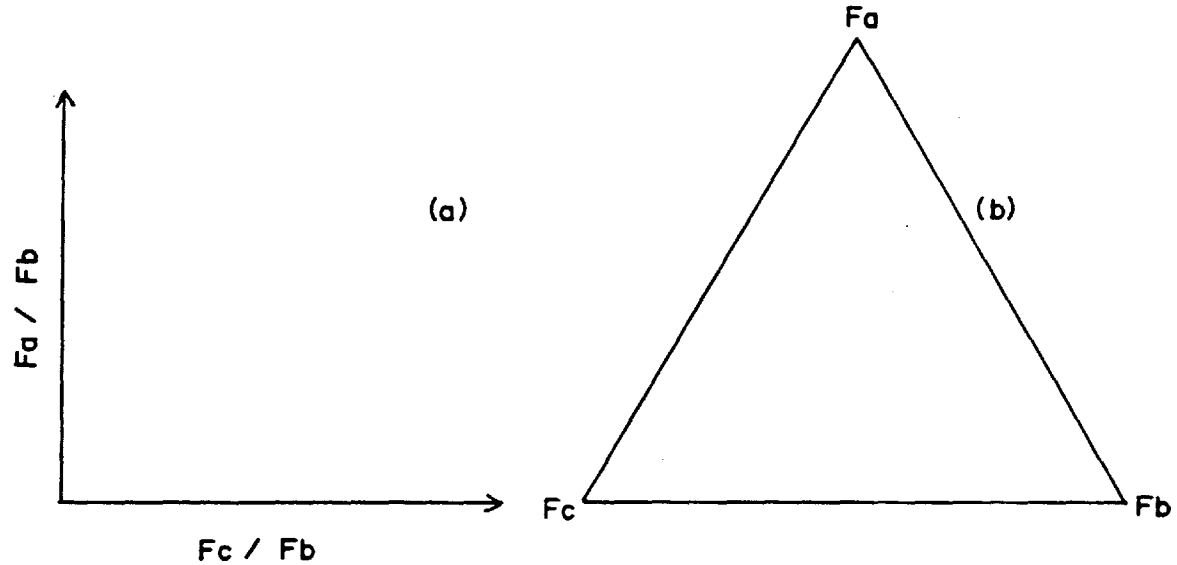


Figure B-2: Binary and ternary diagrams representing discriminant functions Fa, Fb, and Fc on orthogonal and apices of the diagrams.

and

$$S_K = \sum_{i=1}^{N_K} (X_{ijK} - \bar{X}_{jK})(X_{iLK} - \bar{X}_{LK}) \qquad (2)$$

where J=1,2,3,...,m and
L=1,2,3,...,m are variables,

and I=1,2,3,...,Nk are sample numbers.

The mean of each variable of each group is required for 2:

$$\bar{X}_{jK} = \sum_{i=1}^{N_k} X_{ijK} \div N_K \qquad (3)$$

For all groups combined the common means are obtained by:

$$\bar{X}_j = \sum_{K=1}^{g} N_K \bar{X}_{jK} \div \sum_{K=1}^{g} N_K \qquad (4)$$

Using this information we can calculate a discriminant function Fk of the form:

$$F_K = a_{1K} X_{1K} + a_{2K} X_{2K} + \ldots + a_{nK} X_{mK} + C \qquad (5)$$

for each group of samples by the following equations:

$$C_{jK} = \sum_{J=1}^{m} D_{jL} \bar{X}_{jK} \qquad (6)$$

where Djl= the inverse element of the pooled dispersion matrix P

and

$$C_{oK} = -\tfrac{1}{2} \sum_{J=1}^{m} \sum_{L=1}^{m} D_{jL} \bar{X}_{jK} \bar{X}_{LK} \qquad (7)$$

The parameters Cik and Cok are the matrices of the variable coefficients and constants of Fk respectively.

For each i-th case in each k-th group the g discriminant functions are calculated as follows:

$$F_K = \sum_{J=1}^{m} C_{jK} X_{ijK} + C_{oK} \qquad (8)$$

The function Fk with the largest numerical value is the group k which the i-th sample was taken from. The probability of correct classification is:

$$P_L = 1 \div \sum_{k=1}^{g} e^{(F_k - F_L)} \qquad (9)$$

where Fl= the value of the largest discriminant function

l= the subscript of the largest discriminant function.

By making a number of assumptions about the nature of the data it is possible to test the significance of the seperation between the groups. Davis (1973) outlines five basic assumptions:

a) The observations in each group are randomly chosen;

b) the probability of misclassifying a specimen is the same for all groups considered;

c) variables are normally distributed within each group;

d) the variance-covariance matrices Sk of all groups are equal in size;

e) none of the observations used to calculate the discriminant functions were misclassified.

Assumptions "b" and "d" are considered to be justifiable while "a", "c", and "e" are uncertain. Fortunatly, small departures from normality do not greatly affect the behavior of the discriminant functions (Davis,1973) and consequently we can assume that "c" will hold true. On the other hand it is difficult to verify the correctness of "a" because although samples were collected randomly from various outcrops, the distribution of outcrops is controlled by geomorphic conditions which may or may not be probabilistic in nature. However, this effect is probably minimized as samples have been collected from many flows in the volcanic cycle. Assumption "e" may also be problematical. The main difficulty lies in the determination of the boundary between the Watson Lake and Wabassee groups on the northern limb of the anticlinorium. The result of misclassification of the witness samples in this case is to make the measured distance between McGeehan's and MacLean's samples less than the maximum possible if assumption "e" was true and verifiable.

The distance in N-dimensional space between two or more groups of samples is defined by the Mahalanobis D-square statistic:

$$D^2 = \sum_{j=1}^{m} \sum_{L=1}^{m} D_{jL} \sum_{k=1}^{g} N_k (\bar{X}_{jk} - \bar{X}_j)(\bar{X}_{Lk} - \bar{X}_L) \quad (10)$$

The D-square statistic can be used as a CHI-square test under the assumption of normality with m(g-1) degrees of freedom.

Using the Mahalanobis D-square coefficient it is possible to test the significance of the distance between the various groups taken two at the time by transforming the D-square statistic into a standard F-test by the following (Davis,1973):

$$F = \left(\frac{N_a + N_b - m - 1}{(N_a + N_b - 2)\, m}\right) \left(\frac{N_a N_b}{N_a + N_b}\right) D^2 \quad (11)$$

with m and (Na+Nb-m-1) degrees of freedom.

The hypothesis tested by the F-distribution is that the multivariate means of the two groups are equal against their not being equal.

To test the significance of the results, discriminant analysis was run on the samples taken two groups at one time. Three values of D-square and F obtained by this process are presented below (table B-1).

Table B-1: Computed D-square and F-distribution values and critical F-distribution values for samples from MacGeehan (1979), MacLean (unpublished), and this study. * Value taken from Davis (1973), p.102 for =0.05 level of significance.

	D-square	F	critical F-distribution value*
MacGeehan vs MacLean	347	457	1.84
MacGeehan vs this study	784	778	1.93
MacLean vs this study	664	659	1.93

Also shown are the critical F-distribution values for each group pair. Pairs of groups with F values less than the critical value are considered to be equal because they cannot be resolved on the basis of their variances. As can be seen in the table the F values are very much greater than the critical value, demonstrating that the groups are in effect different.

Example of computer output

A typical output from the discriminant analysis routine in Statpak is presented in the following pages. The output contains:

-the pooled dispersion matrix,
-the common means,
-the generalized Mahalanobis D-square index,
-number of degrees of freedom,
-statistical significance of D score,
-discriminant functions,
-group means,
-if requested, the evaluation of each sample.

POOLED DISPERSION MATRIX

ROW 1 (VAR. 1)					
8.061	-0.134	-0.035	-3.311	-1.992	-3.185
0.573	0.196	0.169	-0.016		
ROW 2 (VAR. 2)					
-0.134	0.056	-0.093	0.231	-0.018	-0.036
0.000	-0.001	0.014	-0.002		
ROW 3 (VAR. 3)					
-0.035	-0.093	0.750	-0.363	0.064	-0.171
0.033	0.037	-0.031	-0.001		
ROW 4 (VAR. 4)					
-3.311	0.231	-0.363	2.695	0.608	0.715
-0.421	-0.055	0.005	0.010		
ROW 5 (VAR. 5)					
-1.992	-0.018	0.064	0.608	1.285	0.265
-0.008	-0.011	-0.088	0.001		
ROW 6 (VAR. 6)					
-3.185	-0.036	-0.171	0.715	0.265	3.484
-0.891	-0.230	-0.079	0.010		
ROW 7 (VAR. 7)					
0.573	0.000	0.033	-0.421	-0.008	-0.891
0.760	0.013	-0.011	-0.007		
ROW 8 (VAR. 8)					
0.196	-0.001	0.037	-0.055	-0.011	-0.230
0.013	0.049	0.009	0.002		
ROW 9 (VAR. 9)					
0.169	0.014	-0.031	0.005	-0.088	-0.079
-0.011	0.009	0.021	0.001		
ROW 10 (VAR.10)					
-0.016	-0.002	-0.001	0.010	0.001	0.010
-0.007	0.002	0.001	0.001		

COMMON MEANS

51.623	1.487	13.703	14.483	5.192	8.813
2.672	0.308	0.245	0.209		

DO YOU WISH TO COMPUTE THE GENERALIZED MAHALANOBIS D-SQUARE
?

yes

GENERALIZED MAHALANOBIS D-SQUARE 926.8894
DEGREES OF FREEDOM 20
SIGNIFICANCE 0.0

DISCRIMINANT FUNCTIONS

1	CONSTANT	-7330.62629				
	COEFF.	155.87025	77.15299	123.79683	160.68869	134.67373
		166.79428	162.19577	244.23463	15.74916	-32.67400
2	CONSTANT	-7520.48927				
	COEFF.	158.07556	81.35176	122.49406	164.72384	135.58538
		168.59601	165.11993	246.04357	7.29309	30.90423
3	CONSTANT	-7712.64176				
	COEFF.	159.51478	100.06827	126.21640	165.86887	135.78026
		168.79891	166.33470	238.70475	1.28185	104.64561

DO YOU WISH TO EVALUATE DISCRIMINANT FUNCTIONS FOR EACH OBSERVATION
?
yes

	CASE NO.	LARGEST FUNCTION	ASSOCIATED PROBABILITY	LARGEST FUNCT.NO.
GROUP 1				
	1	7284.23186	1.00000	1
	2	7382.78200	0.71317	1
	3	7404.79365	1.00000	1
	4	7539.40081	1.00000	1
	5	7390.18777	1.00000	1
	6	7347.01456	1.00000	1
	7	7122.06516	1.00000	1
	8	7075.66609	1.00000	1
	9	7468.33608	1.00000	1
	10	7376.62580	1.00000	1
	11	7303.56530	0.99998	1
	12	7436.05789	0.59602	2
	13	7184.33358	0.99855	1
	14	7263.74884	1.00000	1
	15	7368.46367	1.00000	1
	16	7257.88663	1.00000	1
	17	7243.14897	1.00000	1
	18	7395.41960	1.00000	1
	19	7421.39449	0.99994	1
	20	7347.79189	1.00000	1

GROUP 2

1	7866.07497	0.99762	2
2	7824.24921	0.99939	2
3	7687.19014	0.66475	2
4	7452.07738	0.99705	2
5	7697.12278	0.98209	2
6	7666.78010	0.99845	2
7	7632.61546	0.99881	2
8	7551.05004	0.99970	2
9	7401.98347	0.99996	2
10	7652.40506	0.89808	2
11	7752.61646	0.99998	2
12	7551.98830	0.99667	2
13	7462.40494	0.99999	2
14	7621.55494	0.99998	2
15	7472.38014	0.99981	2
16	7542.11928	0.99999	2
17	7539.06323	0.99998	2
18	7561.87737	0.99997	2
19	7528.25818	0.99998	2
20	7488.00605	0.99995	2
21	7590.04116	0.99997	2
22	7301.55378	0.99991	2
23	7149.65882	0.99997	2
24	7467.06440	1.00000	2
25	7343.38161	0.99984	2
26	7455.69893	0.61646	3
27	7607.73625	0.99595	2
28	7295.05281	0.99961	2
29	7470.23955	0.99999	2
30	7198.79404	0.99975	2
31	7304.60313	0.99431	2

GROUP 1 MEANS

54.214	0.745	15.622	9.051	5.447	9.159
2.561	0.372	0.077	0.128		

GROUP 2 MEANS

50.169	1.438	12.847	15.164	5.757	9.929
2.371	0.275	0.198	0.216		

GROUP 3 MEANS

51.405	2.015	13.320	17.306	4.463	7.472
3.043	0.300	0.402	0.254		

GROUP 3

1	7716.06140	0.99998	3
2	7685.58898	0.99952	3
3	7716.40511	0.99974	3
4	7677.06512	0.99979	3
5	7726.21977	1.00000	3
6	7671.51432	0.99998	3
7	7581.02165	0.99997	3
8	7591.03275	1.00000	3
9	7746.32865	1.00000	3
10	7755.91261	1.00000	3
11	7719.41744	0.99999	3
12	7681.28813	0.99980	3
13	7764.20703	0.99620	3
14	7753.55029	0.99896	3
15	7770.89111	1.00000	3
16	7756.63529	0.98760	3
17	7744.70049	0.90435	3
18	7725.22409	0.99990	3
19	7786.96504	0.99961	3
20	7750.75039	0.61839	3
21	7657.28737	0.99950	3
22	7680.13433	0.94100	3
23	7695.41512	0.99337	3
24	7728.79112	0.99711	3
25	7741.86683	0.99991	3
26	7706.23846	0.99999	3
27	7723.84392	0.99999	3
28	7687.20381	1.00000	3
29	7684.33566	0.99876	3
30	7748.17759	0.99961	3
31	7717.82073	0.99999	3

Listing of program to calculate the values of discriminant functions for each sample with a typical output.

```
100 REM      PROGRAM TO CALCULATE DISCRIMINANT DIAGRAM FROM
110 REM              THREE DISCRIMINANT FUNCTIONS
120 REM
130 REM
180 DIM COEFI(3,11)
182 DIM CONST(3)
184 DIM ELEM(11)
186 DIM SUM(3)
200 OPEN "COEFI.LIB" FOR INPUT AS #1
210 FOR N=1 TO 3
220 FOR M=1 TO 11
230 INPUT #1, COEFI(N,M)
240 NEXT M
245 LET CONST(N)= COEFI(N,11)
250 NEXT N
260 CLOSE #1
266 LPRINT TAB(10);"SAMP #";TAB(25);"F1";TAB(36);"F2";TAB(47);"F3";
268 LPRINT TAB(57);"F1/F2";TAB(67);"F3/F2"
280 OPEN "INFO.LIB" FOR INPUT AS #1
300 WHILE NOT EOF(1)
310 LINE INPUT #1, DUM$
320 LET SAMP$= LEFT$(DUM$,5)
330 FOR M=1 TO 11
340 LET ELEM(M)= (VAL(MID$(DUM$,6+4*(M-1),4))/100)
350 NEXT M
360 LET ELEM(4)= ELEM(4)*.89+ELEM(5)
370 FOR M=5 TO 10
380 LET ELEM(M)= ELEM(M+1)
390 NEXT M
392 FOR N=1 TO 3: LET SUM(N)= 0!: NEXT N
500 FOR N=1 TO 3
510 FOR M=1 TO 10
520 LET SUM(N)=SUM(N)+(ELEM(M)*COEFI(N,M))
530 NEXT M
540 LET SUM(N)= SUM(N)+CONST(N)
550 NEXT N
600 LET F1= SUM(1): F2= SUM(2): F3= SUM(3)
700 LPRINT TAB(10); SAMP$;TAB(21);F1;TAB(32);F2;TAB(43);F3;
710 LPRINT TAB(54);F1/F2;TAB(65);F3/F2
720 WEND
```

SAMP #	F1	F2	F3	F1/F2	F3/F2
1135A	7176.556	7170.289	7151.57	1.000874	.9973893
1177A	7270.308	7251.334	7233.71	1.002617	.9975695
1184	7505.865	7492.869	7473.115	1.001734	.9973636
1012B	7403.324	7386.248	7363.689	1.002312	.9969458
1072	7262.237	7240.901	7219.149	1.002947	.9969961
1166	6733.666	6701.449	6674.866	1.004807	.9960332
1001	6956.867	6934.739	6920.402	1.003191	.9979326
1030B	7417.175	7413.103	7396.905	1.000549	.997815
1013A	7147.461	7126.885	7102.802	1.002887	.9966209
1140A	7237.896	7221.612	7191.453	1.002255	.9958237
1024A	6945.232	6921.088	6887.933	1.003488	.9952096
1024B	6905.702	6891.204	6864.205	1.002104	.996082
1017	6829.088	6807.562	6790.567	1.003162	.9975036
1097	6975.901	6951.844	6924.012	1.003461	.9959965
1028B	6941.218	6923.102	6900.094	1.002617	.9966768
1158	7051.896	7039.535	7028.192	1.001756	.9983886
1029	7582.392	7566.583	7551.084	1.002089	.9979516
1101A	7793.483	7778.314	7760.938	1.00195	.9977661
1013B	7518.684	7508.57	7488.201	1.001347	.9972872
1056B	7258.063	7242.018	7219.289	1.002216	.9968615
1056A	7255.52	7236.595	7221.712	1.002615	.9979433
1135B	7378.507	7373.076	7355.181	1.000737	.9975729
1041	7136.84	7121.22	7096.827	1.002193	.9965746
1142B	7507.639	7499.307	7476.011	1.001111	.9968936
1038	7249.589	7244.464	7222.953	1.000707	.9970307
1036	7375.429	7360.682	7340.201	1.002004	.9972175
1030A	7005.865	6994.072	6966.25	1.001686	.9960219
M39	7512.256	7522.429	7521.128	.9986476	.999827
M43	7391.914	7404.846	7408.934	.9982536	1.000552
M37	7434.558	7448.909	7453.632	.9980734	1.000634
M50	7392.414	7404.443	7409.327	.9983755	1.00066
M48	7364.072	7386.644	7395.65	.9969442	1.001219
M33	7378.913	7392.088	7399.639	.9982176	1.001022
M34	7283.634	7302.862	7309.709	.9973672	1.000938
M92	7186.521	7203.859	7218.775	.9975932	1.002071
M89	7391.185	7412.841	7423.526	.9970786	1.001442
M1	7422.568	7446.465	7457.133	.9967908	1.001433
M473	7445.341	7457.411	7451.709	.9983815	.9992352
263	7381.829	7396.92	7404.635	.9979598	1.001043
M256	7376.211	7387.109	7392.209	.9985248	1.00069
M307	7433.002	7451.418	7453.506	.9975284	1.00028
M309	7437.147	7454.114	7457.515	.9977238	1.000456
M9	7420.649	7450.599	7459.8	.9959802	1.001235
3062	7460.772	7477.044	7478.004	.9978237	1.000128
3061	7491.465	7503.658	7502.592	.9983749	.9998579
M300	7421.235	7438.64	7444.397	.9976602	1.000774
M338	7463.195	7486.941	7491.18	.9968284	1.000566
M14	7440.67	7458.143	7455.063	.9976572	.9995871
M579	7478.075	7482.579	7480.397	.999398	.9997084
M335	7491.461	7515.731	7534.467	.9967708	1.002493
M327	7586.959	7597.465	7585.204	.9986171	.9983861
319	7394.652	7399.694	7403.965	.9993186	1.000577
584	7431.724	7436.372	7435.84	.999375	.9999284

322	7440.66	7447.232	7448.91	.9991176	1.000225
M36	7456.17	7468.273	7470.602	.9983794	1.000312
M40	7440.569	7455.294	7460.982	.9980249	1.000763
M85	7345.679	7367.698	7376.263	.9970114	1.001163
M47	7368.649	7390.447	7398.771	.9970504	1.001126
M274	7344.386	7364.827	7378.425	.9972245	1.001846
585	7434.879	7434.019	7431.067	1.000116	.999603
317	7474.912	7476.28	7471.807	.9998169	.9994017
M310	7368.163	7380.065	7383.416	.9983872	1.000454
M311	7416.497	7432.908	7437.345	.997792	1.000597
M305	7380.27	7395.339	7403.041	.9979624	1.001041
L3	7590.3	7599.687	7590.313	.9987648	.9987666
L41	7552.283	7559.683	7548.944	.9990211	.9985794
L42	7304.873	7312.243	7304.156	.998992	.998894
L5	7363.018	7359.704	7357.305	1.00045	.999674
L6	7285.98	7288.254	7289.187	.999688	1.000128
L7	7397.429	7407.539	7403.564	.9986352	.9994634
L7D	7165.895	7174.246	7165.185	.998836	.998737
L9	7394.402	7403.825	7396.438	.9987272	.9990022
L101	7395.9	7402.591	7392.775	.9990961	.998674
L102	7362.175	7370.251	7360.184	.9989042	.9986341
L111	7272.965	7284.262	7272.797	.9984491	.998426
L112	7130.953	7139.576	7126.182	.9987922	.9981239
L12	7278.696	7291.399	7288.052	.9982579	.9995411
L13	7248.229	7244.69	7238.091	1.000489	.9990892
L141	7162.824	7174.957	7169.229	.9983089	.9992016
L142	7205.77	7216.955	7212.205	.9984501	.9993418
L15	7376.07	7387.868	7382.28	.998403	.9992436
L16	7500.401	7506.526	7492.108	.9991841	.9980794
L17	7361.418	7361.678	7345.27	.9999646	.9977712
L18	7216.439	7222.123	7205.84	.999213	.9977452
L19	7369.277	7376.529	7362.33	.9990169	.9980751
L20	7242.456	7248.409	7236.598	.9991786	.9983705
L21	7283.787	7290.689	7276.077	.9990534	.9979959
L221	7275.247	7283.711	7269.574	.9988379	.998059
L222	7313.239	7320.872	7307.108	.9989573	.9981199
L23	7275.238	7282.334	7268.12	.9990256	.9980481
L24	7239.808	7246.092	7232.921	.9991328	.9981823
L251	7345.888	7349.977	7335.525	.9994438	.9980338
L252	7058.756	7061.278	7043.448	.9996429	.997475
L261	6888.498	6891.614	6870.877	.9995478	.9969909
L262	7200.566	7207.224	7190.029	.9990762	.9976142
L27	7241.949	7245.727	7229.489	.9994786	.997759
M802	7077.341	7085.501	7073.472	.9988484	.9983023
M803	7217.807	7228.302	7225.367	.9985481	.999594
M804	7347.088	7358.141	7349.351	.9984978	.9988054
M806	7044.197	7045.091	7031.403	.9998731	.9980571
M807	7223.25	7228.335	7212.673	.9992964	.9978331
M808	6932.754	6940.725	6929.198	.9988515	.9983392
M809	7079.787	7078.569	7063.313	1.000172	.9978448
M8011	6854.839	6870.921	6873.831	.9976593	1.000423